SINTEF

A26122- Unrestricted

FINAL report

Subsurface oil releases – Experimental Study of Droplet Distributions and Different Dispersant Injection Techniques - version 2

A scaled experimental approach using the SINTEF Tower basin

Authors
Per Johan Brandvik, Øistein Johansen, Umer Farooq, Glen Angell and Frode Leirvik

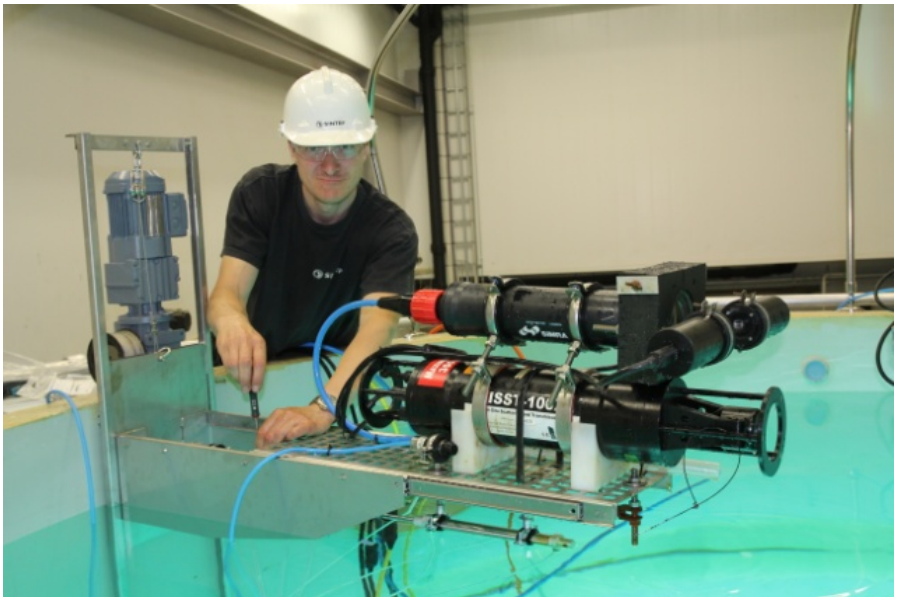

Preparing the instrumentation (LISST and in-situ camera) for monitoring of droplet size distributions in the Tower basin.

SINTEF Materials and Chemistry
Environmental Technology
2014-05-08

SINTEF Materials and Chemistry
Environmental Technology
2014-05-08

SINTEF Materialer og kjemi
SINTEF Materials and Chemistry
Address:
Postboks 4760 Sluppen
NO-7465 Trondheim
NORWAY
Telephone:+47 73593000
Telefax:+47 73597043
info.mk@sintef.no
www.sintef.no/mk
Enterprise /VAT No:
NO 948007029 MVA

KEYWORDS:
Oil spill
subsurface
release conditions
droplet size
modeling

Final report

Subsurface oil releases – Experimental Study of Droplet Distributions and Different Dispersant Injection Techniques - version 2

VERSION
FINAL Report ver. 2

DATE
2014-05-08

AUTHOR(S)
Per Johan Brandvik, Øistein Johansen, Umer Farooq, Glen Angell and Frode Leirvik

CLIENT(S)
The American Petroleum Institute – API JITF D3

CLIENT'S REF.
Patrick Twomey, EM&A

PROJECT NO.
102001616

NUMBER OF PAGES/APPENDICES:
100 + Appendices

ABSTRACT
The main objectives with this project have been to answer the following questions regarding dispersant injection during a subsea blowout.

1. How do dispersant injection method, dispersant to oil ratio (DOR) and dispersant type affect oil droplet size (Volume Median Diameter – VMD)?
2. How does the dispersant-oil mixing vary as a function of distance from the orifice for different injection methods and how does this affect oil droplet size?

The experimental work has been performed in SINTEFs Tower basin in Trondheim, Norway. This unique facility consist of a 6 meter high, 3 meter wide tank that holds 42 m^3 of natural sea water and is equipped with the latest technology for such experiments.

- A clear correlation between DOR and the shift in droplet size distribution towards smaller droplets was observed. Very limited effect was observed for the lowest concentrations (DOR 1:1000-1:500), steadily increasing up to a shift corresponding to a third of the initial VMD at the highest concentration (1:25).

- The three different injection methods tested in this project gave similar results (reduction or shift in VMD), independent of whether the dispersant was injected immediately before the outlet (simulated injection tool) or immediately after the outlet.

PREPARED BY
Per Johan Brandvik, Senior Scientist/Professor

SIGNATURE

CHECKED BY
Ivar Singsaas, Research Director, QA coordinator

SIGNATURE

APPROVED BY
for Tore Aunaas, Vice President

SIGNATURE

REPORT NO.	ISBN	CLASSIFICATION	CLASSIFICATION THIS PAGE
A26122	9788214057393	Unrestricted	Unrestricted

Document history

VERSION	DATE	VERSION DESCRIPTION
Draft version 1	2012-08-15	First version - To be discussed with API D3 committee in Houston early in October 2012.
Draft version 2	2012-10-21	Updated version for the October meeting, now postponed to 24. October. Updates based on comments from API D3 steering committee members.
Draft version 3	2012-12-20	Updated version based on feedback and comments on and after the October meeting.
Final version	2013-03-05	Final unrestricted version implementing comments on third draft.
2nd Final version	20014-05-08	Final unrestricted version implementing additional comments.

Recommended reference:

Brandvik, P.J., Johansen, Ø., Farooq, U., Angell G., and Leirvik, F. 2014 *Sub-surface oil releases – Experimental study of droplet distributions and different dispersant injection techniques- version 2. A scaled experimental approach using the SINTEF Tower basin*. SINTEF report no: A26122. Trondheim Norway 2014. ISBN: 9788214057393.

This study has been funded by the American Petroleum Institute (API) under contract 2012-106675.

SINTEF

Table of contents

1 Introduction

SINTEF received in November 2011 a request for proposal (RFP) from API called "Evaluation of subsea dispersant injection methods / equipment and effectiveness". This RFP was a part of the Joint Industry Task force (JITF) D3 and was managed by Ecosystem Management & Associates (EM&A), Maryland, USA.

API requested a proposal from SINTEF to conduct large-scale laboratory studies on the physical and chemical characterization of oil droplets associated with physically and chemically dispersed crude oil from uncontrolled well events in deep-water environments. The goal of this research is to understand droplet formation as a function of release conditions (e.g. diameter and flow rate) and oil properties (e.g. viscosity, density and interfacial tension). The important variables should be varied systematically to produce a data set suitable to calibrate and improve existing algorithms for estimation of droplet sizes. Topics of immediate interest to API include oil droplet characterizations that can be used to predict (model) the behaviour of physically and chemically dispersed oil droplets based on the oil release flow rate, configuration and size of the orifice releasing oil, and properties of the crude oil and dispersant used. For the initial research efforts, API is particularly interested in experimental work that will further increase our understanding and ability to define the dispersion process for deep water releases of crude oil with and without the use of dispersants for atomization break-up regimes, generating data to support predictive modelling of the processes with different crude oil release conditions and varying types of crude oil.

The requested experimental work from API was listed in the following prioritized order:

1) Studies of dispersant injection method
2) Studies of DOR dependence.
3) Studies of dispersant dependence

The experimental work listed above only covers parts of the overall objectives for the D3 program. The main focus of these experiments is how the dispersant injection techniques and dispersant concentrations affect the droplet size distribution.

To clarify this, SINTEF took an initiative for a meeting with the API D3 management and team members on 15th November 2011 (during SEATAC in Boston). The main conclusions from this meeting are listed below (See minutes issued by EM&A for further details):

- "Studies of dispersant injection techniques, DOR dependency and dispersant products have priority as this knowledge is needed to inform on-going development of new response equipment designed to combat deep sea releases."
- "This RFP describes the first phase of the D3 project. Later studies will focus on how release conditions and oil properties affect droplet size distribution."
- "This RFP must be regarded as a starting point of an iterative process between the D3 management and SINTEF. The project description should include inherent flexibility to change the experimental program if necessary as the project progresses and further insight is gained."

Based on the recommendations from this meeting, this project was described as a Phase I and contains only activities covering the prioritized areas 1-3 listed above. Activities for possible Phase-II will be discussed as a part of the reporting of Phase-I.

2 Objectives

The main objectives with this study are to answer the following questions regarding dispersant injection during a subsea blowout:

1. How do dispersant injection method, dispersant to oil ratio (DOR) and dispersant type affect oil droplet size?
2. How does the dispersant-oil mixing vary as a function of distance from the orifice for different injection methods and how does this affect oil droplet size?

3 Deliveries

According to the contract, this final report includes the following sections:

1. Description of test tank, measurement methods, etc.
2. Summary of the experiment test matrix.
3. Summary of data analysis with special emphasis on effectiveness of the different dispersant injection techniques, DOR, dispersant type and the effect on oil droplet size distribution.
4. Discussion of scaling the results from the Tower basin dispersant injection testing to field scale.
5. Summary of further research needs and opportunities.

The main findings from this study will be published in a relevant peer reviewed scientific journal focusing on the effectiveness of the different dispersant injection techniques.

4 Droplet formation in turbulent flow

The size distribution of oil droplets formed in deep water oil and gas blowouts is known to have strong impact on the subsequent fate of the oil in the environment. Large droplets will rise relatively rapidly and come to the surface relatively close to the discharge location, while small droplets will rise more slowly and can be transported long distances from the discharge location with ambient currents before reaching the sea surface. The smallest droplets may even be kept suspended in the water masses for prolonged periods by vertical oceanic turbulent mixing, and this mechanism is the main rational for application of chemical dispersants. Releases which are predominantly producing large oil droplets (in the millimetre size range) may thus result in relatively thick surface oil slicks, while thin surface films may be expected from releases producing small droplets (micrometre range). Thin oil films are more susceptible to natural dispersion and will have distinctly shorter persistence on the sea surface than thicker oil slicks, and the possibility of oiling of adjacent shorelines may thus be strongly reduced.

Reliable predictions of the droplet size distribution in deep water blowouts will thus improve our ability to forecast the fate of oil in the environment, provide guidance for oil spill response operations and relevant information to the public. The present study was initiated to get a better understanding of the mechanisms that governs droplet break up in deep water blowouts, with and without application of chemical dispersants. In order to achieve this, we need to understand the basic mechanisms that govern droplet breakup, and empirical data to support the theoretical understanding. This chapter deals with the theoretical aspects, while the empirical findings will be presented in the subsequent chapters.

4.1 Break up regimes

Droplet breakup may be caused by different mechanisms depending on the properties of the fluid and outlet conditions, ranging from pendant droplets that separate from the nozzle when the buoyant forces outrange the interfacial tension forces, through various axial or transverse instabilities of the jet, to full atomization where droplets of a wide size range are generated almost instantaneously at the jet exit.

The full range of breakup regimes of oil jets in water was investigated in laboratory experiments reported by Masutani and Adams (2000) and Tang and Masutani (2003). Examples of the various breakup regimes of oil jets are shown in Figure 4.1. As previously observed from breakup experiments with liquid jets in air, Masutani et al. found that the breakup regimes of oil jets in water could be delimited in a Reynolds number (re) vs Ohnesorge number (Z or Oh) diagram (Figure 4.2). The two non-dimensional numbers are defined as $Re = \rho U D/ \mu$ and $Oh = \mu/(\rho \sigma D)^{1/2}$, where U is the exit velocity, D the orifice diameter, and ρ and μ are the density and dynamic viscosity of the jet fluid. The Ohnesorge number can also be expressed as a combination of the Reynolds number and the Weber number, i.e. $Oh = We^{1/2}/Re$, where $We = \rho U^2 D/\sigma$. The two boundaries which are shown in the diagram were derived from visual inspection of the breakup conditions. The broken line shows the boundary between laminar and transitional breakup, while the dashed dotted line shows the boundary between the transitional and turbulent (atomization) break regimes. Both lines were found to represent linear relationships of the form $Oh = c\ Re^{-1}$, where c is a constant of proportionality. From the definition of Ohnesorge number mentioned above, this relationship implies that both boundaries are lines for a constant Weber number, with $We = c^2$, or $We = 18 \times 18 = 324$ for the boundary between the transitional and turbulent breakup regime.

In the present study, where the main focus will be on turbulent break up, these findings are useful as a basis for limiting the experimental conditions for the breakup experiments. Figure 4.3 shows how the Ohnesorge vs. Reynolds number diagram can be used to delimit the range of discharge conditions. The parallelogram formed grid in the diagram depicts a range of possible orifice diameters and oil flow rates that might be used in the tower tank experiments. The orifice diameters are here limited to the range from 0.5 to 20 mm, with oil flow rates in the range from 0.1 to 20 L/minute. The thick solid line drawn in the diagram shows the boundary between the transition regime and the turbulent breakup (or atomization) regime.

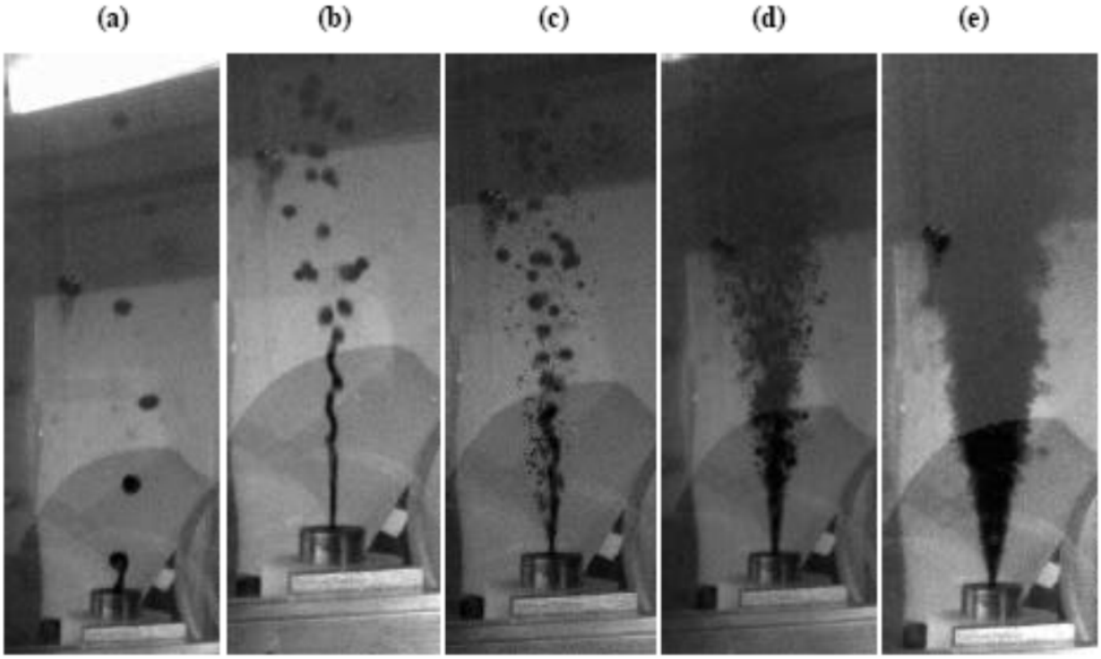

Figure 4.1: Illustration of oil jet breakup regimes from Tang and Masutani (2003). At low velocities, Rayleigh instability dominates, producing a near mono-dispersion of droplets larger than the orifice (a). As velocity is increased, the breakup location moves away from the nozzle and at some point the instability changes to a sinuous mode (b). At higher velocities, two instability mechanisms appear to operate in parallel: the surface of the jet becomes unstable to short wavelength disturbances and disintegrates close to the nozzle into fine droplets, while the core of the jet persists as a continuous fluid filament that breaks up further downstream into large droplets (c). Raising the velocity moves the breakup location of the jet core filament closer to the nozzle and also increases the fraction of fine droplets (d). Finally, atomization is attained (e).

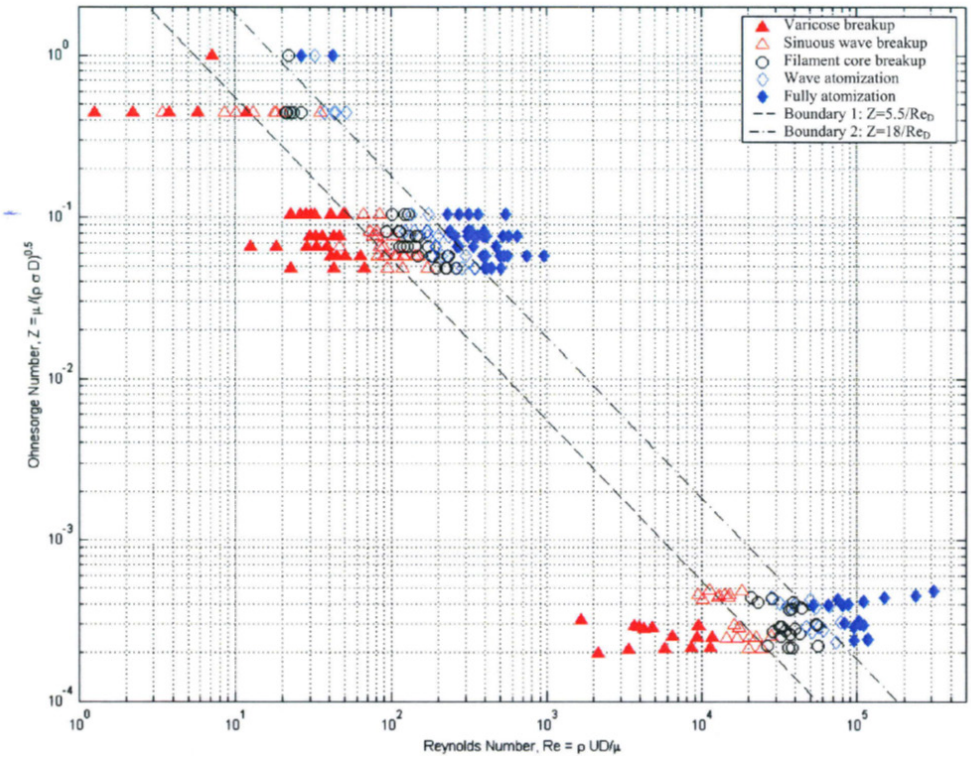

Figure 4.2: Liquid-liquid jet breakup regimes based on experiments with oil and silicone injection tests (upper two sets) and liquid CO2 injection tests (lower right hand corner). After Tang and Masutani (2003).

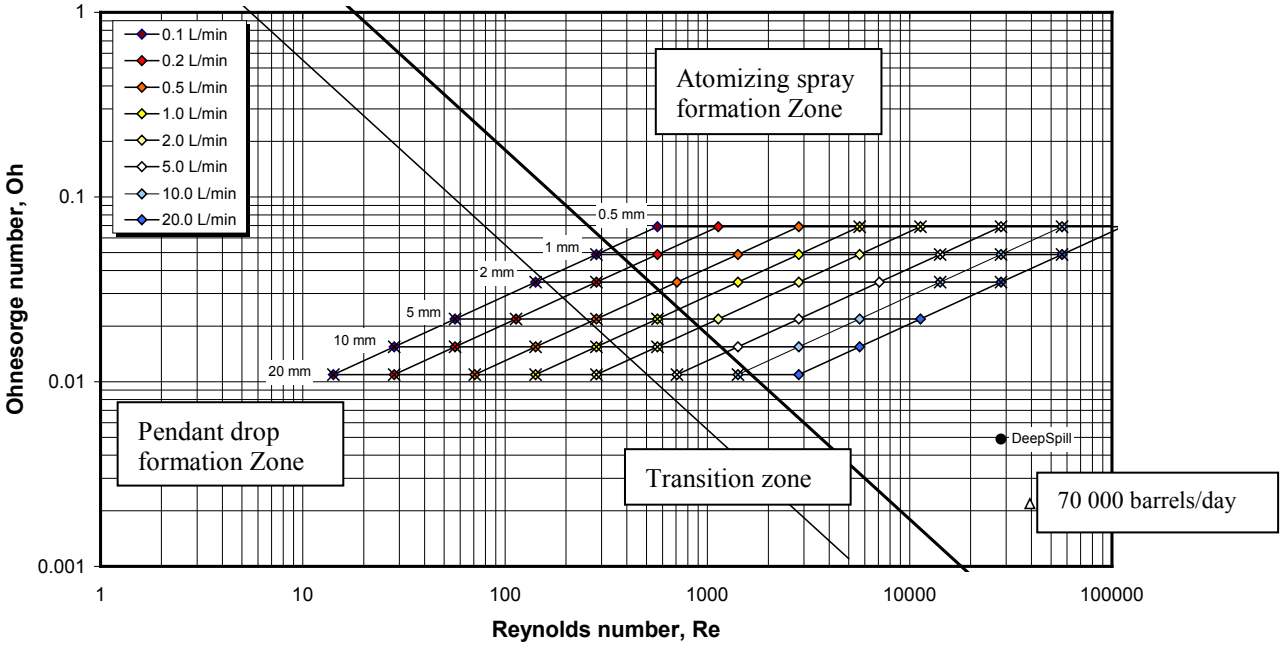

Figure 4.3: Experimental conditions plotted in an Ohnesorge vs. Reynolds number diagram. Injection rate varied from 0.1 to 20 L/min, with nozzle diameters from 0.5 to 20 mm. Oil viscosity is presumed to be 5 cP (50°C). Approximate location of the SINTEF DeepSpill experiment and a tentative large scale release are shown for comparison.

The preferred range of experimental conditions are depicted with open markers, while the cases that falls outside the turbulent regime are shown with crossed markers. Some of the cases in the turbulent breakup regime that will produce high outlet velocities (> 40 m/s) are also crossed out. These cases may be difficult to realize due to high pressure drops. The range of experimental conditions are also limited due to the size of the tank, however, nozzle sizes up to 15 mm and rates up to 100 L/min can be tested. The duration of such experiments will be limited to 10-30 seconds.

4.2 Weber number scaling

The classical theory of droplet splitting in turbulence predicts a maximum stable droplet size $d_{max} = C(\sigma/\rho)^{3/5}\varepsilon^{-2/5}$, where C is a constant of proportionality, σ is the interfacial tension (oil-water), ρ is the density of the continuous phase (water), and ε is the stationary turbulent dissipation rate (Hinze1955). However, in an oil jet emitted into water from a nozzle, the droplets will be carried downstream in the jet during the splitting process. Consequently, in a Lagrangian framework, the turbulent dissipation rate will diminish rapidly with time, and the assumption of stationary turbulence will not be applicable.

However, this theoretical model may still serve as a starting point for experimental design and development of more practical empirical equations. For example, by taking into account that the exit turbulent dissipation rate in a jet scales with the exit velocity U and diameter D, $\varepsilon \sim U^3/D$, the equation given above for d_{max} can be expressed in non-dimensional form: $d_{max}/D = A\ We^{-3/5}$, where A is a factor of proportionality, while the exit Weber number $We = \rho U^2 D/\sigma$. The factor of proportionality will depend on the flow conditions in the break up zone, and have to be determined empirically.

This scaling law is supposed to be valid when the breakup is limited by the interfacial tension of the jet liquid. However, as Hinze (1955) also pointed out, internal viscous stresses in the fluid droplets may also influence the breakup. Hinze introduced a dimensionless viscosity group N_{Vi} to account for this effect. Hinze's viscosity group is actually identical to the Ohnesorge number defined above. More recently, Wang and Calabrese (1986), proposed to replace Hinze's viscosity group by the viscosity number $Vi = \mu U/\sigma$ to account for the effect of viscous stresses. This dimensionless number is also defined as the ratio between the Weber number and the Reynolds number, i.e. Vi = We/Re.

Wang and Calabrese (1986) found that droplet breakup was governed by the Weber number scaling for small viscosity numbers ($Vi \rightarrow 0$), but that a Reynolds number scaling would apply for large viscosity number ($d_{max}/D = C\ Re^{-3/4}$, $Vi \rightarrow \infty$). For intermediate values of Vi, a combination of the two scaling laws might be applied. We will return to this relationship in the discussion of the experimental results, but it should be pointed out here that the viscosity numbers usually are small in conjunction with oil jet breakup, but large numbers may result in conjunction with application of chemical dispersant, since this can result in reductions in the interfacial tension by several orders of magnitude.

4.3 Bubbly jets

Most oil jet breakup experiments are conducted with a single fluid into water (crude oil or silicone fluid). In subsea blowouts, however, gas is in general discharged together with the oil, and the oil is quite often mixed with certain amounts of formation water. Different flow conditions can occur in

such multiphase flows, from bubbly flow with oil as the continuous phase, via slug flow where plugs of oil and gas occupy sequential sections of the pipe, to mist flow where oil droplets are suspended in the gas flow, and some of the oil might flow along the surface of the pipe (annular flow). Bubbly flow in vertical pipes are normally associated with low to moderate gas void fractions ($0 < n < 60$ %), while mist flow is limited to very high void fractions ($n > 95\%$). However, the actual flow conditions are also influenced by the velocity of the flow, often defined by the superficial velocities of the two fluids. In the present context, we will only consider the bubbly flow condition, which in this study is of most interest because of concerns about high flow rate oil blowouts.

The main issue here is how to account for the presence of gas in the normalized variables defined above (i.e. the Reynolds, Weber and Ohnesorge numbers). For example, Neto et al. (2008) defined the nozzle Reynolds number in a series of bubbly water jet experiments in terms of the superficial water velocity $U_W = Q_W/A$, where Q_W is the volume flow of water and A is the nozzle cross section $A = \pi D^2/4$ corresponding to a nozzle diameter D, i.e. $Re_W = U_W D/\nu_W$, where ν_W is the kinematic viscosity of water.

However, this definition will not discriminate between a pure water jet and a bubbly jet with the same water flow. In order to account for this, the "water only" velocity may be substituted with an "effective" water velocity U_E derived from the principle of conservation of momentum flux. In the following, M is the exit momentum flux of the bubbly water jet, while M_E is the momentum flux of an "equivalent" pure water jet. The effective water velocity is then defined as the velocity of a pure water jet producing the same momentum flux as the bubbly water jet:

$$M = (\rho_W Q_W + \rho_G Q_G) U_{W+G},$$

$$M_E = \rho_W Q_E U_E, \text{ where } Q_E = A U_E$$

If we neglect the contribution of the gas to the momentum flux (due to the much smaller density of the gas), $M_E = M$ will imply $U_E = U_{WO}/(1 - n)^{1/2}$.

Since we now have defined the Reynolds number is in terms of the continuous phase, it is reasonable to do the same for the Weber and the Ohnesorge numbers. We then get the following definitions of the non-dimensional variables:

$$Re = \rho U_E D/\mu,\ We = \rho U_E D^2/\sigma \text{ and } Oh = \mu/(\rho \sigma D)^{1/2}$$

In the following, when we consider a system with oil and gas (instead of water and gas), oil properties will be substituted for water properties, and the subscripts will be dropped in the density and viscosity terms (implicitly implying oil).

Figure 4.4 shows a Re vs. Oh plot based on these definitions with results from the bubbly water jet experiments reported by Neto et al. (2008), covering gas volume fractions in the range from approximately 5 to 80 %. Experiments where atomization is observed are represented by filled markers, while open markers represent the transition regime. The thick red line depicts the

transition to full atomization based on the liquid only experiments of Tang and Masutani 2003 (with oil or liquid CO_2).

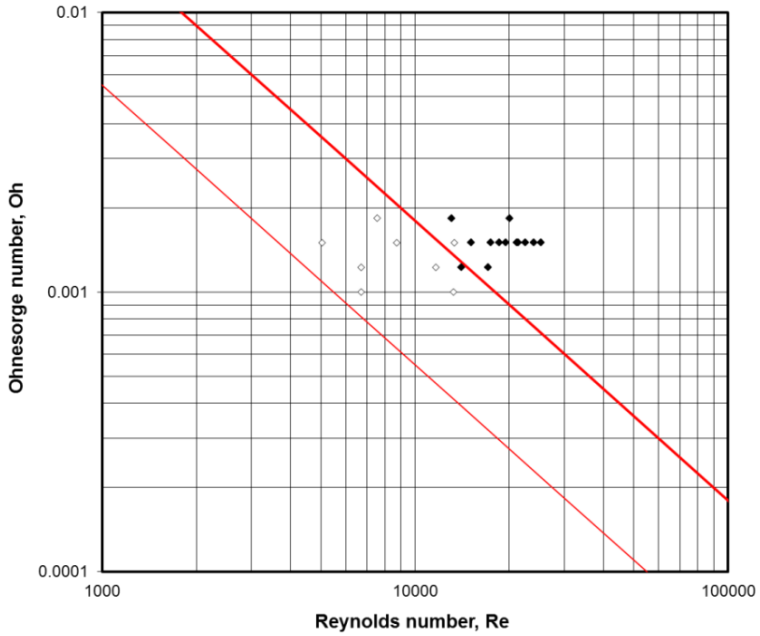

Figure 4.4: Ohnesorge – Reynolds number plot of data from bubbly water jet experiments reported by Neto et al. 2008. Filled diamonds represent cases with atomization, while the open diamonds are cases in the transition regime. The thick red line depicts the transition to full atomization based on liquid only experiments of Tang and Masutani 2003.

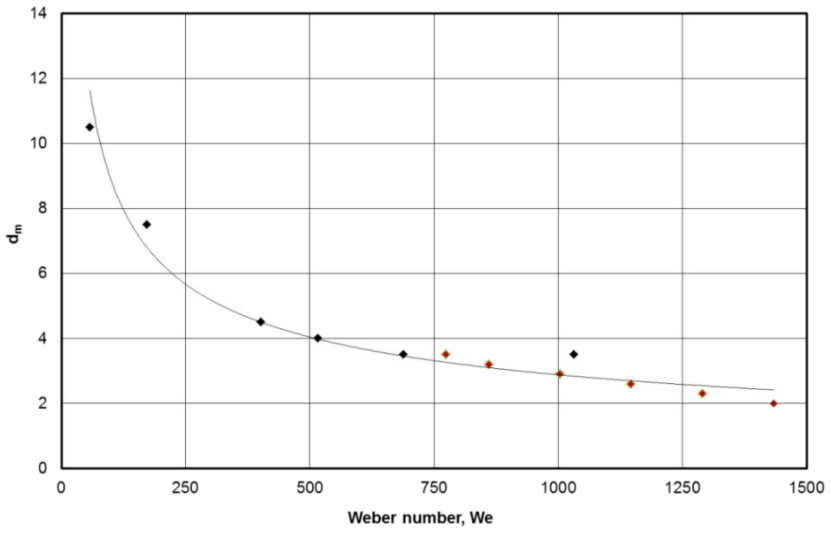

Figure 4.5: Volumetric mean bubble diameter plotted as a function of the Weber number computed from the equivalent liquid velocity U_{LE} defined above. The results shown here were obtained by Neto et al. 2008 with a 6 mm nozzle, with water only velocities in the range from about 0.5 to 3 m/s and gas volume fractions in the range from 7 to 80%. The red markers represent experiments with a fixed water only velocity (U_{LO} = 2.95 m/s), but with gas volume fraction varied from 7 to 50 %.

Figure 4.5 shows a plot of the mean bubble diameter reported by Neto et al. for a set of experiments with a 6 mm nozzle. The gas volume fractions varies in a range from about 7 up to about 80 %, while the water only velocities are in the range from about 0.5 to 3 m/s. It is promising that the transition line derived from single liquid flows also applies to bubbly jets when we use the definitions given above of the non-dimensional numbers. The same can be said for the quite systematic variation observed in Figure 2 of the mean bubble size with our definition of the Weber number. In conjunction with the planned oil experiments, these findings seem to imply that a situation with a gas volume fraction n and an oil volume flow $Q^{(n)}$ might be represented by an oil only experiment with an adjusted oil volume flow $Q = Q^{(n)}/(1–n)^{1/2}$.

4.4 Buoyant jets

The gas fraction in a bubbly jet will also contribute to the buoyancy flux of the discharge. The buoyancy flux is defined as $B = g' Q$, where Q is the total exit volume flow and $g' = g (\rho_w – \rho)/ \rho_w$ is the reduced gravity, where g is the acceleration of gravity, ρ_w is the density of water, and ρ is the density of the mixture of liquid and gas. Papanicolaou and List (1988) made an experimental investigation of the dynamics of round vertical buoyant jets, and found that buoyant jets differs from momentum jets in many aspects. While most experiments of droplet breakup in oil jets are made with jet-like outlet flow conditions due to restriction in volumetric flow rates and nozzle diameters, the conditions in deep water blowouts with large volume flows and large outlet diameters may tend to be more plume-like.

Papanicolaou and List (1988) found that the transition from jet-like to plume-like behavior in buoyant plumes is defined by a characteristic length $l_M = M^{3/4}/ B^{1/2}$. They conducted experimental studies with buoyant plumes and showed that the flow behaves like a jet at distances $z < l_M$, and like a plume for $z > 5\ l_M$. The relative distance l_M/D may indicate whether droplet splitting will take place in the jet-like or plume-like section of the buoyant plume. By insertion of the expressions for Q, B and M in this equation, this ratio is found to correspond to the exit Froude number, $Fr = U/(g'D)^{1/2}$. Exit conditions (defined by the exit velocity and the orifice diameter) that give high exit Froude numbers will thus imply that droplet splitting will occur in jet-like flow, while low exit Froude number implies buoyant plume flow in the breakup zone.

The authors also showed that in jet-like flow, the centerline velocity w_c at a distance z downstream from the exit will scale with the exit velocity, i.e. $w_c \sim U\ z/D$. In plume-like flow, the buoyancy flux will be the primary factor that determines the velocity development, i.e. $w_c \sim (B/z)^{1/3}$. This implies that in plume-like conditions, the exit velocity will not be a characteristic velocity for droplet breakup. From the scaling law for plume like flow, we find that at a distance $z = 5\ l_M$ where the flow shifts to plume-like behavior, the centerline velocity will be $w_c \sim (g'D)^{1/2}$. Thus, we may define a modified characteristic velocity $U' = U (1 + b\ Fr^{-1})$,where b is a factor of proportionality in the order of 1, to account for both jet-like and plume-like breakup conditions. The last term will vanish for large exit Froude numbers (i.e. $U' \approx U$ for jet-like flow), while for small Froude numbers (plume-like flow), the modified velocity will approach $U' = b\ Fr^{-1} = b\ (g'D)^{1/2}$, corresponding to the velocity at the transition to plume-like behavior. The factor of proportionality b should be determined from droplet breakup studies with buoyant flow conditions, but b = 1 could be used as a provisional estimate.

4.5 Droplet size distributions

In the previous section, we have focused on models for prediction of the characteristic droplet size, e.g. defined as the volume median droplet diameter, d_{50}. However, we also need to consider the statistical distribution of the droplet sizes around the characteristic diameter. Of the many available options, two distribution functions are most commonly found in the literature on droplet breakup; the lognormal distribution and the Rosin-Rammler distribution (Lefebvre1989).

The former can be understood as a normal distribution of the logarithms of the droplet sizes, i.e. a normal distribution of $x = \ln(d)$, with a mean value $M = \langle x \rangle$, and a standard deviation σ_x based on x. The mean value M is also equal to the logarithm of the median droplet diameter, $M = \ln(d_{50})$. Thus, the lognormal distribution is defined by two parameters, M and σ_x.

The Rossin-Rammler distribution is also a two-parameter distribution function, defined in terms of a characteristic diameter d_i corresponding to a certain cumulative volume fraction V_i (e.g. 50%), and a spreading parameter n. The cumulative volume distribution function is given as:

$V(d) = 1 - \exp[- k_i (d/d_i)^n]$, where $k_i = - \ln(1-V_i)$

For $V_i = 50\%$, d_i is the median diameter, and $k_i = -\ln(0.5) = 0.693$.

A third option is the Upper Limit lognormal distribution (UL), which is based on the lognormal distribution, but truncated at an upper limit diameter d_{max}. The cumulative probability function for the Upper Limit lognormal distribution is simply $V_U(d) = V(d)/V(d_{max})$ for $d < d_{max}$ and $V_U(d) = 1$ elsewhere, where $V_U(d)$ corresponds to the upper limit distribution and V(d) corresponds to the lognormal distribution. This distribution function will also be skewed, as shown in Figure 4.6. Figure 4.6 shows examples of distributions for the three distribution functions, with cumulative distributions shown in the top graph and frequency distributions in the bottom graph. Both graphs are presented in terms of relative droplet diameters d/d_{50}. The spreading parameter n = 1.8 in the Rosin-Rammler distribution is chosen to give an approximate fit to the lognormal distribution with the chosen standard deviation (here $\sigma_x = 0.78$ in natural logarithmic units). The UL distribution has the same nominal median and standard deviation, but is truncated at $d/d_{50} = 3$. The top graph shows that the lognormal distribution is symmetric on a logarithmic x-axis, while both the Rossin-Rammler distribution and the UL distribution is skewed with a shortened high-end tail ($d/d_{50} > 1$). However, at the low-end ($d/d_{50} < 1$), the three distributions have almost the same shape.

The same tendency is found in the bottom graph. This graph is made by binning the diameters in equal logarithmic intervals, corresponding to the data obtained from the LISST instrument. In the output from that instrument, the top value of each bin d_n is 1.18 times the top value of the previous bin D_{n-1}, and the same increment is used here, i.e $d_n = 1.18\ d_{n-1}$. The values given on the x-axis in the bottom frame are median diameters in each bin, i.e. $d_M = (d_{n-1}\ d_n)^{1/2}$. The height of the columns represent the volume fraction contained in each bin, i.e. $\Delta V = V_n - V_{n-1}$. A close inspection of the bottom chart shows that the maximum bin volume fraction falls in the bin centered near $d/d_{50} = 1$ for all distributions, but with a slightly higher value for the Rosin-Rammler distribution ($d/d_{50} = 1.3$). However, for larger values of the spreading parameter, the peak diameter of the Rosin-

Rammler distribution is found to approach the median diameter: with n = 2.5, the peak diameter is found to fall in the bin centered at $d/d_{50} = 1.1$.
While the arithmetic mean for a normal distribution is known to coincide with the median value, for a lognormal distribution, the arithmetic mean is given as $E = \exp(M + \sigma_x^2/2)$, where M is the logarithmic mean and σ_x is the logarithmic standard deviation. With the given parameters, M = 0 and σ_x =0.78, this gives E = 1.36. We have estimated the arithmetic mean value for the Rosin-Rammler distribution from the binned distribution as $E = \Sigma\, d_i\, \Delta V_i$, summarized over all bins. With n =1.8, the arithmetic mean diameter was found to be $d/d_{50} = 1.09$, while for larger values of n, the arithmetic diameter was found to be closer to $d/d_{50} = 1$: with n = 2.5, the arithmetic mean was found at $d/d_{50} = 1.03$. The same method gave an arithmetic mean at $d/d_{50} = 1.34$ for the lognormal distribution, which is close to the theoretical value given above.

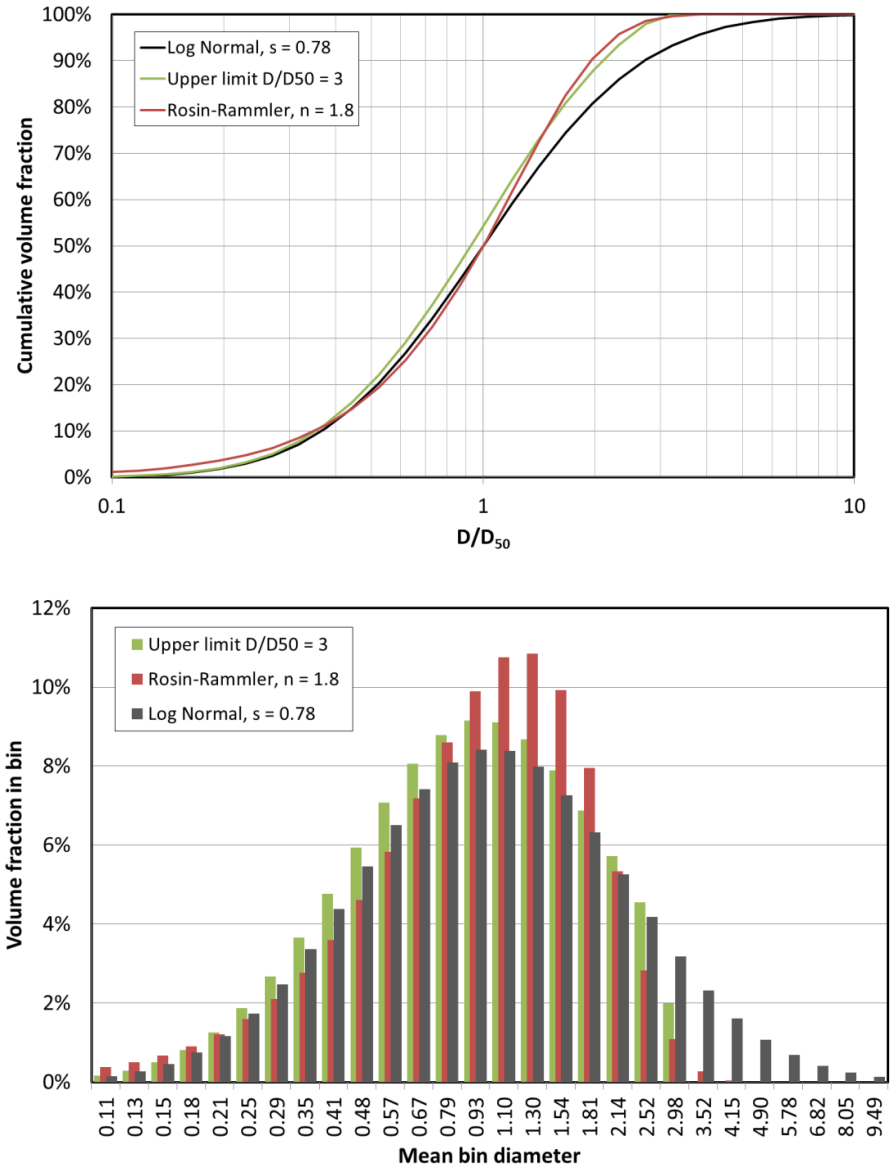

Figure 4.6: Comparison of lognormal and Rosin-Rammler distributions. Top: Cumulative distributions, bottom: Frequency distributions. The latter is based on data binned in equal logarithmic intervals, comparable to results from the LISST-instrument (see text).

The lognormal distribution may be linearized by plotting the number of standard deviations S that corresponds to a given cumulative probability V against x = ln(d) (see Figure 4.7, upper graph). The value of S(d) is computed from the given cumulative probability V(d), presuming that the distribution follows a lognormal distribution. In algorithmic notation, this can be expressed as S(x) = Norm.Inv(V(x), 0, 1), where Norm.Inv represents a function that returns the inverse of a normal distribution with a mean value M = 0 and standard deviation $\sigma_x = 1$. If the data are from a true lognormal distribution, the data points will then fall on a straight line y = a x, where the coefficient of proportionality will be $a = 1/\sigma_x$. By plotting an observed distribution in this way, we may thus assess whether the data follows a lognormal distribution, and if that is the case, determine the standard deviation of the distribution from the slope of the line.

The Rosin-Rammler distribution can be linearized in a similar way by plotting the variable –ln[1-V(d)] versus the diameter (see bottom graph in Figure 4.7). If the data follows a Rosin-Rammler distribution, the data will follow a power law function $y = b\ d^p$, where the exponent p = n and the coefficient $b = k/d_{50}^n$. This implies that by plotting an observed distribution in this way, we may assess whether the data follows a Rosin-Rammler distribution, and if that is the case, determine the median diameter d_{50} and the spreading parameter n of the distribution.

The examples shown in Figure 4.7 demonstrate the point, but also show that the Upper Limit distribution may look like a lognormal distribution at the lower end ($d/d_{50} < 1$), and as a Rosin-Rammler distribution at the upper end ($d/d_{50} > 1$).

We may also conclude that the peak diameter of the logarithmic binned distributions will coincide closely with the median diameter when the data fits a lognormal distribution. The same assumption may be made when the data fits a Rosin-Rammler distribution, but in that case, the median diameter may be slightly overestimated.

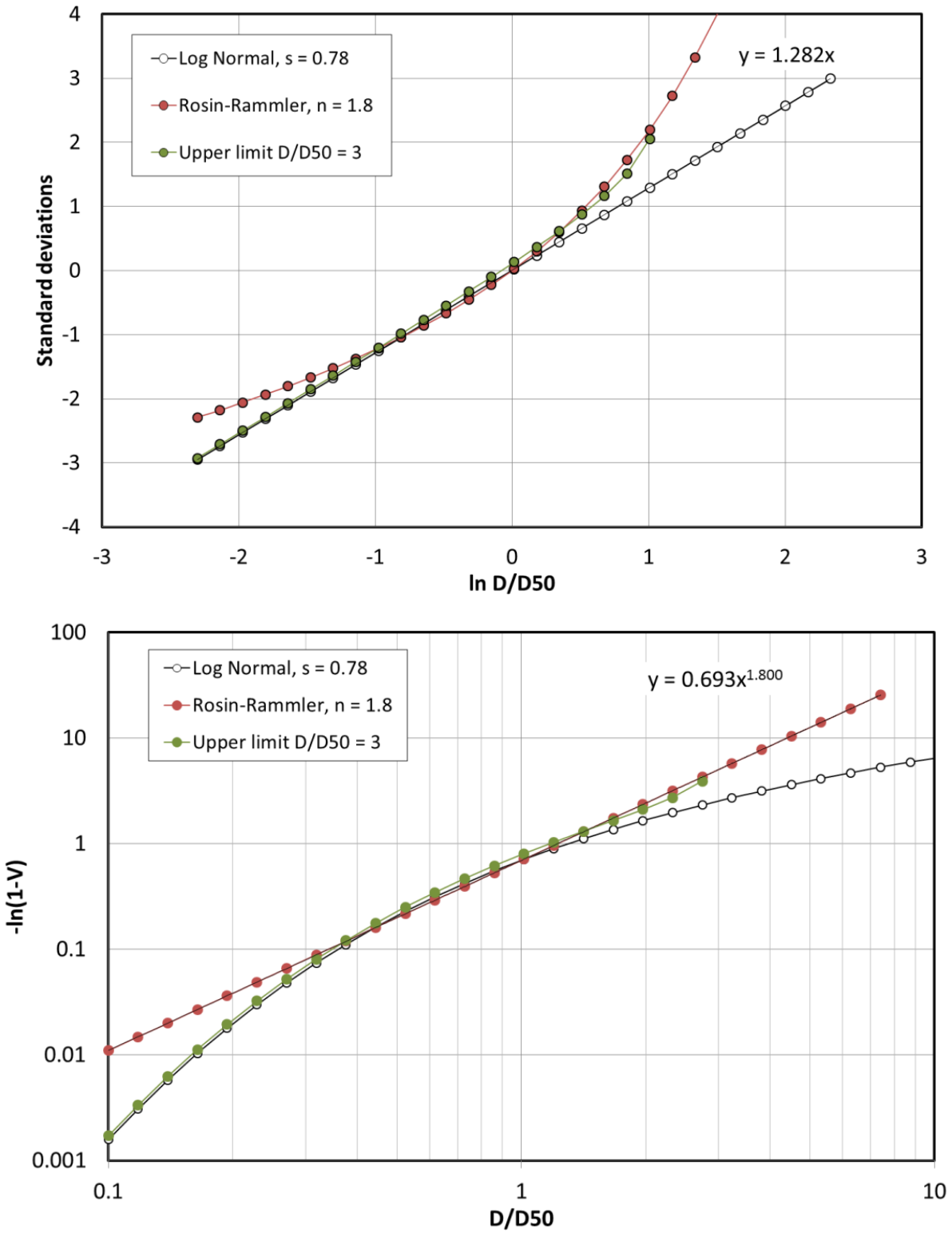

Figure 4.7: Linearization of lognormal and Rossin-Rammler distributions. Top: Log normal linearization. Bottom: Rosin-Rammler linearization.

5 Experimental

This section contains a description of the experimental methods and the experimental work performed in this project.

5.1 Selection of oil types

The experiments in this study are performed with the Norwegian Oseberg blend. Oseberg is a light paraffinic crude with high evaporative loss and is a representative candidate for a deep water high flow rate blow out scenario. However, the chemical composition and properties for such light oils can vary significantly and influence droplet sizes and dispersant effectiveness. Table 5.1 presents details for Oseberg Blend and MC252. The data for both oil types is from earlier weathering studies at SINTEF.

Table 5.1: Properties of MC252 and Oseberg blend.

	Macondo MC252 (ID 2012-0347)	**Oseberg blend** (ID 2012-0347)
Specific gravity (kg/l)	0.833	0.832
Pour Point (°C)	-27	-6
Viscosity (mPas at shear rate 10 s^{-1} and 40°C)	4	5
Asphaltene (wt%)	0.2	0.3
Waxes (wt%)	1.6	3.2
150°C – Evaporative loss (vol%)	27	22
200°C – Evaporative loss (vol%)	39	34
250°C – Evaporative loss (vol%)	50	45

Properties for different batches of Oseberg blend can vary. This batch had some higher wax content and slightly higher pour point compared to earlier batches. However, the same batch of oil is used for all experiments in this study. The oil was received from the Sture oil terminal in January 2012 and given the SINTEF ID 2012-0347. The oil IDs were tracked during the experimental work in the Tower Basin and each experiment is linked to this ID.

5.2 Selection of dispersants

Corexit 9500 was selected for this study since it was the main dispersant used during the Macondo incident and it is stored worldwide as a part of operational oil spill contingency. Two different varieties of Corexit c9500 are used in this study; Corexit EC9500A and Corexit EC9500A with reduced content of solvent (approx. double concentration of surfactants).

The first was labelled "CXIL0004" from Nalco and received in March 2012 (SINTEF ID: 2012-0062). The second was received from Nalco in June 2012 with the label "VX10612" and given SINTEF ID: 2012-0224. The dispersant was used as received and IDs were tracked during the experimental work in the Tower Basin and each experiment with dispersant is linked to a dispersant ID.

5.3 Overview of SINTEF Tower basin

The basin tower was constructed and built in 2005, but was not assembled or tested before it was used in this project. An outline of the tower basin mounted into SINTEFs ice basin is presented in Figure 5.1. The mounted tower basin during the first filling with water is seen in Figure 5.2 and Figure 5.3 and a drawing showing the scaffolding/railing around the tower basin together with the ventilated hood and oil collecting system is shown in Figure 5.4. More details can also be found in Brandvik et al., 2013.

The assembling of the basin shell, the rebuilding of the hall to fit these type of experiments and the preparation of the necessary HSE arrangements demanded more resources than initially anticipated. The following activities were part of this preparation.

a. Mounting the different parts of the tower basin and making it leak proof
b. Establishing the necessary arrangements/procedures for filling and emptying the tower basin
c. Establishing the necessary HSE arrangements for this new type of large-scale experiments
   - scaffolding/railing around the tower and a staircase to reach the top section for inspection and sampling
   - ventilated hood to prevent light hydrocarbons / vapors from entering the laboratory hall. This allowed operators to avoid working with external air masks or other breathing protection.
   - overflow system to collect or skim off surfacing oil from the top of the tower
   - disposal system/procedure for the used oil and the large volumes (42 m^3) of water containing small oil droplets. The dispersion experiments create very small droplets with very long rising/settling times.

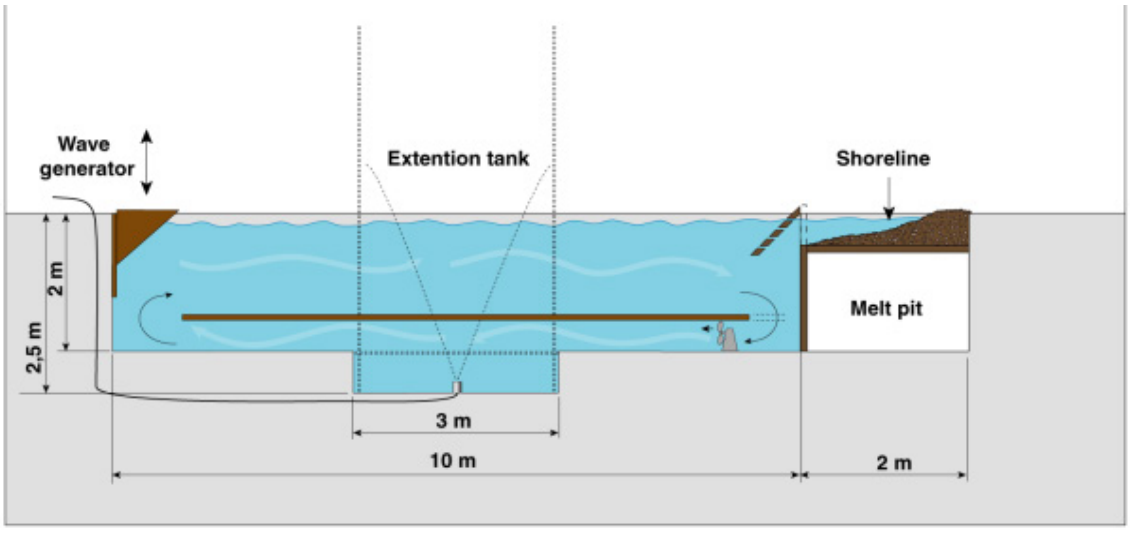

Figure 5.1: Overview of the tower basin inserted into the ice basin.

Figure 5.2: Ice basin without propellers and other equipment used for circulation showing the fundament for the Tower basin (left) and the initial mounting of the Tower basin (right).

Figure 5.3: First filling of water in the SINTEF Tower Basin, January 2011.

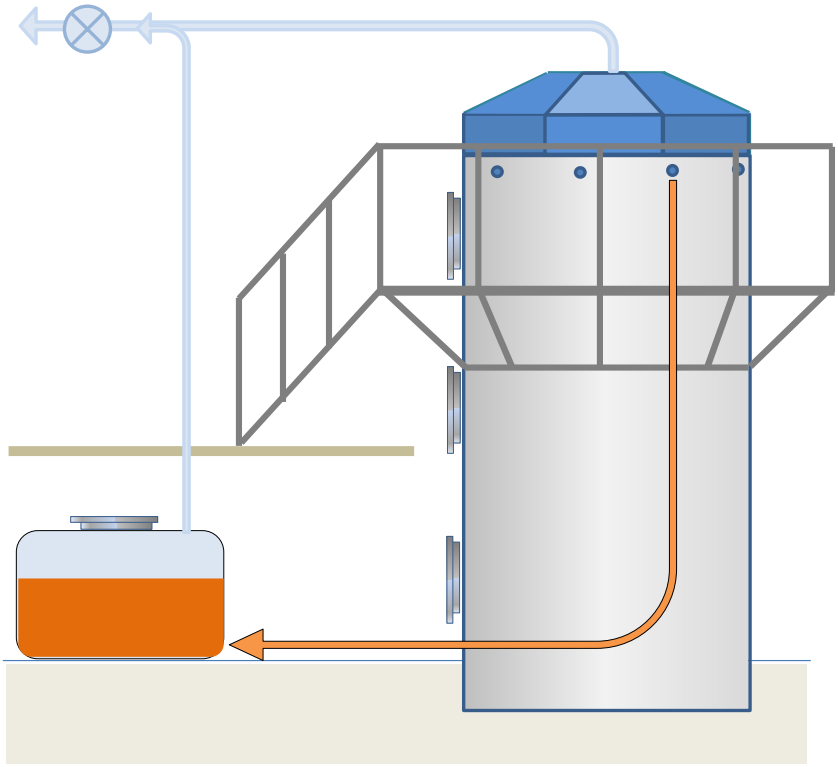

Figure 5.4: Principles for the scaffolding/railing around the tower, ventilated hood and overflow system to collect surface oil from the top of the tower.

Figure 5.5: The Tower basin per March 2012 showing the ventilated hood, scaffolding, staircase and the railings to ensure safe working conditions.

Trying to fully simulate a deep water, large-scale oil and gas blow out in a 6 meter high basin is not possible. Therefore, we have focused on some important aspects and scaled down and simulate these. The main objectives have been to study oil droplet size distribution as a function of:

1. Oil release conditions (release diameter and release rates).
2. Dispersant to oil ratio (DORs).
3. Different dispersant application techniques.

The droplets are formed by turbulent droplet splitting immediately after the release nozzle where the oil/gas/water plume will quickly stabilize with respect to droplet size distribution. The plume will rise mainly due to the buoyancy of gas (air) bubbles and oil droplets. It is in this zone in the middle of the tank, approximate 3 meters above the release nozzles, where the droplet size distribution measurements are performed. The distance from the nozzle is based on dilution of the oil plume from the turbulent zone. Due to instrument limitations, this dilution should approximately be 100. This distance will also depend on the release rates.

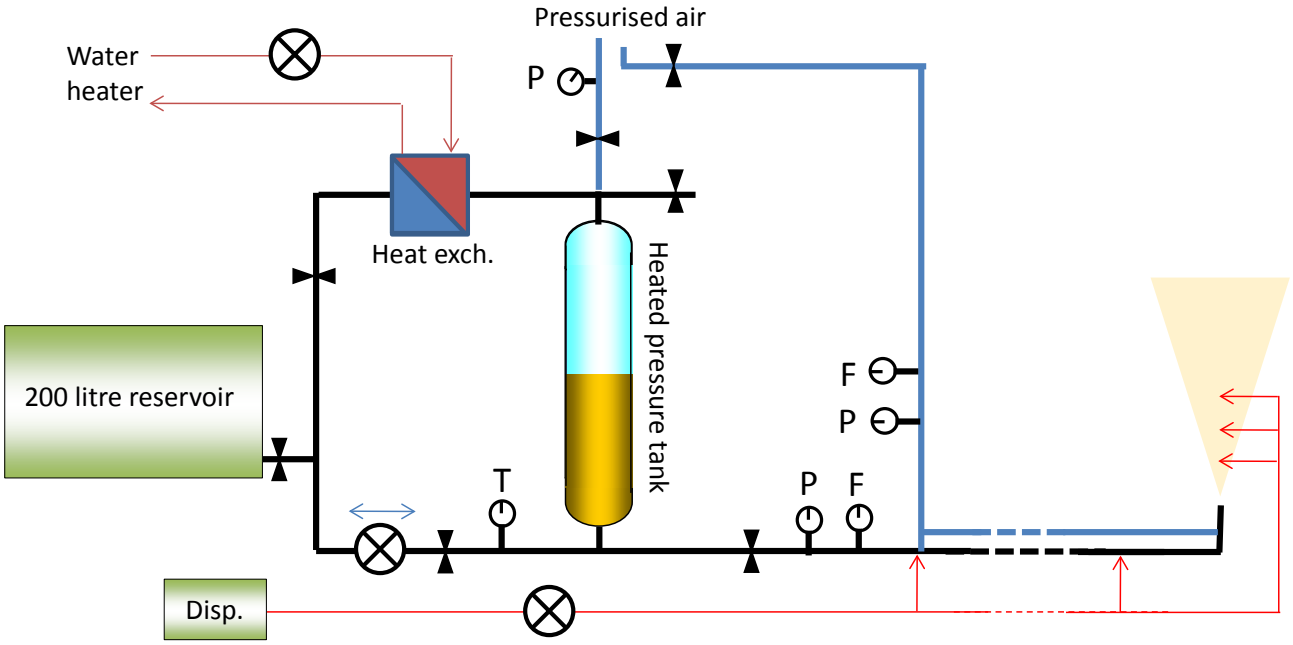

Figure 5.6: Principle overview of the set-up showing how oil, gas and dispersant are released during the experiments. The oil flow is controlled by regulating pressurized air (P) with a mass flow controller (F). The oil temperature (10-95 ºC) is controlled by a heat exchanger. The dispersant is delivered by a high precision piston pump to several alternative injection points. Gas flow is controlled by pressure (P) and a mass flow controller (F).

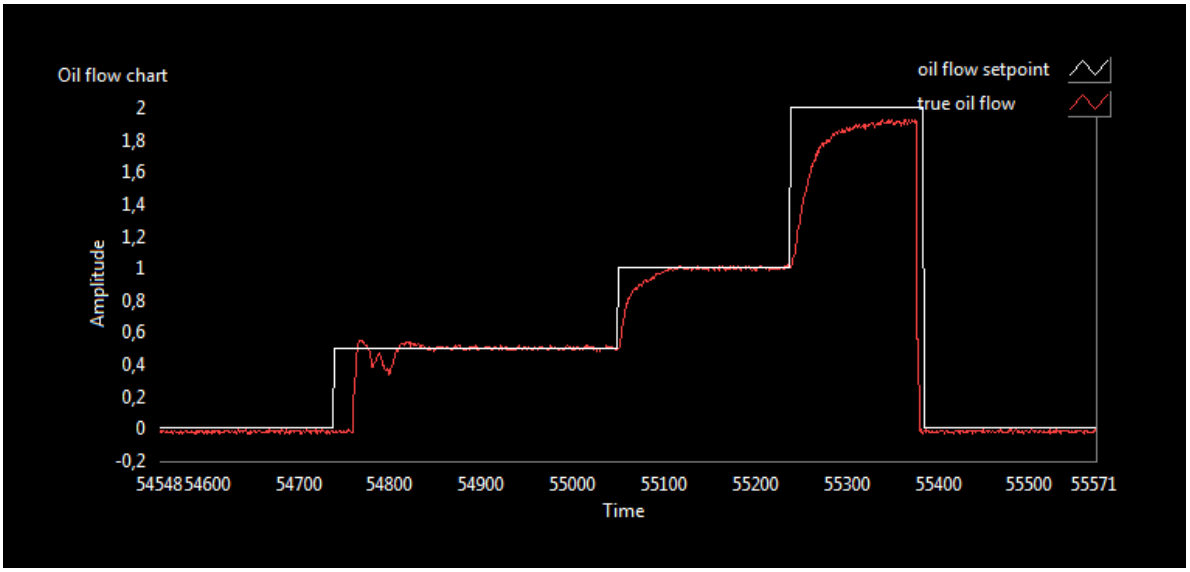

Figure 5.7: Oil flow rate (L/min) as a function of time during one Tower basin experiment. Both the set point (white) and the obtained values (red) are monitored and logged.

5.4 Description of a Tower basin experiment

A more specific procedure for operating the tower basin is described in operational procedures (Lab. procedure 507). This procedure is a part of SINTEFs general QA system for laboratory procedures.

A short version of the procedure for a blow-out experiment in the tower basin can be summarized like this:

a. Fill tower basin with water and check for leaks.
b. Install and test all release and monitoring equipment.
c. Check background values (particle/oil concentration, droplet size distribution, temperature, and pictures/video).
d. Determine and set test conditions (oil type and rate of gas (air)/oil).
e. Check and confirm status on monitoring and release equipment.
f. Prepare for experiment, background monitoring (three radial positions at approximately 3 meters above release nozzle)
g. Initiate experiment, start release of oil/gas (air)/dispersant (dependent of experiment type)
h. Monitoring of plume (3 x 3 minutes in three radial or horizontal positions)
   - Video cameras (3 to 6 cameras)
   - Oil droplet size distribution (LISST 100X, particle visual microscope (PVM) and macro camera/laser).
   - In-situ UVF monitoring of oil content/dissolved components and water sampling
   - Water temperature
i. Stop release
j. Settling of oil droplets and removal/skimming of surface oil
k. Emptying/disposal of used water containing small oil droplet and dissolved oil components according to lab. procedure
l. Cleaning and control of equipment.
m. Collection and initial quality control of monitoring data.

In general it takes 1-2 days to prepare for a Tower basin experiment, depending on the type of experiment. The experiment itself takes only 1-2 hours. After the experiments are finished, the cameras are recovered and the oil is left to settle overnight. The surface oil is skimmed off and the oily water is rinsed (if necessary, oil content < 50 ppm) by an oil-ware separator. Surface oil is collected and later delivered as hazardous waste, while the oily water is injected into the local sewer system according to SINTEFs discharge permit (low rates and oil concentration). Recovery and pre-treatment of data, cleaning the tank and equipment, rinsing of water and discharge usually takes 1-2 days.

Performing one Tower basin experiment a week has been the normal procedure in the project. From March to the end of May 2012 totally 16 experiments were performed. See Appendix A for an overview of all experiments.

5.4.1 Calibration of oil mass regulators

The following two oil mass regulators (see Figure 5.6) are used in this project.

Table 5.2 Mass regulators used in the project

Type	Range (L/min)	Period (experiments)
Digimesa FHK	0,1-5 l/min	March-April 2012 (Exp. 1 - 3)
Burkert S020 D8	0,8-30 l/min	April-June 2012 (Exp. 4 - 16)

The calibration data for the different regulators are presented in Chapter 6.2.4. Experiment numbers can be found in Appendix A.

5.5 Monitoring during an experiment

This chapter contains the description of the different monitoring techniques used during the blow-out simulation experiments. The monitoring was performed in the centre of the plume approximately 3 metres above the release point to ensure sufficient dilution of the oil & gas (air) plume. A suit of instrumentation was mounted on a piston operated platform which is inserted into the plume. The platform was mounted on a slide on the inner wall of the basin and its vertical position could be continuously changed.

Since documentation of oil droplet size distribution is central in this project, three different approaches are used to measure droplet size distribution of the rising oil droplets. The presence of a wide range of gas (air) bubbles in the plume complicates the measurements of the oil droplet.

a. The LISST-100X instrument is a laser difractometer for in-situ observations of particle size distribution and volume concentration. It also records the optical transmission, pressure and temperature. The instrument used in this project is a shorter version more suitable for laboratory work in confined areas.
b. Particle visual microscope (PVM)
c. High resolution camera and two green lasers defining a focal plane.

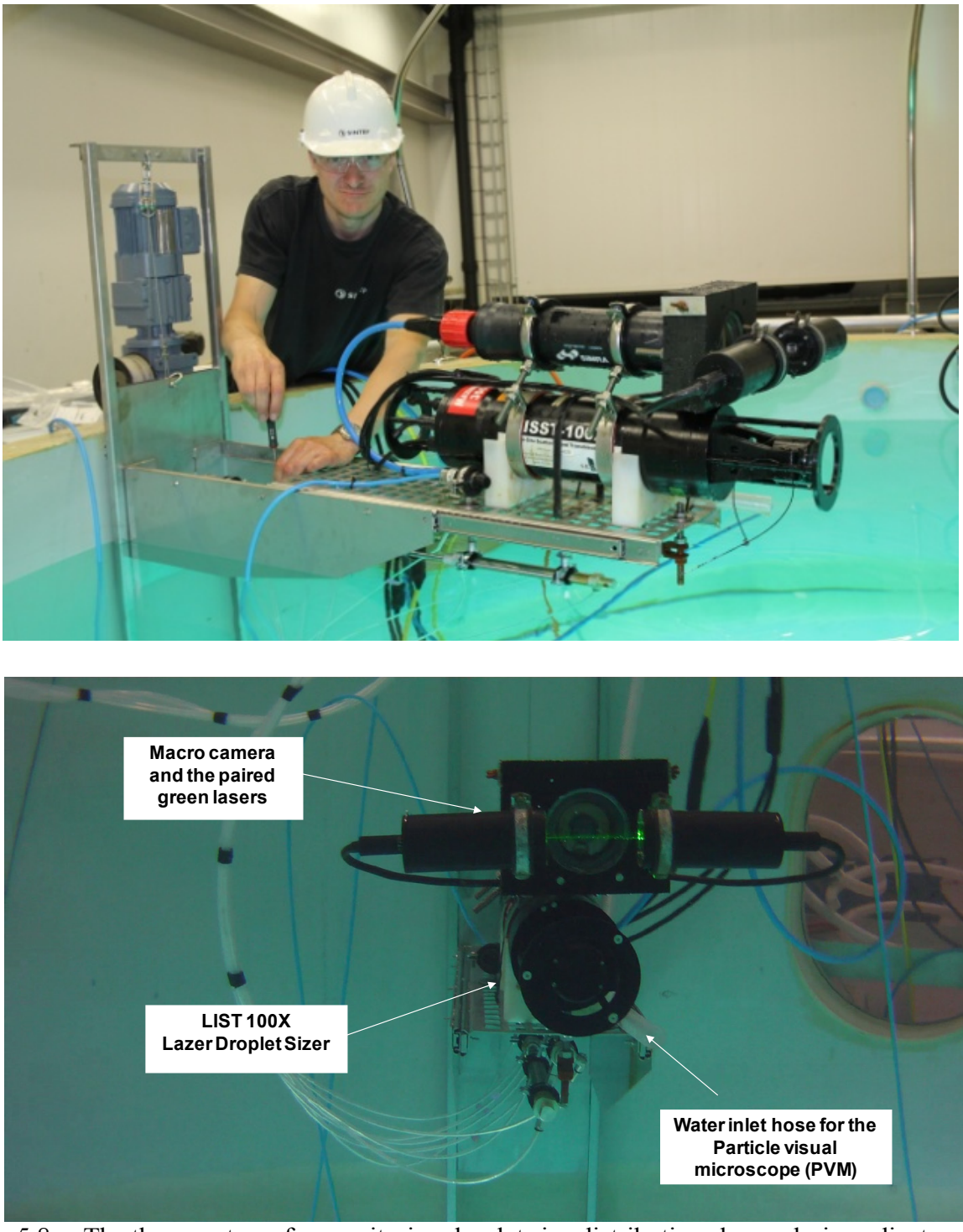

Figure 5.8: The three systems for monitoring droplet size distribution shown during adjustment over the water surface and submerged.

5.5.1 In-situ macro camera

Specifications of the 5-megapixel Sony macro camera (GC2450) are given below:

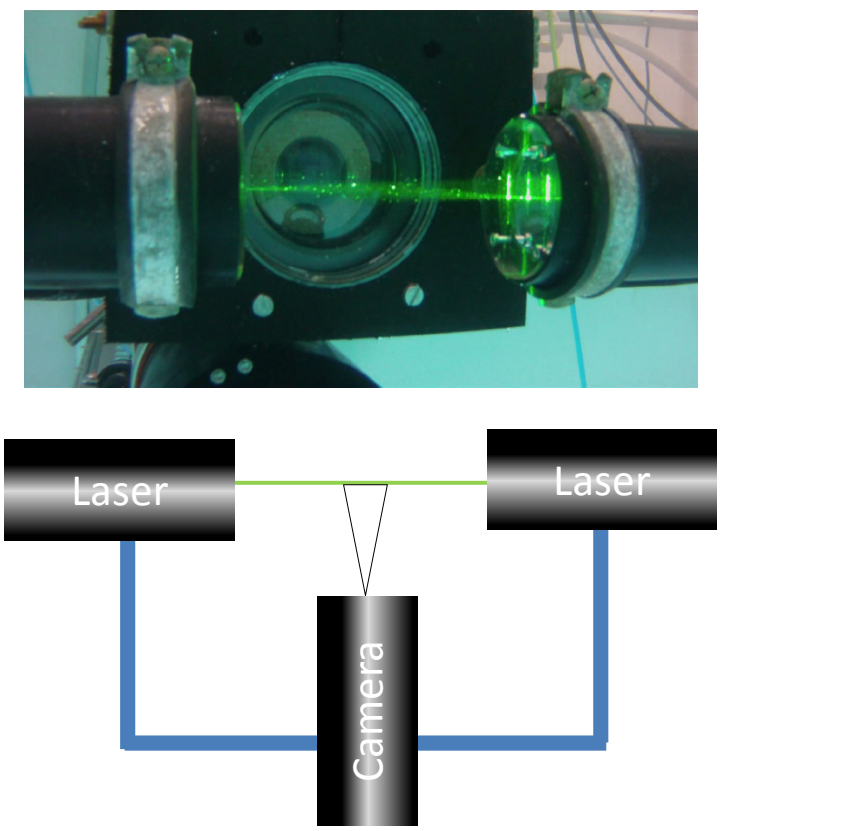

Figure 5.9: Close-up photo, a principle drawing of the macro camera and the green laser focusing plane and a picture of the camera module.

The built-in camera has the following specifications:

- Ultra-compact high resolution CCD camera - 5 Megapixels, 15 fps
- The 5-megapixel GC2450 is a very high-resolution CCD camera with Gigabit Ethernet output (GigE Vision®). The GC2450 has a frame rate of 15 fps at 2448x2050 resolution.
- The sensor used in the GC2450 is the high-quality Sony ICX625 CCD image sensor that provides high image quality, high sensitivity, and low noise.
- 5 Megapixels (2448x2050)
- Models used: GC2450, 2448x2050, 15 fps, CCD, mono

5.5.2 External Particle Visual Microscope – PVM V819

The PVM is a miniature version of the in-situ macro camera and is mounted as a probe in a water stream coming out of the tower basin. The water is not pumped, but flows out due to the ambient pressure at 3 meter depth in the Tower basin.

Figure 5.10: Illustration of the PVM probe and image analyser.

The Particle Visual Microscope has the following specifications:

- Illuminations Class 1M laser product
- Sources: 6 pulsed laser diodes
- Wavelength: 808nm
- Energy: 39µJ (at window), 6.5µJ (3mm beyond window)
- Imaging Field of view (nominal): 1075mm x 825mm
- Resolution: 2 µm
- Focus Adjustment: Manual
- Pressure Standard: Vacuum to 150psi (10bar)
- Probe Head Length: 163mm
- Diameter: 69mm

5.5.3 Light scattering sensor – LISST 100X

This method determines size distribution of an ensemble of particles, as opposed to counting type devices that size one particle at a time. The reason that laser diffraction is unaffected by composition of particles is that the scattering of laser light is observed at multiple, small forward angles. At these small angles, light scattering is determined almost entirely by light diffracted by the particle. The light transmitted through the particle makes only a weak contribution to the measured scattering. Since the light transmitted through the particle would experience the composition of the particle, i.e. its refractive index, and since it makes only a weak contribution to the observed scattering, the method of laser diffraction is mostly independent of particle composition. In the aquatic sciences, particle refractive index is poorly known. Thus, except for shape effects, laser diffraction offers an excellent method for size-distribution estimation. Shape effects are a matter of continuing research and no definite generalized guidelines are available to account for them by any method. Consequently, laser diffraction methods deliver the equivalent-spheres size distribution. By

calibrating for concentration with ISO standard natural particles, shape effects are empirically included.

The instrument is calibrated, both with a flow through cell and in the tower tank with a mono-disperse particle standard containing particles over a range of 6 – 346 microns.

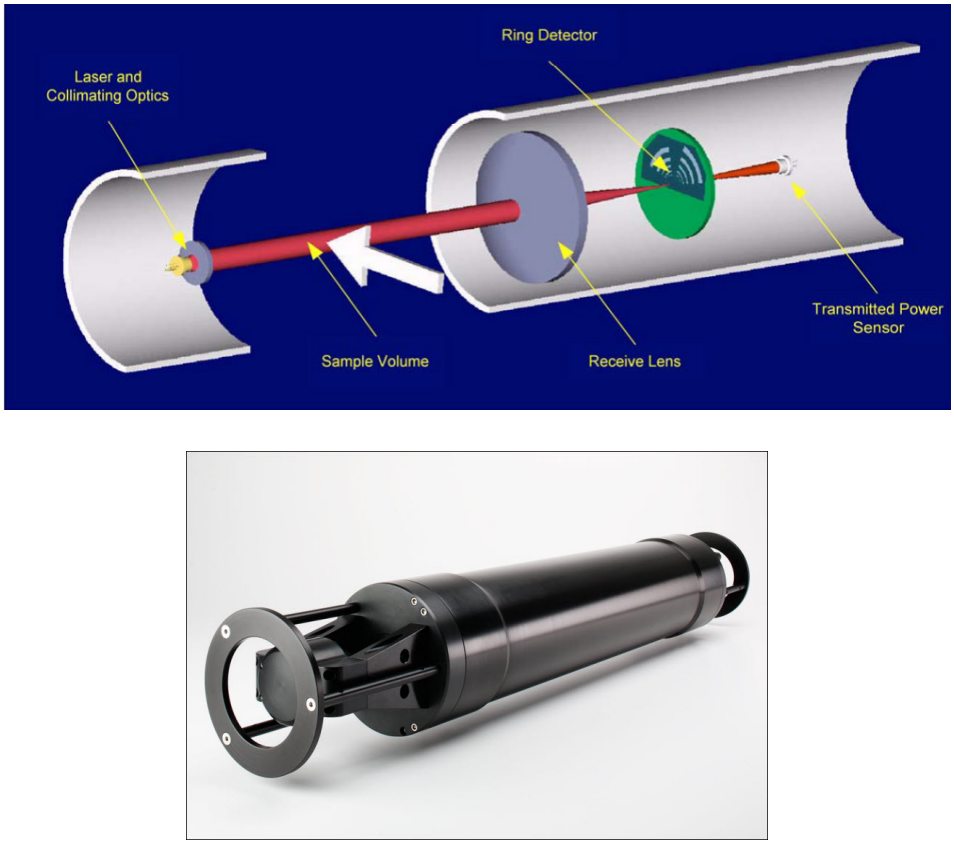

Figure 5.11: Principle drawing and close-up of the LISST

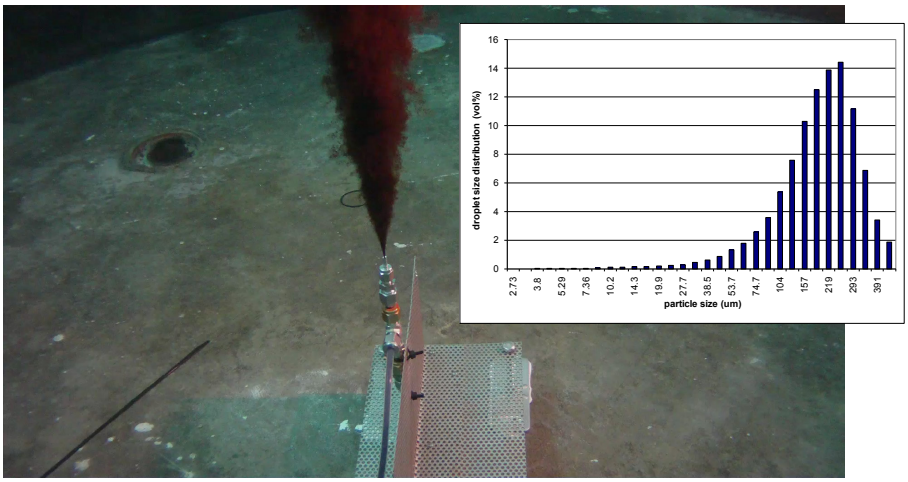

Figure 5.12: Initial release of model oil and an example of measured droplet size distribution (LIST 100X system).

5.5.4 Image analysis to produce droplet size distributions

The images from the in-situ macro camera or the Particle Visual Microscope are via image analysis, particle identification and diameter identification used to produce a droplet size distribution, see Figure 5.13. This process is performed with a program utilizing the Visual Basic procedures in LabView.

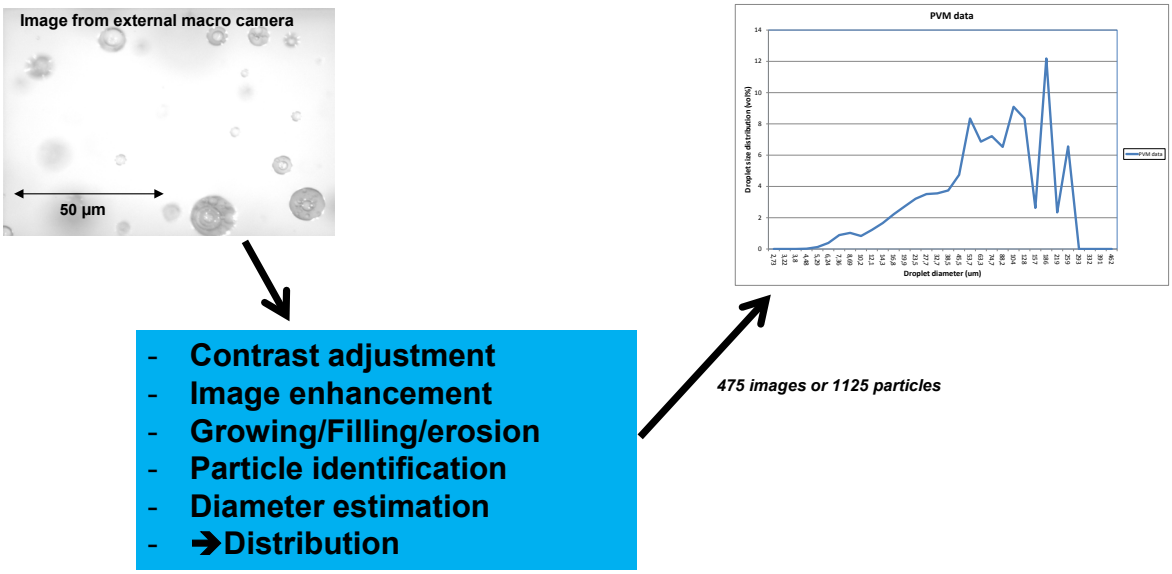

Figure 5.13: Principles for the image analysis producing a droplet size distribution from the in-situ macro camera or the particle Visual microscope.

5.5.5 Calibration of droplet size measurement

The LISST instrumentation was calibrated in a container with natural sea water (900 Litres). Different standards of polyethylene mono disperse with different size (6 – 346 microns) were injected into the experimental container used for the verification.

Commercial standard material in the size range of interest is not available. The needed standards were for this reason synthesised by SINTEFs Materials and Chemistry, Department of Synthesis and Properties, Research team: Polymer Particles and Surface Chemistry.

Table 5.3: Mono disperse standards used in LISST verification

STD ID	STD micron	STD Volume	STD Conc. weight%	mL added	ppm (900L)	Relative conc. weight%
1A	6	1000	1	240	2.7	0.5
2B	20	1000	2	240	5.3	1.0
3	38	1000	1	1000	11.1	2.0
4B	80	1000	4	1000	44.4	7.9
6	165	1000	42	120	56.0	10.0
8	346	2000	37.5	130	27.1	4.8

The corresponding droplet size distribution was recorded by the LISST instruments (see Figure 6.3).

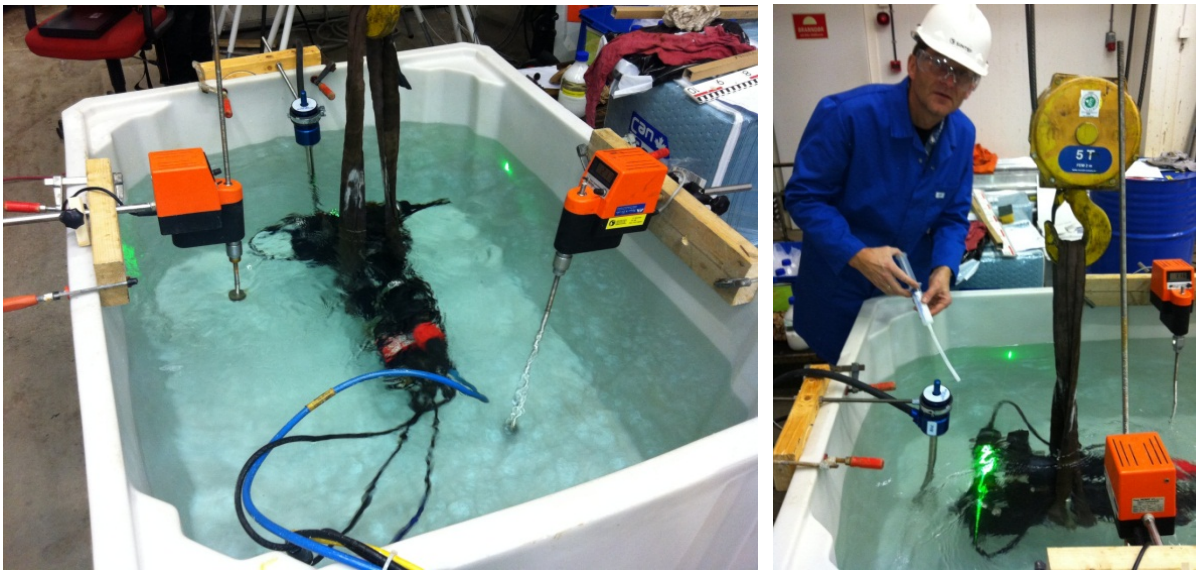

Figure 5.14: Verification of the LISST instrument in a 900 Litre container injecting batches of mono disperse particles.

A particle standard is also injected in front of the LISST instrument before a Tower basin experiment was initiated as a part of the general quality assurance procedure.

5.5.6 Water sampling

Water samples were taken in the same position in the tank as droplets sizes are measured. The water was sampled through a short flexible hose located on the moving sampling platform. The water samples were analyzed for oil content by solvent extraction (dichloromethane) and UV adsorption spectroscopy. See SINTEF laboratory procedures for further details.

5.5.7 In-situ measurement of oil in water (UVF cell)

The overflow hose (no pumping) used for water sampling above was also used for monitoring of oil-in-water content (droplets and dissolved components). This was done by ultraviolet fluorescence (UVF) with an UviLux flow-through cell. The water flows through this cell before being sampled. The set up used to calibrate the UVF instrument involved pumping a solution with a known concentration of dispersed oil through the cell as shown in Figure 5.15.

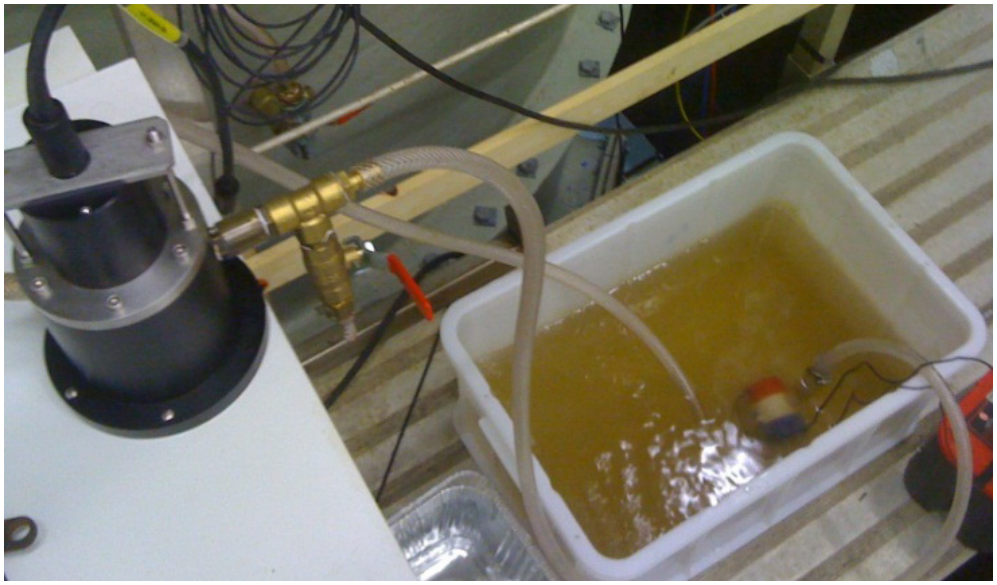

Figure 5.15: Calibration of the UVF cell (UviLux) by circulating solutions with known oil concentrations.

5.5.8 Oil sampling

Oil sampling was performed from two different locations. One is located together with the LISST and in-situ camera and used for water sampling. The other is located 1.5 meter above the nozzle and is used for more concentrated oil samples (more oil, less water). The oil that was sampled from this location was used for interfacial tension analysis (when dispersants are applied).

5.5.9 Video documentation

Three to nine HD video cameras (1280 x 960 pixels) were used to document the conditions during a Tower basin experiment. The cameras were mounted to monitor the following locations:

a. Conditions around the release nozzle (dispersant injection into the oil/gas(air)/water stream)
b. Nature of the rising plume
c. Downward looking camera from the top section of the tank giving an overview of the experiment

5.6 Interfacial tension measurements

Crude oil - sea water interfacial tension (IFT) plays a key role in the process of oil droplet formation during oil spills. Addition of dispersants reduces the interfacial tension between oil and sea water (brine) that subsequently promotes the formation of a larger number of small oil droplets when surface waves entrain oil into the water column. The effectiveness of chemical dispersion is known to depend on the specific combination of oil type, dispersant composition, dispersant concentration (dispersant-to-oil ratio), and the environmental conditions (temperature, waves, pressure etc) under which dispersion occurs. Depending on different dispersant to oil ratios and types of crude oils, the IFT between oil/brine/dispersant interfaces ranges from 28.5mN/m to an ultra-low value of 0.0002 mN/m (Khelifa and So., 2011).

Numerous methodologies have been developed for the measurements of interfacial tensions. But all different approaches have certain limitations. Oil/water IFT measurements are generally based on

drop methods e.g. spinning drop and pendant drop (Miller et al., 2001). These methods can also be used to measure oil/water IFT when dispersants are used. At ambient conditions, relatively high values of IFT (> 1mN/m) are traditionally being measured by using a pendant drop technique and ultra-low values (< 0.1mN/m) are measured with a spinning drop method (Zhang et al., 2001). We used the spinning drop method for the IFT measurements of oil/water/dispersant system in this project.

5.6.1 Spinning drop method

In the spinning drop method [SDM], two immiscible fluids are placed in a capillary tube, which is rotated, as shown in Figure 5.16. Fluid A (oil droplet) is the less dense fluid, while fluid B (sea-water) is the more dense fluid. The centrifugal field generated by rotation forces keeps the less dense fluid in the centre of the capillary tube where it forms an elongated drop. The configuration of the drop is determined by the balance of the centrifugal force and interfacial tension force. The centrifugal force elongates the drop, while the IFT suppresses this elongation to minimize the interfacial area. In the pendant drop method, gravity forces are applied for drop deformation, while SDM employs centrifugal forces (Liu, 2007). Determination of interfacial tension is related only to the diameter and does not require measurement of the drop volume.

This method is perfectly suitable for measurement of ultra-low tensions and the measurable values of IFT may range from 0.0005 to 0.5 mN/m (Zhang et al., 2001). Oil/sea-water/surfactant interfaces for ultra-low IFTs values are commonly measured by spinning drop technique (Khelifa and So., 2011), (Liu, 2007), (Zhu et al., 2008) and (Standness and Austad., 2000).

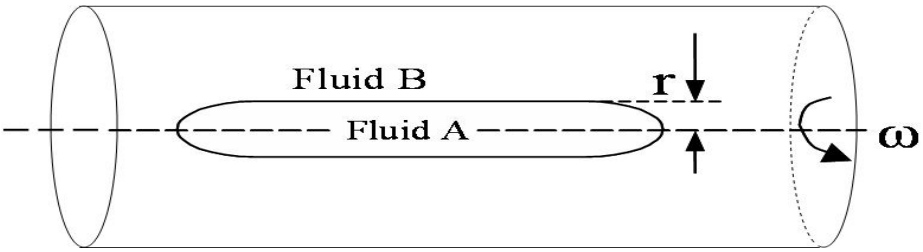

Figure 5.16: Schematic of the spinning drop method

For the interfacial tension measurements by spinning drop method, the Dataphysics Spinning Drop Tensiometer SVT-20N with control and calculation software SVTS 20 IFT was used (Figure 5.16). The Julabo F12-ED Refrigerated and Heating Circulator was used for temperature control. Disposable 1ml plastic syringes were used to inject the oil sample into the SVT 20N capillary tube.

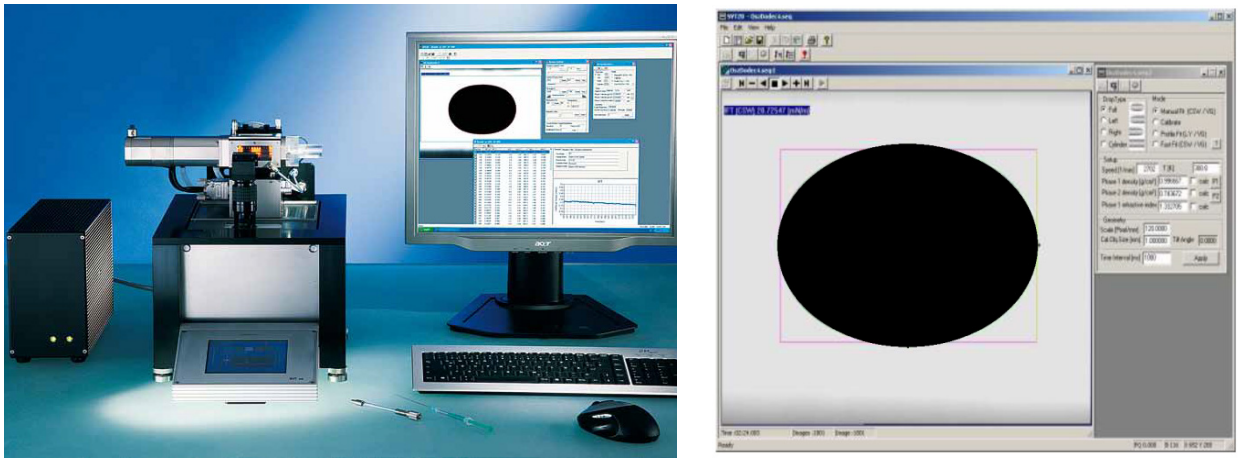

Figure 5.17: The Dataphysics Spinning Drop Tensiometer SVT-20N and its software used to measure small interfacial tension values of oil/water/dispersant interfaces.

Prior to each measurement, the capillary tube was rinsed three times with dichloromethane (DCM), acetone and deionized water, dried with nitrogen gas, and then rinsed three times with the sea-water. The capillary was carefully filled with the sea-water (outer phase liquid) to ensure the absence of air bubbles (Figure 5.18A). After the filling of capillary with sea-water, the open side of the capillary (Figure 5.18B) was closed and inserted into the measuring cell.

Figure 5.18 A-B: Filling of capillary with the sea-water (outer-phase) and closed capillary with septa holder

After closing the quick lock on the motor mounted the plastic protection cover on the measuring cell. The injection of a drop of the oil sample (inner phase) into the filled capillary was done by use of the 1 ml syringe with a long needle. Depending on the oil sample, the capillary may be stationary or rotating when the drop of oil is injected and the rotation speed may also vary. Measurements of IFT were taken as soon as the drop elongation was stable. Depending on the interfacial tension, different oil samples have different volumes of droplet. Parent oil and their mixture with low DOR formed relatively big droplets while oil with high DOR formed very small droplets, Figure 5.19A, B, C and D. Each measurement was run for 30-60 minutes and repeated at least two times. The reported IFT values were the mean IFT of different droplets measured during first 50-150 seconds.

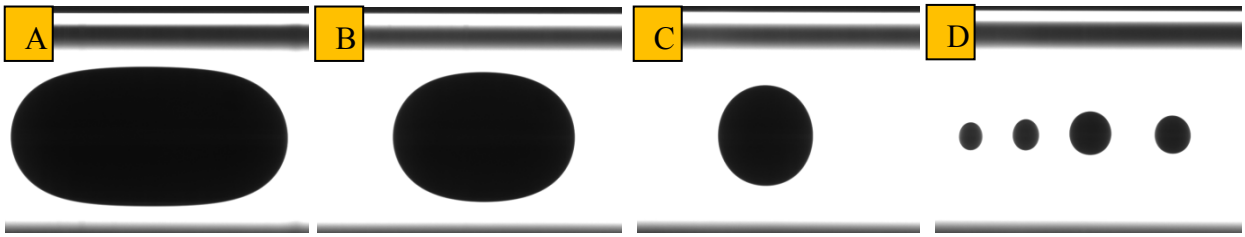

Figure 5.19: Oil droplets with different DOR; A) Oil alone, B) DOR: 1:500, C) 1:250, D) 1:50

5.6.2 Oil sampling for IFT measurements

During different injection sequences of dispersants into the oil, oil/water samples were taken 1.5 meters above the nozzle after 60 seconds of each dispersant injection. Each oil/water sample was collected in a 1 litre, long-necked measuring flask. Oil appeared as droplets depending on the DOR and method of application. Oil settled as a layer in the narrow neck of the bottle and was collected for IFT measurements after 24 hours. The settling time was important for collecting the smaller droplets in experiments with high dispersant effectiveness. The collected oil samples were stored in a dry and cool place overnight. No homogenization or heating was done before the IFT measurements.

6 Results

6.1 Overview of experiments

The Tower Basin experiments reported from this study were performed from March to June 2012. Totally, 16 experiments were performed in this period. Each experiment usually takes a week, consisting of two days of preparation, one day for performing the experiment and another two days for cleaning and post processing of data. A summary overview of the experiments is given in Appendix A. The experiments were divided into the following groups or phases.

1. **Initial experiments** (Experiments 1, 2 and 15): Initial testing to document calibration of monitoring equipment and find suitable conditions (nozzle size and flow rate) for the later experiments. Experiments with oil:air and water:air.
2. **Flow rate experiments** (Experiments 5-7 and 14): Droplet sizes as a function of three flow rates and three nozzle sizes (0.5, 1.5, and 3 mm). Experiments marked with red circles in Figure 6.1.
3. **DOR testing** (Experiments 3, 11 and 16): Droplet sizes as a function Dispersant to oil ratio (1:1000-1:25) and interfacial tension. Experiments with premixed dispersant (Corexit 9500). Blue experiments and, to some degree, blue centre point in Figure 6.1.
4. **Dispersant injection techniques** (Experiments 5, 10, 12 and 13): Droplet sizes as a function of different dispersant injection techniques (simulated insertion tool, wand and injection into the oil jet). Blue centre point in Figure 6.1.
5. **Testing with warm oil** (Experiment 13): Experiment with cold/warm oil and different DORs. Heater used to raise temperature of the oil before injection. (Experiments 22, 23, 27).
6. **Testing with an alternative dispersant** (Experiment 16): Testing with Corexit 9500A with reduced solvent content at different DORs (centre point in Figure 6.1).

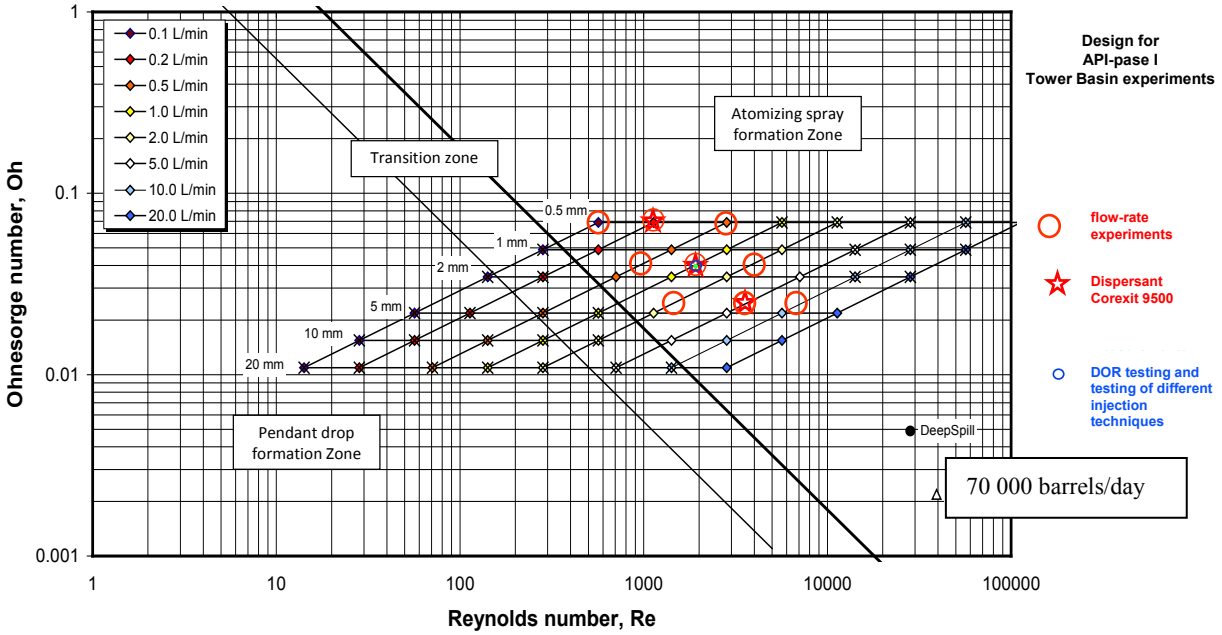

Figure 6.1: The different types of Tower basin experiments performed in the second part of this project plotted in the Ohnesorge vs. Reynolds number diagram (see Figure 4.3 for details).

The background or basic theory for the initial experiments (rate and turbulence levels) is based on earlier tank experiments in smaller scale described in Chapter 4 Droplet formation in turbulent flow (see Figure 4.3). This figure presents the release conditions based on Ohnesorge vs. Reynolds number and has been used in this study to find a suitable starting point for the initial testing and to determine the total design of this study. The solid lines drawn in an Ohnesorge vs. Reynolds number in Figure 4.3 indicates the different droplet formation regimes for oil jets in water (without air/gas). Three different zones are indicated; Pendant drop, Atomizing and a transition zone. The experiments in this project were all performed in the Atomization regime in Figure 4.3.

6.2 Initial experiments

The main objectives with the initial experiments were to test and verify the main components of the tower basin (release and monitoring equipment). These experiments were also needed to see how often it was needed to change the water and to determine the time/resources needed for each experiment.

6.2.1 Ultra Violet Fluorescence sensor

The initial experiments were used to test and verify the sensors used to quantify the oil concentrations in the oil/gas (air) plume during a tower tank experiment. Water samples were taken 3 meters above the release in the same position as the LISST and were directed through the UVF cell.

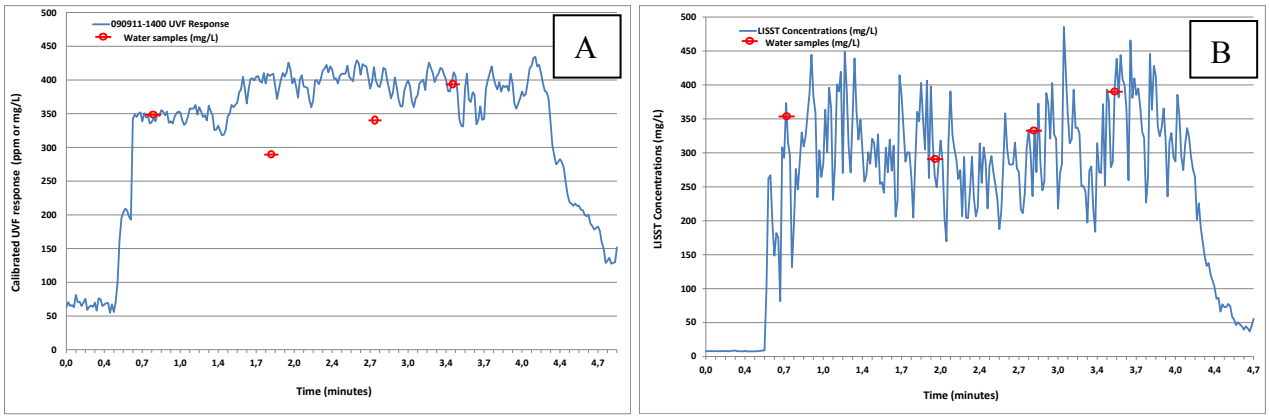

Figure 6.2: Comparison of measured oil concentration (red circles – quantified from water samples) with oil concentrations measured in-situ with UVF cell (A) and LISST (B). Vertical axes are measured oil concentration (ppm) and horizontal axes are time (minutes).

Results from the initial experiments, see example in Figure 6.2, showed that the measured oil concentration from the LISST (B) correlated better with the measured values from the water samples than the UVF sensor (A). This was as expected since the concentrations were high (50-350 ppm) and there was a variation in droplet sizes, which influences the UVF sensor.

The high oil concentrations are also above the linear response range for the UVF cell, indicating that a more thorough calibration of the UVF cell would be useful. The wide range of droplet sizes during the Tower basin experiments is also a challenge for the UVF cell. Fluorescence is a surface phenomenon and the difference in total surface is strongly dependant of droplet sizes. A shift from

230 µm to 70 µm gives a very large increase in surface area and a large increase in response from the UVF cell even if the concentration is constant. The oil concentrations from the LISST are calculated from the measured concentration of droplets in the different size groups or bins. This gives concentration readings from the LISST that are not biased in relation to droplet sizes. This is also seen in Figure 6.2 (right). However, oil concentrations in the rising oil and gas (air) plume is not a critical parameter to fulfil the objectives of this project since they can be calculated from the release rates and dilution factors.

6.2.2 Verification of droplet size measurements

The droplet size measurements from the LISST instrument were verified with a mixture of polystyrene particle standards (6, 20, 38, 80, 165 and 346 µm). Comparison of the LISST measurements and the calculated distribution of the standard mixture are shown in Figure 6.3, see chapter 5.5.5 Calibration of droplet size measurement for details.

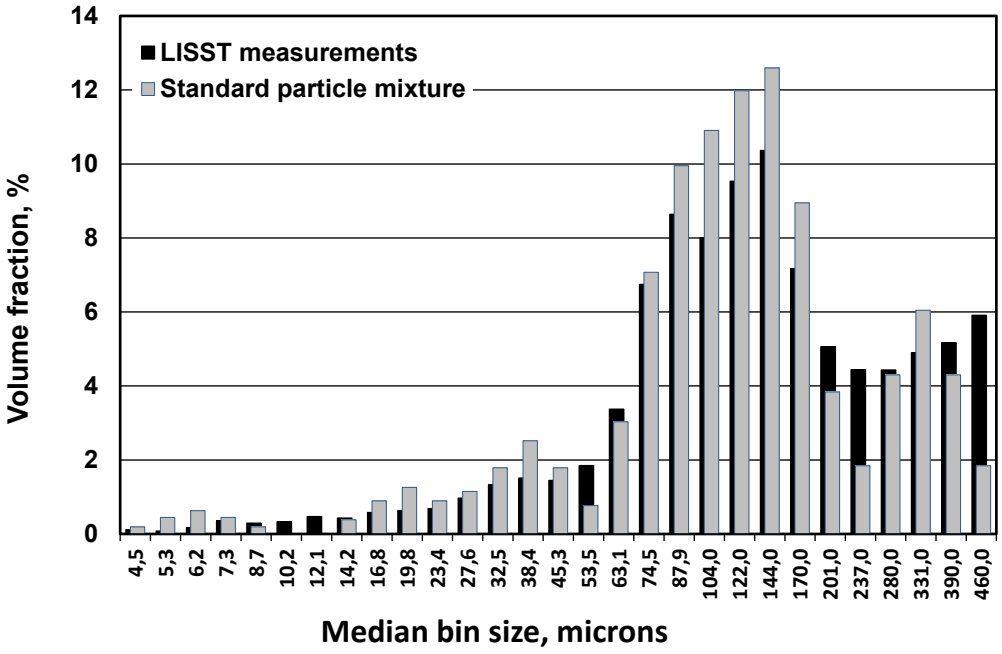

Figure 6.3: Droplet size distributions from the calibration experiments with the LISST instrument comparing measured and real distribution of the standard particle mixture.

A particle standard (80 and 346 micron) was also injected in front of the LISST instrument before Tower basin experiments were initiated as a part of the general quality assurance procedure.

6.2.3 Quantification of droplet sizes by image analysis

The data obtained from the two image based techniques (In-situ macro camera and the external PVM) contained very limited information regarding sizes of the large droplets in most experiments. This is probably due to the small focusing area of these macro methods (mm range) combined with the short time for data acquisition (usually 30 seconds). During this period a very limited number of large droplets were captured and quantified on the images.

Due to this limitation the images were only analysed and used for the large nozzle experiments (3 mm) and low flow rates (5 and 8 L/min). In these experiments the maximum peak of the distributions were not visually identified in the 2-500 micron range obtained by the LISST.

6.2.4 Verification of mass flow regulators

The mass flow regulators used in this study have been calibrated and the results are shown in the table below.

Table 6.1: Mass flow regulator verification

Type	Low		Medium		High	
	Setting	Measured	Setting	Measured	Setting	Measured
Digimesa FHK	0.10	0.12	1.5	1.49	3.0	2.96
Burkert S020 D8			1.5	1.20	2.5	2.50

6.2.5 Reproducibility within and between experiments

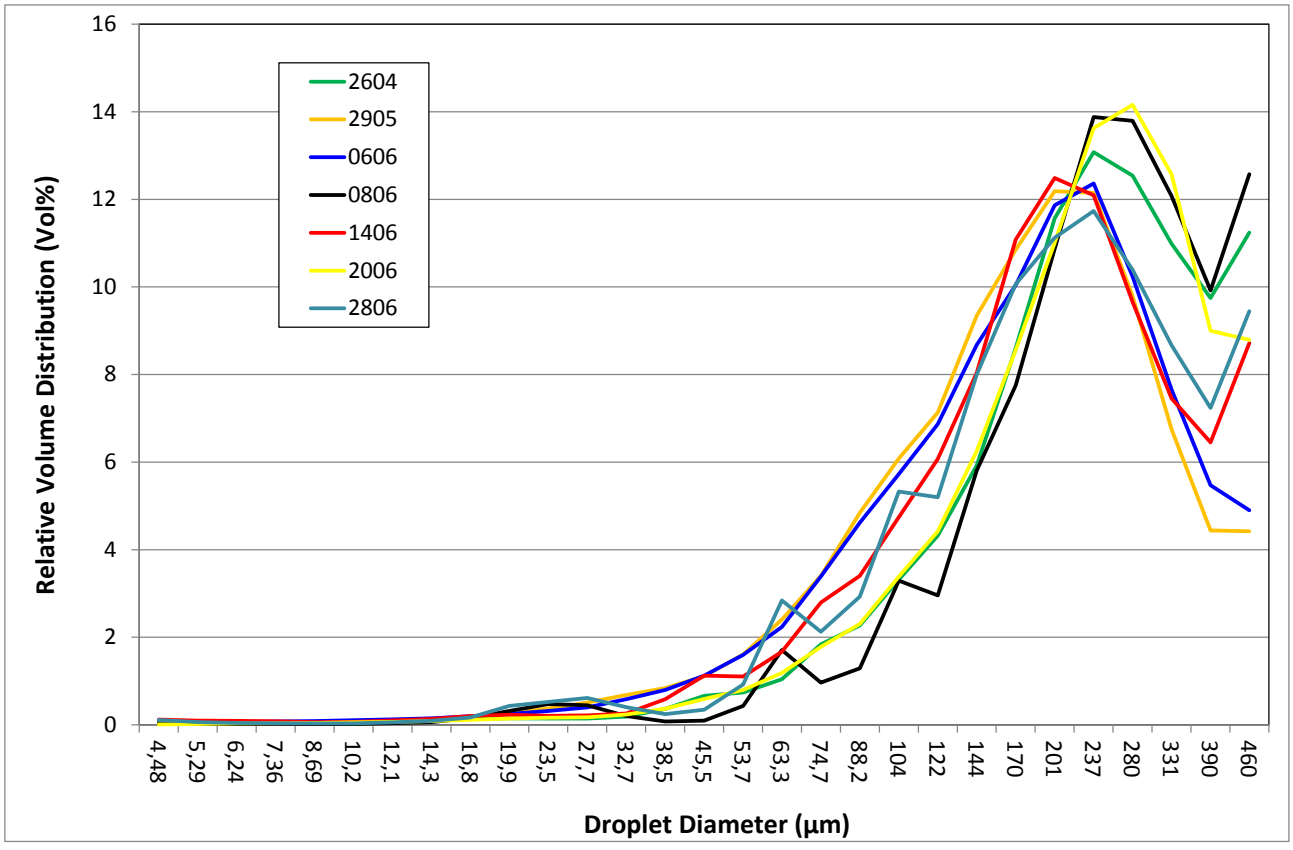

Figure 6.4: Variation in Tower basin experiments between experiments (April – June 2012). Relative droplet size distribution (volume %) for 7 individual experiments with the same experimental conditions (1.5 mm nozzle and 1.5 L/min) measured with LISST instrumentation in SINTEF Tower Basin.

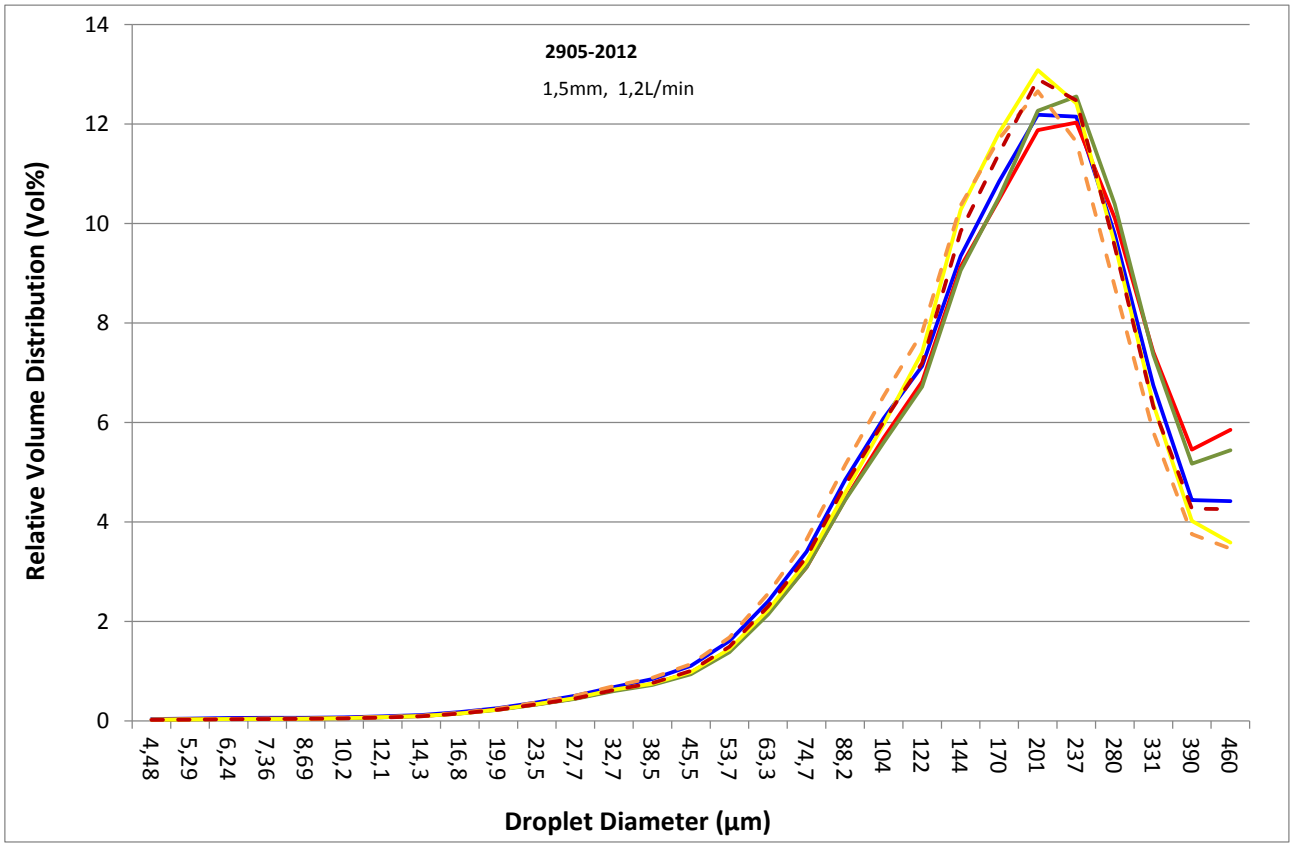

Figure 6.5: Variation within one Tower basin experiment (29. May 2012). Relative droplet size distribution (volume %) for 6 different experimental periods (90 seconds) within one Tower basin experiment with the same experimental conditions (1.5 mm nozzle and 1.2 L/min) measured with LISST instrumentation in SINTEF Tower Basin.

6.3 Flow rate experiments

The data generated in this activity are used to verify and further develop the algorithms used to estimate droplet size distributions as a function of flow rate, nozzle size and oil type (Weber number estimation or scaling), see chapter 4.2 Weber number scaling for details.The following table describes the main part of the experimental work.

Table 6.2: Experimental conditions for the flow rate experiments

Nozzle diameter:	0.5, 1.5 and 3 mm
Flow rates:	0,1 - 8 L/min
Gas-oil-ratio:	Only oil

These experiments (3 nozzle sizes and 3 flow rates for each nozzle) were performed with oil alone with no gas (air) present. The main reason for this approach was that the instrumentation for measuring oil droplet sizes cannot distinguish between oil droplet and gas bubbles. However, some initial experiments were performed with oil and gas (air) and injection of dispersants.

The results from the three nozzles 0.5, 1.5 and 3 mm are presented in Figure 6.6 and Table 6.3. The figure presents the relative volume distributions and the median bin size for each bin is used on the logarithmic x-axes.

Since the LISST is detecting noise or "non-oil" particles in the water in the three smallest bins (2,7, 3,2 and 3,8 microns), these bins are excluded from the relative distributions. Including this noise would introduce a systematic shift in the calibrating data set towards smaller volume median droplet sizes (VMD).

The histograms from the droplet size distributions in this study are presented as graphs in this report. This is not strictly correct since the data are discrete and not continuous. However, graphs were used since projecting several histograms on top of each other is visually difficult to interpret.

The graphs presenting the droplets size distributions are usually averages of 30 individual LISST measurements measured over 30 seconds. For the smallest droplets each bin represents thousands of droplets, while for the largest droplets each bin usually represents an average of 5-20 droplets.

The volume median droplet sizes (VMD) were calculated from both the relative volume distributions (maximum peak) and the cumulative distributions (50% volume). If the assumption that the data can be approximated with a log normal distribution is valid, the difference between these two measures of VMD should be very small. However, for some of the distributions, especially with high VMDs e.g. with the 3 mm nozzle in Figure 6.6, the complete distribution is NOT covered by the distribution. For these distributions the cumulative VMD will be underestimated.

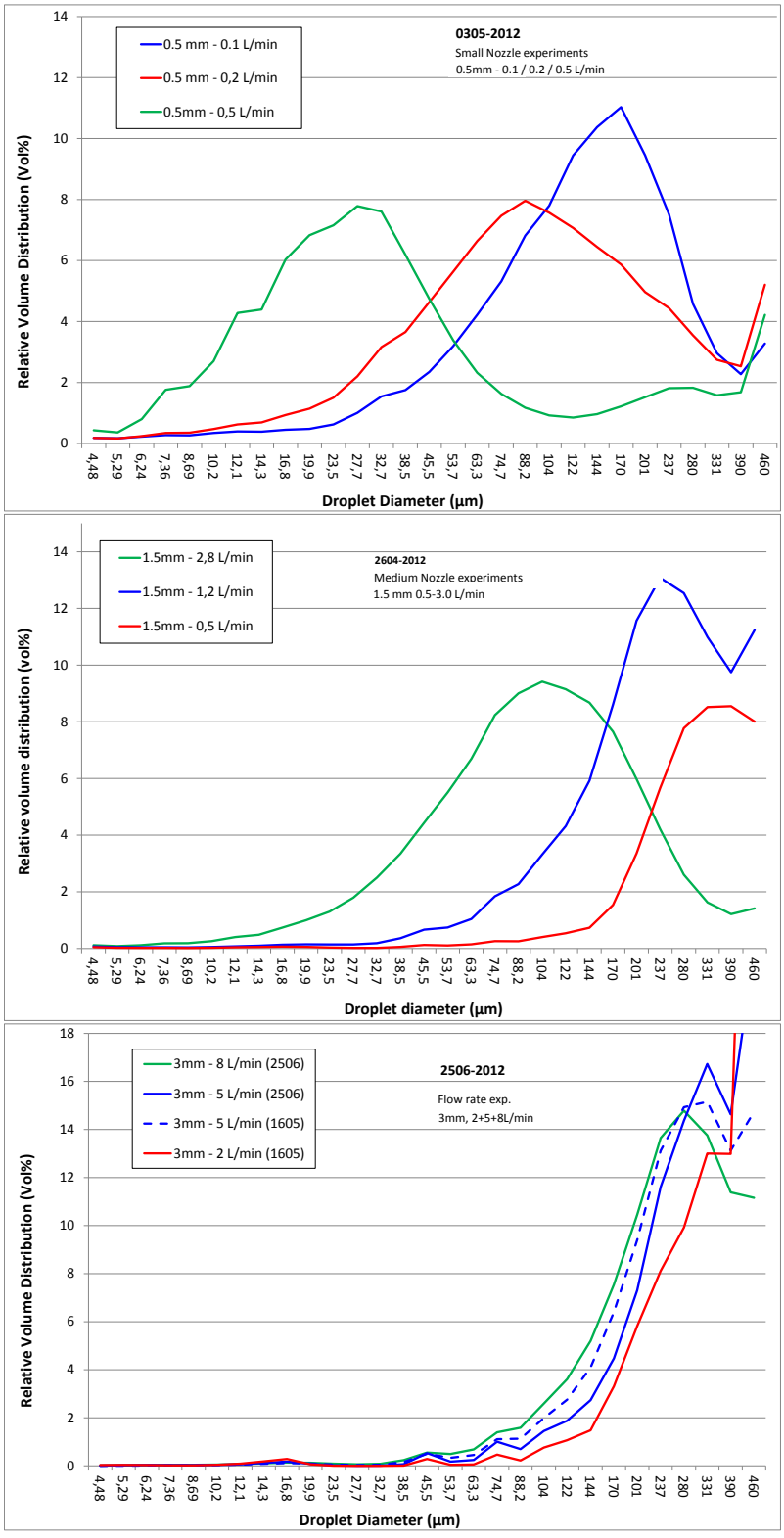

Figure 6.6: Relative droplet size distribution (volume %) as a function of nozzle size (0.5, 1.5 and 3 mm) and flow rate (0.1 – 8 L/min) for the Oseberg oil measured with LISST instrumentation in the SINTEF Tower Basin.

Table 6.3: VMD as a function of nozzle size (0.5, 1.5 and 3 mm) and flow rate (0.1 – 8 L/min) for the Oseberg oil measured with LISST instrumentation in the SINTEF Tower Basin.

Based on maximum peak

0.5 mm		**1.5 mm**		**3 mm**	
Flow rate (L/min)	VMD (µm)	Flow rate (L/min)	VMD (µm)	Flow rate (L/min)	VMD (µm)
0.1	186	0.5	391	2	460*
0.2	88.2	1.2	259	5	332
0.5	27.7	2.8	104	8	293

Based on cumulative distribution (50% volume)

0.5 mm		**1.5 mm**		**3 mm**	
Flow rate (L/min)	VMD (µm)	Flow rate (L/min)	VMD (µm)	Flow rate (L/min)	VMD (µm)
0.1	134	0.5	301	2	450*
0.2	90.7	1.2	243	5	299
0.5	27.5	2.8	93	8	262

* Based on analysis of PVM images

Experiments with oil & gas (air) for one selected nozzle size and flow rates (three experiments) were performed to validate our assumption that "oil alone" experiments could be used to generate data also valid for oil & gas (air) experiments, see Figure 6.24 and Figure 6.25.

6.4 Dispersant-to-oil-ratio (DOR) testing

To be able to evaluate the effectiveness of the different injection techniques, it is important to know the reduction in interfacial tension (IFT) and the resulting effect on droplet size distribution at different DORs. Experiments were performed in the SINTEF Tower basin with premixed dispersants to reduce uncertainty due to the injection methods. The dispersant was injected into the oil stream 3 meters (or 2000 release diameters) before the nozzle (see Figure 5.6). The dispersant is injected into the oil stream via Teflon tubing with an inner diameter of 4 mm. With an oil flow rate of 1,2-1,5 L/min, the residence time of the oil/dispersant blend from the injection point to the nozzle is in the range of 1,5 to 1,9 seconds. The intention was that this would ensure sufficient mixing of the oil/dispersant before oil was released through the nozzle (premixed).

Ideally the dispersant should have been blended into the oil in the pressure tank before injection, but this would demand thorough cleaning between experiments and probably introduce other uncertainties. However, this "premixed mode" could also be regarded as a "deep down-hole or upstream injection".

Table 6.4: Experimental conditions for the DOR experiments

Nozzle diameter:	One – 1,5 mm
Flow rate:	two – 1,2 and 1,5 L/min
Gas-oil-ratio:	Oil alone
Number of replicate experiments:	None
Dispersant application technique:	Upstream injection (Premixed)
Dispersant:	two - Corexit 9500A and a version of C9500A reduced solvent content
Oil type:	Oseberg
DORs	1:25, 50, 100, 250, 500 and 1000

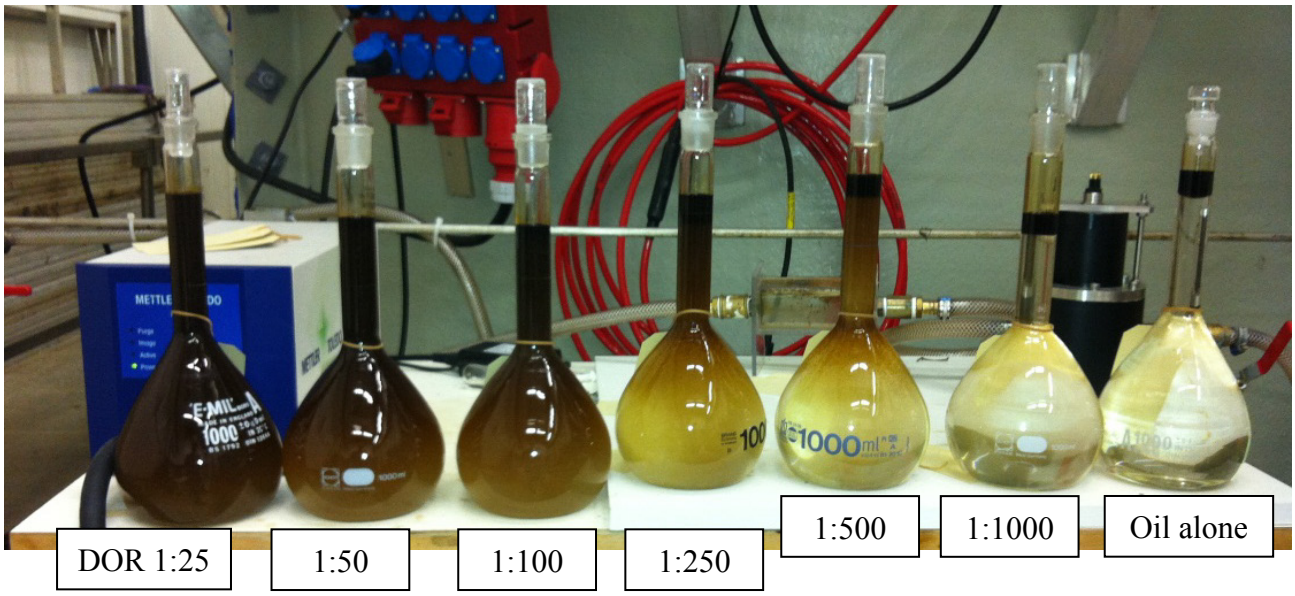

Figure 6.7: Samples of oil and water taken from the Tower basin for IFT measurements on 8. June 2012. The picture is taken after approximate 15 minutes of settling. The large droplets have already risen and formed a surface layer in the neck of the bottles. The colour of the samples reflects the concentration and droplet sizes of the remaining dispersed oil. Dispersant used is C9500. The labels represent the DORs.

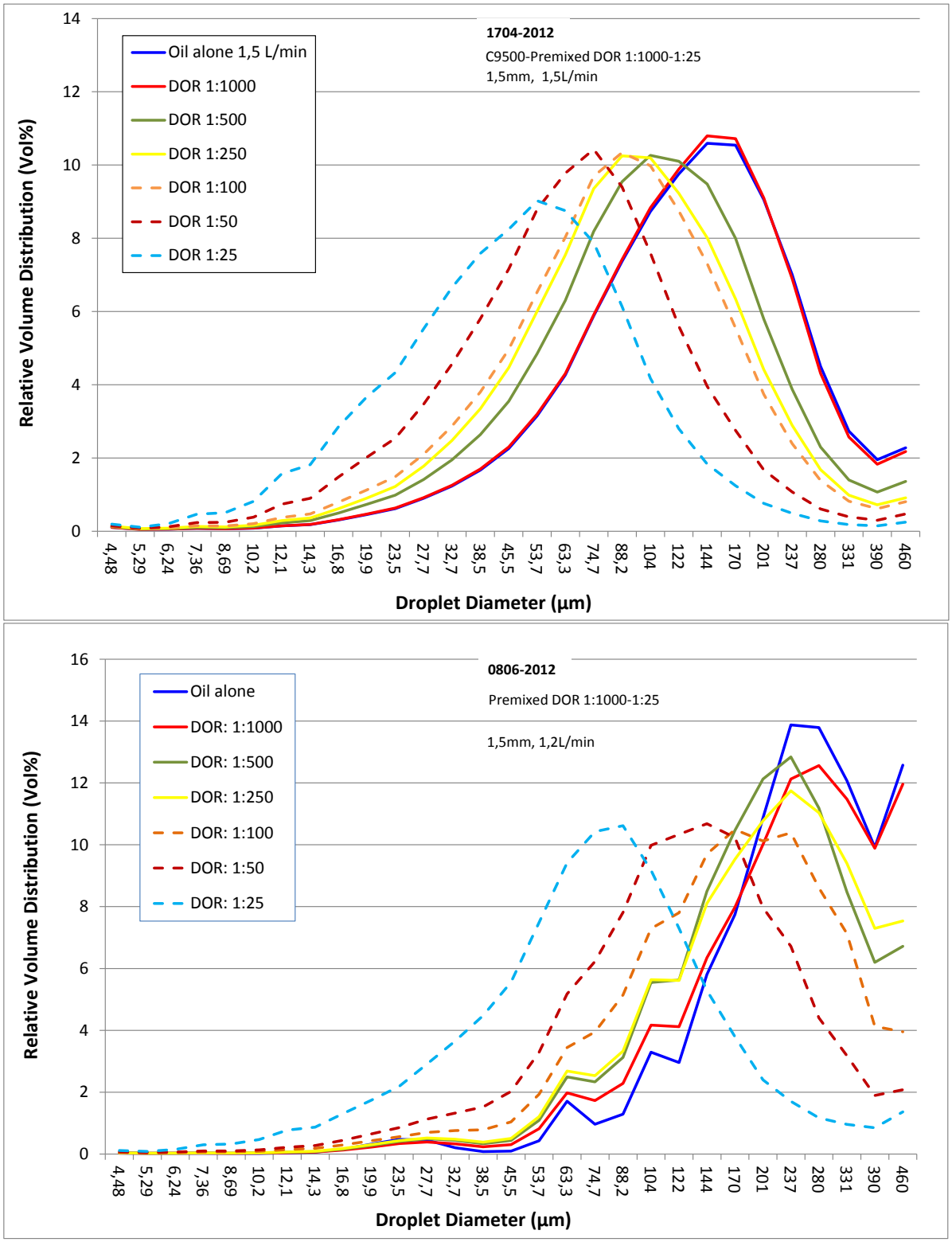

Figure 6.8: Relative droplet size distribution (volume %) as a function of Dispersant to Oil Ratio (DOR) with the Oseberg oil measured with the LISST in the SINTEF Tower Basin. Release conditions 1,5 mm and 1,2 and 1,5 L/min. Dispersant used is C9500.

Table 6.5: DOR experiment with premixed dispersant (1704): VMD as a function of Dispersant to oil ratio (DOR) for premixed dispersant. Nozzle size 1.5 mm and flow rate 1.5 L/min for the Oseberg oil measured with LISST instrumentation in the SINTEF Tower Basin. Interfacial tension measured on oil samples collected in-situ from the oil plume in the Tower basin.

DOR	Maximum peak VMD (µm)	Relative shift in VMD	Cumulative 50% VMD (µm)	Relative shift in VMD	Interfacial tension – Initial (mN/m)	Interfacial tension 30 min (mN/m)
No disp	157	1	130	1	16.5	13.2
1000	157	1	129	1	14.7	11.7
500	104	0.66	97.4	0.75	13.2	9.5
250	88.2	0.57	85.6	0.66	4.5	2.6
100	88.2	0.57	80.3	0.62	1.5	1.2
50	74.7	0.47	61.2	0.46	0.002	0.08
25	53.7	0.34	45.2	0.34	0.07	0.05

Table 6.6: DOR experiment Premixed dispersant (0806): VMD as a function of Dispersant to oil ratio (DOR) for premixed dispersant. Nozzle size 1.5 mm and flow rate 1.2 L/min for the Oseberg oil measured with LISST instrumentation in the SINTEF Tower Basin. Interfacial tension measured on oil samples collected from the oil plume in the Tower basin.

DOR	Maximum peak VMD (µm)	Relative shift in VMD	Cumulative 50% VMD (µm)	Relative shift in VMD	Interfacial tension - Initial (mN/m)	Interfacial tension 30 min (mN/m)
No disp	259	1	255	1	19.6	15.1
1000	293	1.13	246	0.96	9.5	5.0
500	259	1	207	0.81	2.9	1.5
250	259	1	211	0.83	1.3	0.8
100	186	0.72	171	0.67	0.7	0.3
50	157	0.66	123	0.48	0.07	0.008
25	88.2	0.34	71	0.28	0.08	0.07

6.5 Experiments with dispersant injection

This section presents results from tank tests using dispersant injection techniques similar to those used during the Macondo deep water release. Tank injection equipment was designed after the techniques shown in photos in Figure 6.9, taken from the Macondo incident. These techniques were evaluated as they offer the potential for effective subsea dispersants injection.

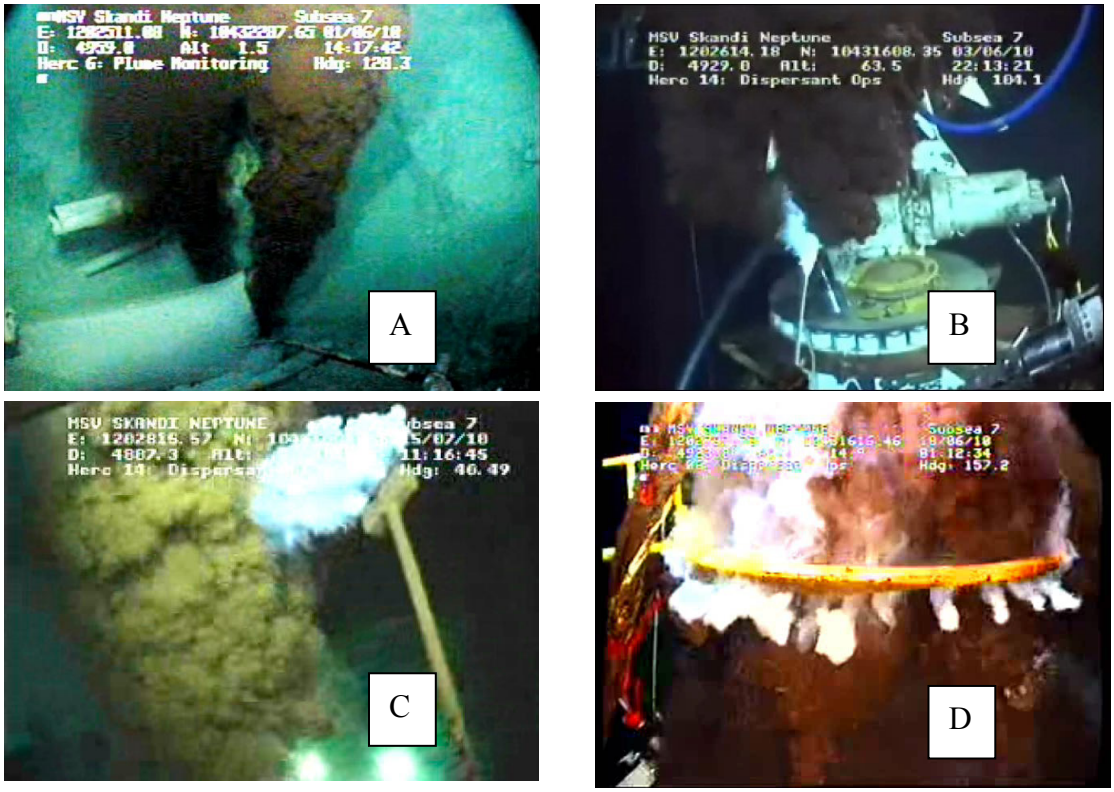

Figure 6.9: Images from the streaming video captured during the DWH deep water oil release showing different methods for injecting dispersant into the oil plume. The insertion tool (A) the wand (B and C) and the dispersant application ring (D).

Table 6.7: Experimental conditions for the dispersant injection experiments

Nozzle diameter:	One – 1.5 mm
Flow rate:	One – 1.2 L/min
Gas-oil-ratio:	No gas (air)
Dispersant application techniques	Three
Dispersant:	One - Corexit 9500A
Number of replicate experiments:	None
Oil type:	One – Oseberg

These experiments were performed with the same nozzle and flow rate used in the DOR experiments (1,2 L/min) and with the same oil type and dispersant (Oseberg/C9500A).

The application techniques tested in this study are (three different techniques):

a. Simulated insertion tool (injected 6 nozzle diameters before the nozzle outlet). See Figure 6.10-A1.
b. Injected above nozzle in the centre of the jet/plume – simulated "Wand" (different distances above nozzle), See Figure 6.10-A2
c. Horizontal injected from the side of the plume 6 diameters above the nozzle (different distances), See Figure 6.11-B.

In these down-scaled laboratory experiments, scaling from field conditions was done by using the release diameter as a scaling factor. The "distances" referred to in the bulleted list above (b, and c) are relative to nozzle diameter of 1,5 mm.

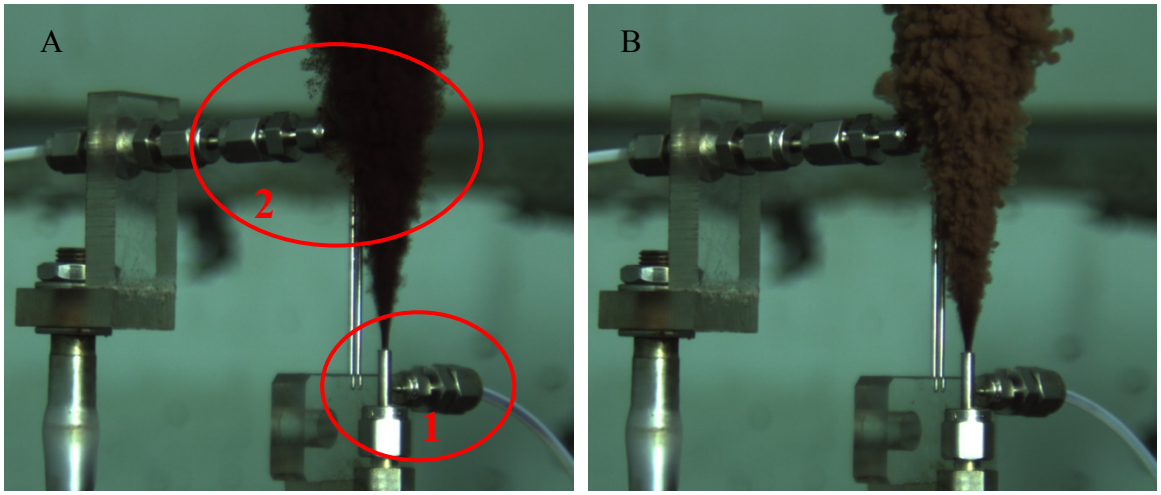

Figure 6.10: Release arrangement (1.5 mm nozzle) with options for injection of dispersant by the "Simulated insertion tool" (1) and "injection in the oil above the nozzle" (2). A: Oil released alone, no dispersant, B: Dispersant injected with the "Simulated Insertion tool" (DOR: 1:25).

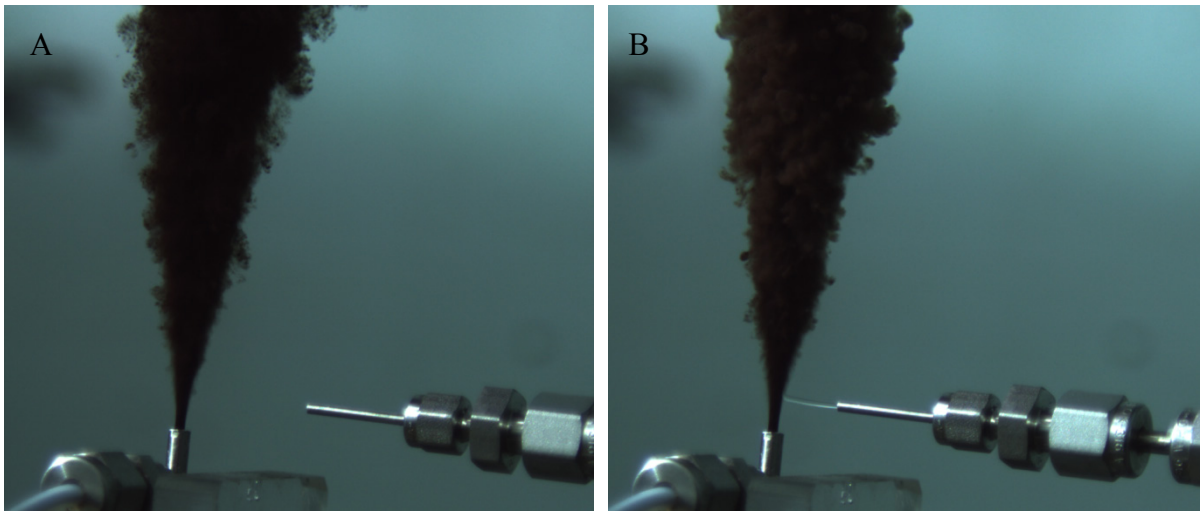

Figure 6.11: Release arrangement (1.5 mm nozzle) with options for injection dispersant horizontally into the oil. A: Oil released alone, no dispersant, B: Dispersant injected at DOR: 1:100.

6.5.1 Simulated injection tools

This section presents the results from the testing with the "Simulated insertion tool".

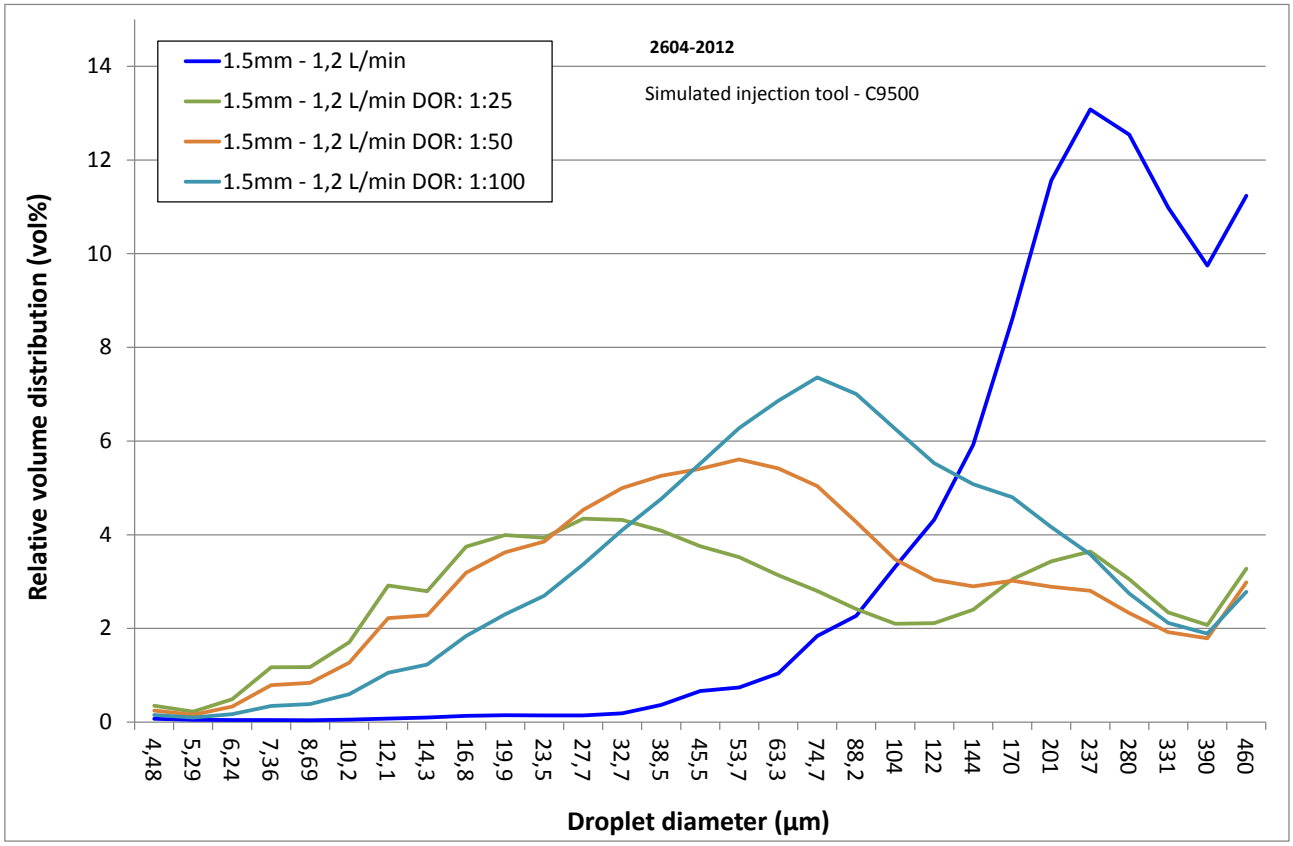

Figure 6.12: Relative droplet size distribution (volume %) with the simulated insertion tool with different Dispersant to Oil Ratio (DOR: 100, 50 and 25) on the Oseberg oil measured with LISST instrumentation in the SINTEF Tower Basin. Release conditions 1,5 mm and 1,2 L/min.

Table 6.8: VMD as a function of Dispersant injection by the "simulated insertion tool" with three different dispersant to oil ratio (1:100, 50 and 25). Nozzle size 1.5 mm and flow rate 1.2 L/min for the Oseberg oil measured with LISST instrumentation in the SINTEF Tower Basin.

DOR	Maximum peak VMD (µm)	Relative shift in VMD	Cumulative 50% VMD (µm)	Relative shift in VMD
No disp	259		243	
100	74	0.29	72	0.30
50	54	0.21	52	0.21
25	28	0.11	46	0.19

6.5.2 Injection into the oil jet above the nozzle

This section presents the results from the Tower basin experiments where the dispersant was injected into the oil at different distances above the nozzle.

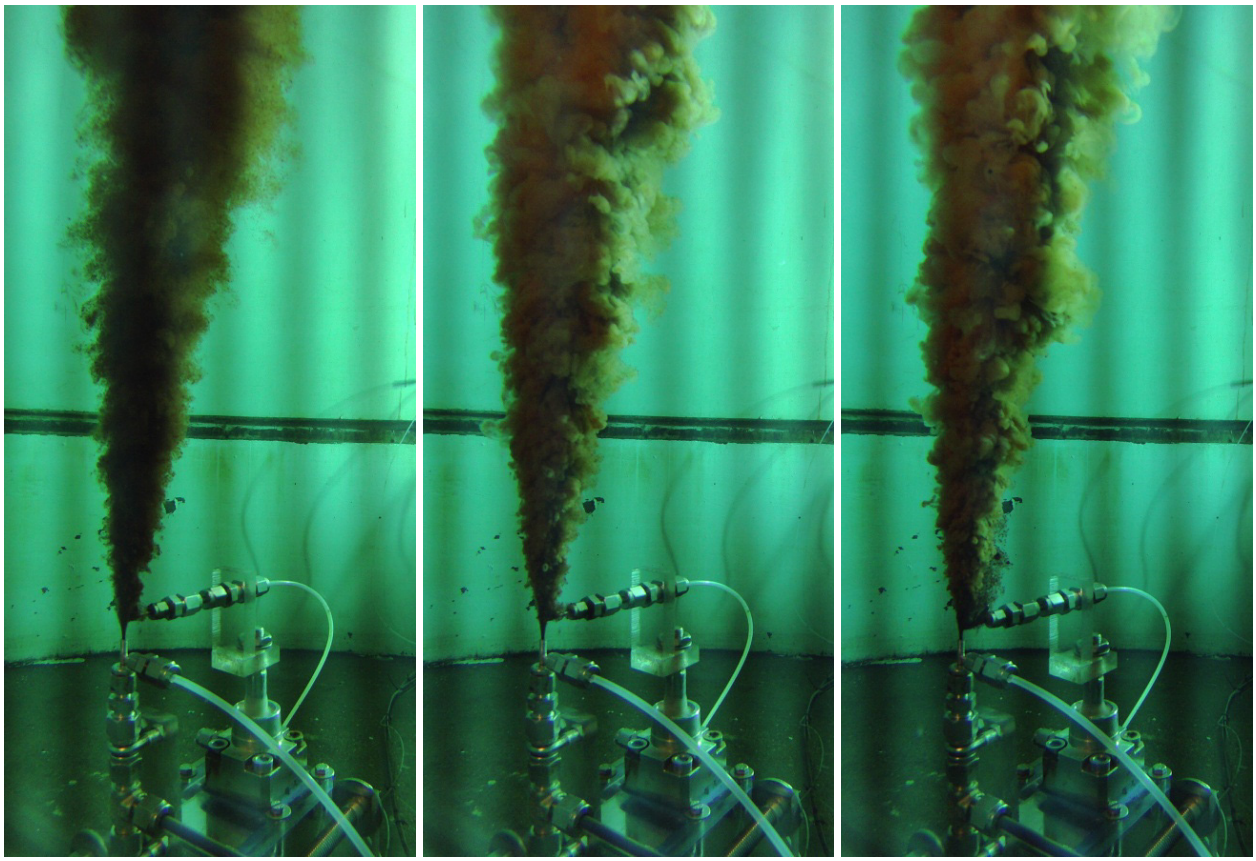

Figure 6.13: Dispersant injected into the rising oil at different distances above the nozzle. A: Before dispersant injection (blue dotted line in Figure 6.15). B: Injection at 8 mm above nozzle (yellow dotted line in Figure 6.17). C: Injection at 1,5 mm above nozzle (light blue dotted line in Figure 6.17).

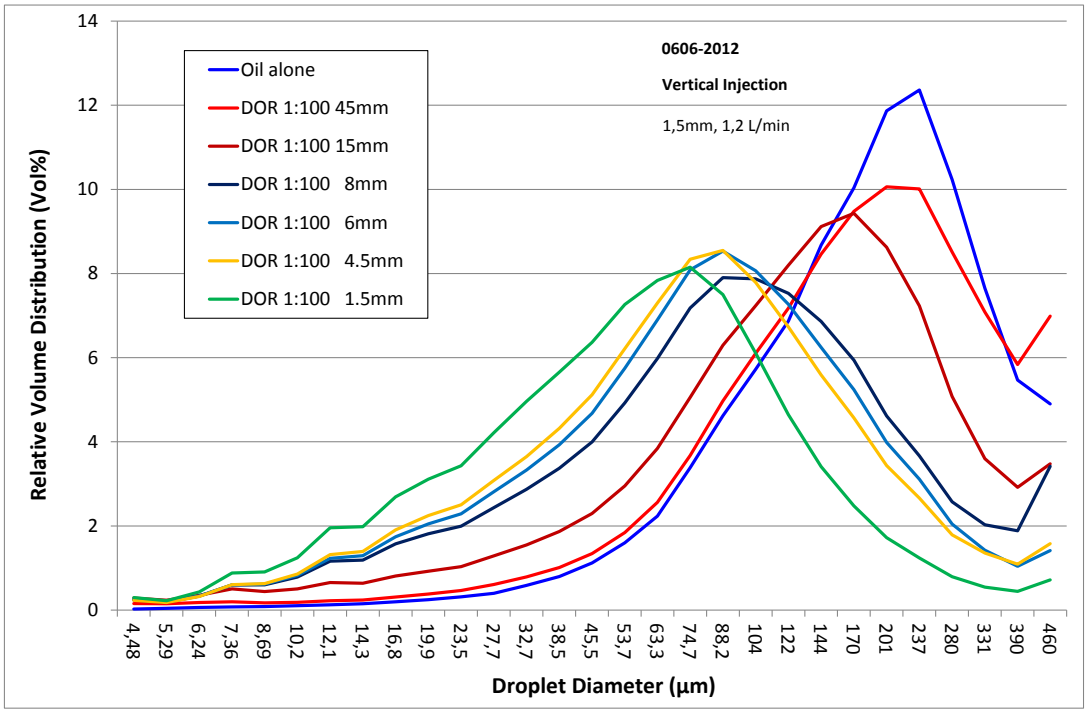

Figure 6.14: Relative droplet size distribution (volume %) with dispersant injected into the rising oil at different distances above the nozzle at DOR 1:100 with the Oseberg oil measured with LISST instrumentation in the SINTEF Tower Basin. Release conditions 1,5 mm and 1,2 L/min.

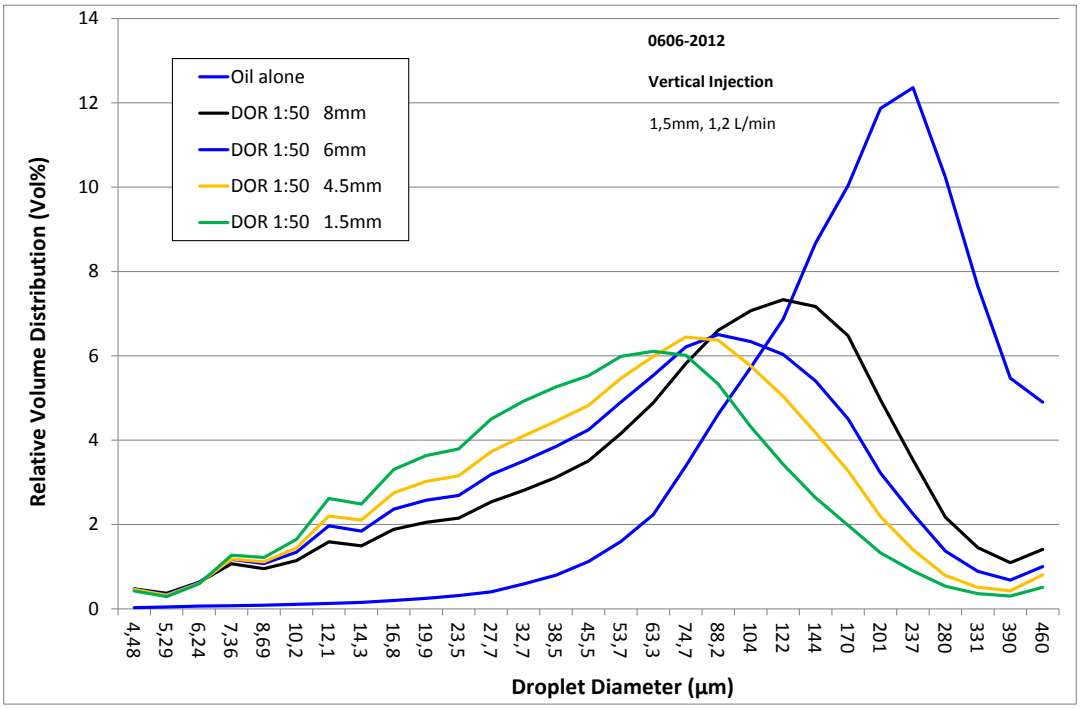

Figure 6.15: Relative droplet size distribution (volume %) with dispersant injected into the rising oil at different distances above the nozzle at DOR 1:50 with the Oseberg oil measured with LISST instrumentation in the SINTEF Tower Basin. Release conditions 1,5 mm and 1,2 L/min.

Table 6.9: Injection above nozzle (0606): VMD for dispersant injected into the oil plume at different distances above the nozzle (DOR 1:100). Nozzle size 1.5 mm and flow rate 1.2 L/min for the Oseberg oil measured with LISST instrumentation in the SINTEF Tower Basin. Interfacial tension measured on oil samples from the oil plume in the Tower basin.

Distance	Maximum peak VMD (µm)	Relative shift in VMD	Cumulative 50% VMD (µm)	Relative shift in VMD	Interfacial tension - Initial (mN/m)	Interfacial tension 30 min (mN/m)
Oil alone	259	1	193	1	18.2	15.5
45	219	0.85	183	0.95	1.4	1.4
15	186	0.72	132	0.68	0.8	0.2
8	88.2	0.34	85.8	0.46	0.7	0.8
6	88.2	0.34	75.9	0.39	0.6	0.3
4.5	88.2	0.34	71.2	0.37	1.3	1.2
1.5	74.7	0.29	53.7	0.28	0.5	0.5

Table 6.10: Injection above nozzle (0606): VMD for dispersant injected into the oil plume at different distances above the nozzle (DOR 1:50). Nozzle size 1.5 mm and flow rate 1.2 L/min for the Oseberg oil measured with LISST instrumentation in the SINTEF Tower Basin. Interfacial tension measured on oil samples from the oil plume in the Tower basin.

Distance	Maximum peak VMD (µm)	Relative shift in VMD	Cumulative 50% VMD (µm)	Relative shift in VMD	Interfacial tension - Initial (mN/m)	Interfacial tension 30 min (mN/m)
8	128	0.49	83.5	0.23	0.1	0.03
6	88.2	0.34	65.8	0.31	0.05	0.009
4.5	74.7	0.29	55.5	0.29	0.04	0.006
1.5	63.3	0.24	44.4	0.17	0.001	0.004

6.5.3 Horizontal injection from the side into the oil jet

This section presents the results from the horizontal injection of dispersants.

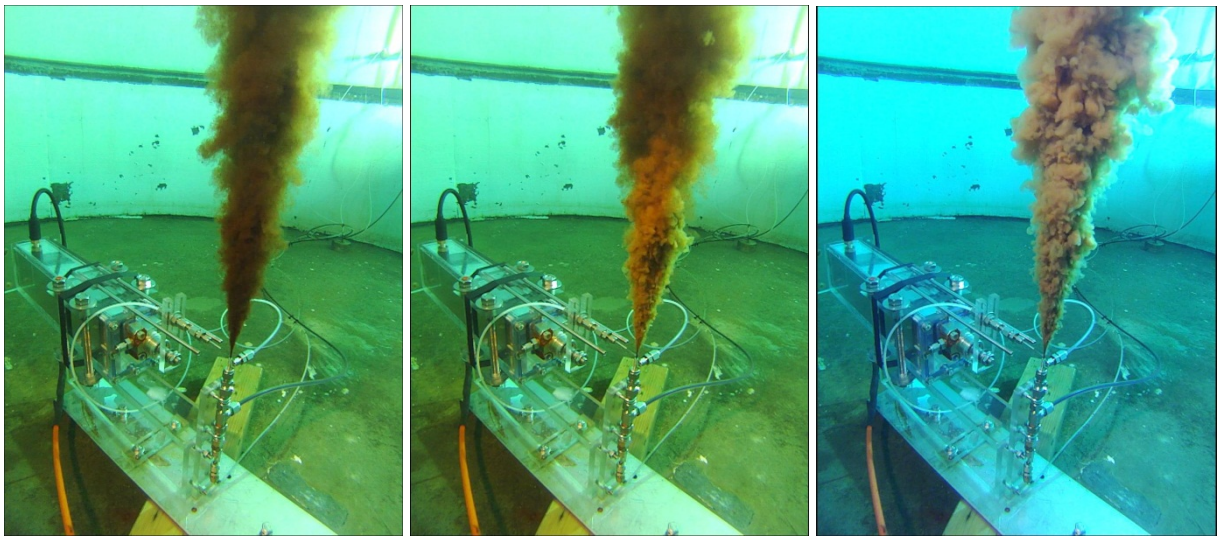

Figure 6.16: Dispersant injected horizontally 4.5 mm (3 release diameters) into the rising oil plume at DOR 1:50 in the SINTEF Tower Basin. A: Before dispersant injection (similar to blue solid line in Figure 6.17). B: Immediately after injection started. C: 30 seconds after injection started (similar to green solid line in Figure 6.17). Release conditions 1,5 mm and 1,2 L/min.

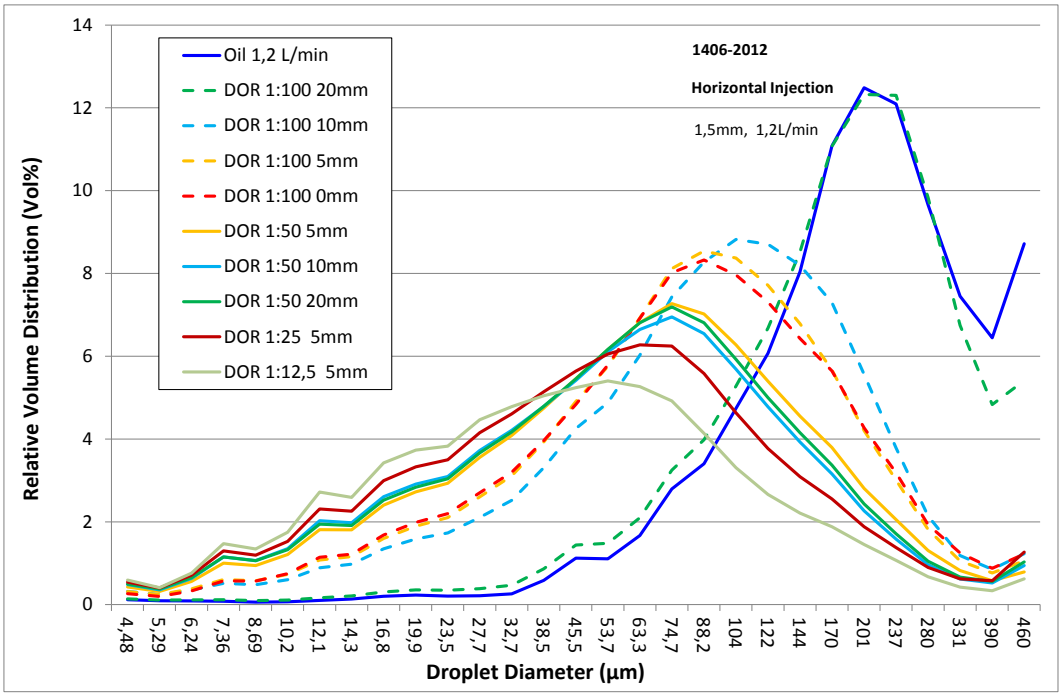

Figure 6.17: Relative droplet size distribution (volume %) with dispersant injected into the rising oil plume from the side at different distances and DORs with the Oseberg oil measured with LISST instrumentation in the SINTEF Tower Basin. Release conditions 1,5 mm and 1,5 L/min.

Table 6.11: Horizontal injection from beside the oil jet (3 diameters above) nozzle (1406): VMD for dispersant injected into the oil plume at different distances above the nozzle (DOR 1:100). Nozzle size 1.5 mm and flow rate 1.2 L/min for the Oseberg oil measured with LISST instrumentation in the SINTEF Tower Basin. Interfacial tension measured on oil samples from the oil plume in the Tower basin.

Distance	Maximum peak VMD (µm)	Relative shift in VMD	Cumulative 50% VMD (µm)	Relative shift in VMD	Interfacial tension - Initial (mN/m)	Interfacial tension 30 min (mN/m)
Oil alone	219	1	205	1	12.4	10
20	219	1	191	0.93	3.7	2.5
10	104	0.48	88.1	0.43	1.8	1.4
5	88.2	0.40	77.0	0.37	1.9	1.0
0	88.2	0.40	76.4	0.34	*	*

*: No sample taken for IFT measurements

Table 6.12: Horizontal injection from beside the oil jet (3 diameters above) nozzle (1406): VMD for dispersant injected into the oil plume at different distances above the nozzle (DOR 1:50, 25 and 12,5). Nozzle size 1.5 mm and flow rate 1.2 L/min for the Oseberg oil measured with LISST instrumentation in the SINTEF Tower Basin. Interfacial tension measured on oil samples from the oil plume in the Tower basin.

Distance	Maximum peak VMD (µm)	Relative shift in VMD	Cumulative 50% VMD (µm)	Relative shift in VMD	Interfacial tension - Initial (mN/m)	Interfacial tension 30 min (mN/m)
20	74,7	0,34	57,3	0,28	1,6	1,4
10	74,7	0,34	55,6	0,27	0,04	0.03
5	74,7	0,34	60,3	0,27	0,03	0.01
5**	63,3	0,28	49,0	0,22	0,05	0.009
5***	53,7	0,24	40,3	0,18	*	*

*: No sample taken for IFT measurements

**: Experiment performed with DOR: 1:25

***: Experiment performed with DOR: 1:12.5

6.6 Experiments with release of warm oil

In case of a subsurface release of oil, the oil would in most cases have a higher temperature than the oil released in the Tower basin experiments (room temperature 15°C). How the temperature shift from e.g. 70 to 15°C influence the droplet distribution can be estimated by existing algorithms (Weber scaling). However, how elevated temperature influences the dispersant physically mixing with the oil, surfactant interaction with the oil/water and finally the IFT and dispersant effectiveness are more complex to incorporate in algorithms for predicting droplet size distributions.

To get a first idea of the temperature effect, one experiment with elevated temperature was performed. The goal was to perform an experiment with a release temperature out of the nozzle of 60°C. This was also obtained during testing with the heat-exchanger (hot water – oil) used with the Tower basin. However, during the experiment only 51 °C was obtained, probably due to the heat lost to cold piping/hoses in the relatively short experiment. The experiment was first run with ordinary "Cold oil" (15 °C) and then the oil was run through the heater for the "Warm oil" experiment, see figure below. The temperature is measured at the release nozzle.

Simulated insertion tool was used as the injection method to ensure that the dispersant was injected into the warn oil before it entered into the cold water (10 °C).

The results from the "warm oil" experiments are compared in the next two figures with both "cold oil results" obtained in the same run as the "warm oil" experiments and with results from an earlier experiment with cold oil and the Simulated insertion tool.

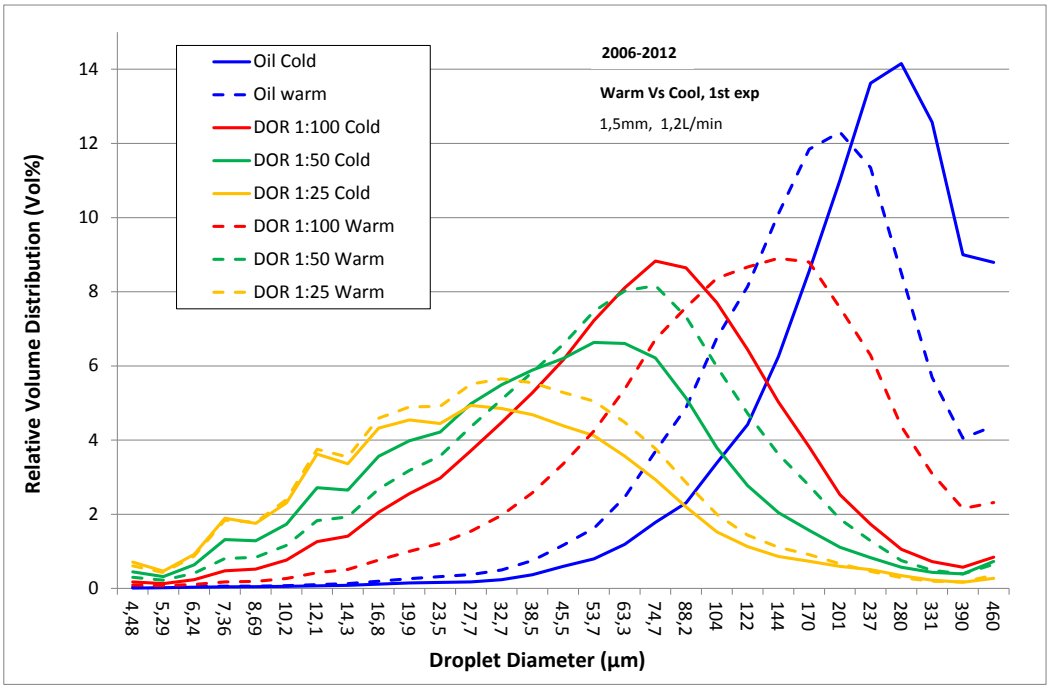

Figure 6.18: Relative droplet size distribution (volume %) as a function of temperature (cold versus warm – 15-51°C) at DOR: 1:100, 50 and 25 with the Oseberg oil measured with LISST instrumentation in the SINTEF Tower Basin. Release conditions 1,5 mm and 1,2 L/min.

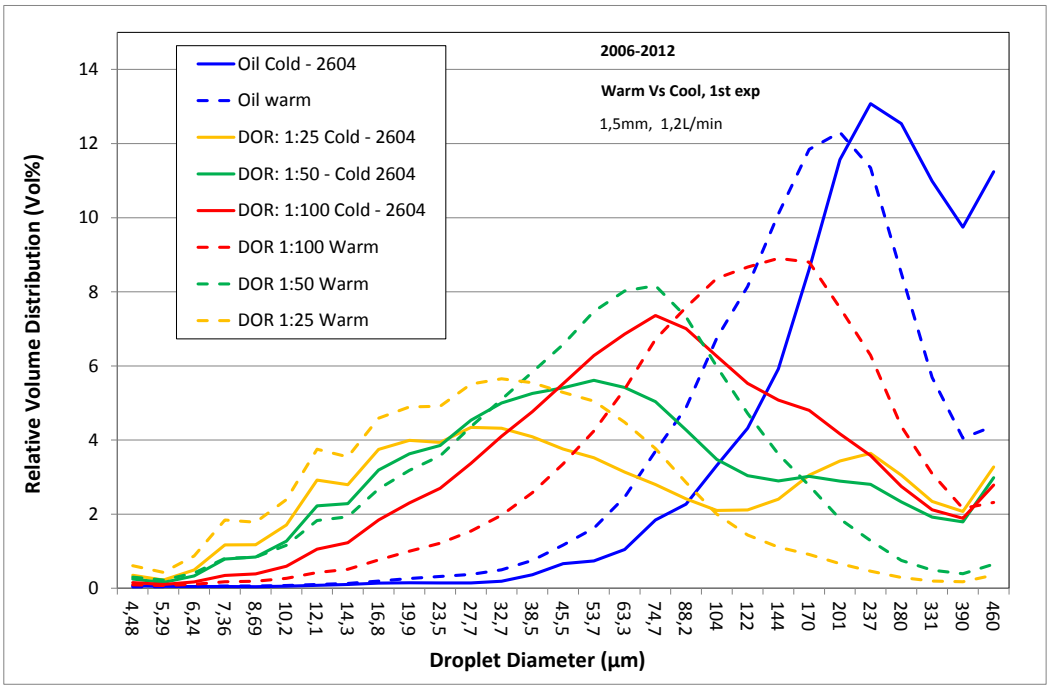

Figure 6.19: Relative droplet size distribution (volume %) as a function of temperature (cold versus warm – 15-51°C) at DOR: 1:100, 50 and 25 with the Oseberg oil measured with LISST instrumentation in the SINTEF Tower Basin. Release conditions 1,5 mm and 1,2 L/min. Warm experiment compared to earlier "cold experiment" performed 2604.

6.7 Modified dispersant with reduced amount of solvent

To study the effect of using a more concentrated dispersant (less solvent), a modified version of Corexit 9500A was used. The dispersant that was tested by "upstream injection" was used as supplied by Nalco.

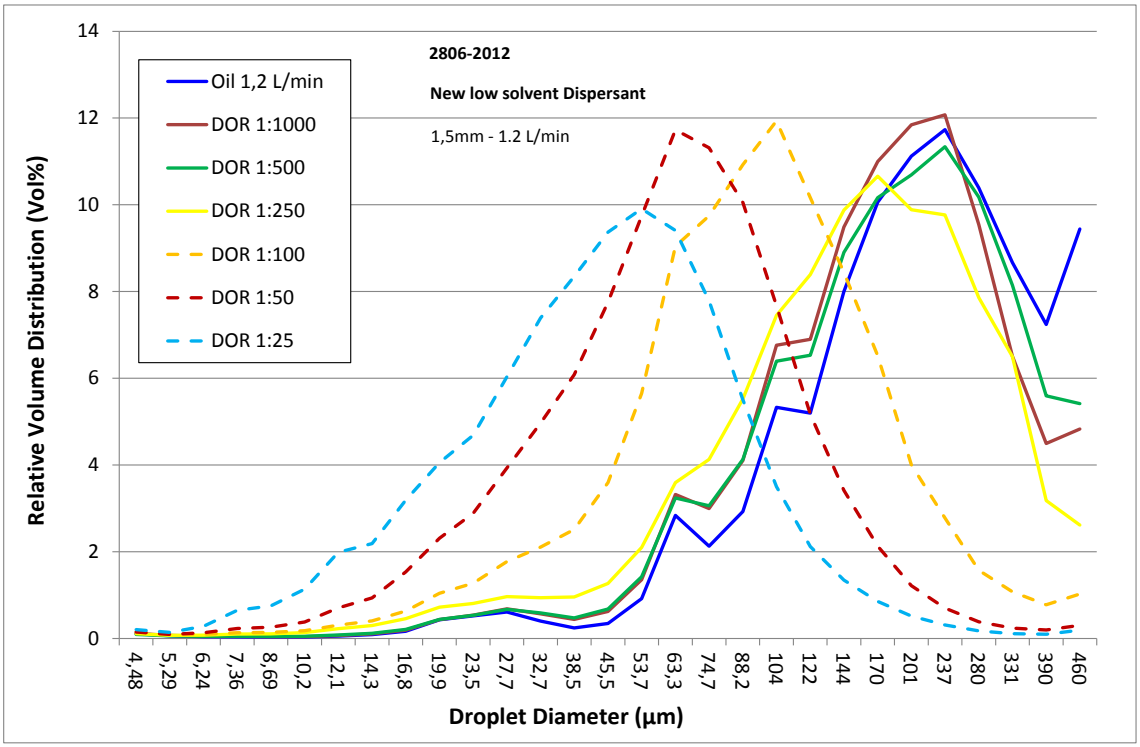

Figure 6.20: Relative droplet size distribution (volume %) with premixed low solvent version of C9500A as a function of Dispersant to Oil Ratio (DOR) with the Oseberg oil measured with LISST instrumentation in the SINTEF Tower Basin. Release conditions 1.5 mm and 1.2 L/min.

Table 6.13: DOR experiment with premixed (upstream injection) low solvent version of C9500A (2806): VMD as a function of nozzle size Dispersant to oil ratio (DOR) for premixed dispersant. Nozzle size 1.5 mm and flow rate 1.2 L/min for the Oseberg oil measured with LISST instrumentation in the SINTEF Tower Basin. Interfacial tension measured on oil samples collected from the oil plume in the Tower basin.

DOR	Maximum peak VMD (µm)	Relative shift in VMD	Cumulative 50% VMD (µm)	Relative shift in VMD	Interfacial tension - Initial (mN/m)	Interfacial tension – 30 min (mN/m)
No disp	259	1	212	1	18,1	11,8
1000	259	1	185	0,87	7,5	2,9
500	259	1	191	0,90	2,4	1,4
250	186	0,72	160	0,75	0,7	0,8
100	104	0,40	87,3	0,41	0,09	0,04
50	63,3	0,24	58,8	0,28	0,07	0,05
25	53,7	0,21	42,3	0,20	0,05	0,007

6.8 Comparison of the different injection techniques

The following figures and tables summarize the data for the different injection techniques and can be used to compare the different injection techniques.

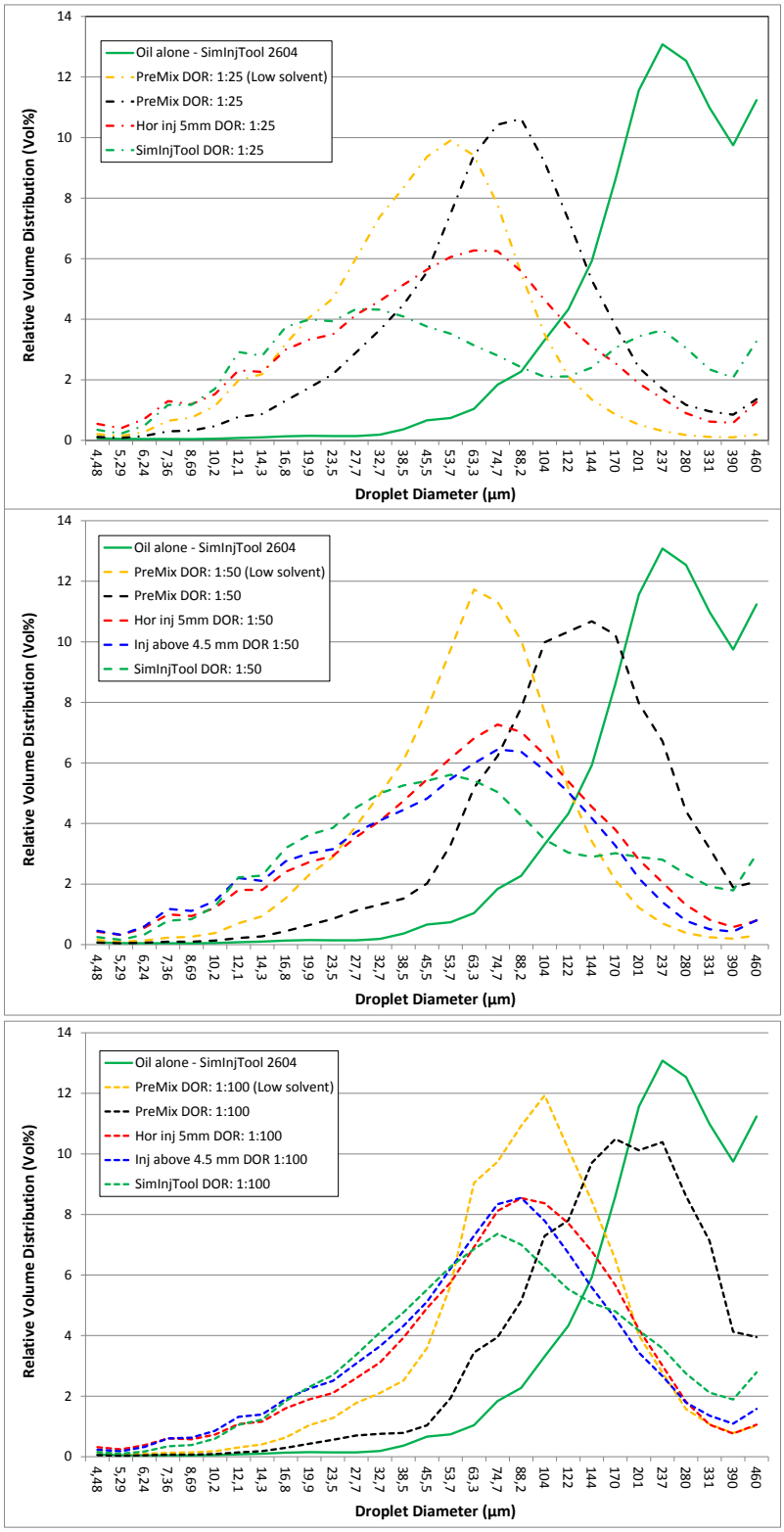

Figure 6.21: Relative droplet size distribution (volume %) for all the injection methods at Dispersant to Oil Ratio (DOR) 1:100/50/25 with the Oseberg blend. Oil alone is also included as a reference. Release conditions 1,5 mm and 1,2 L/min.

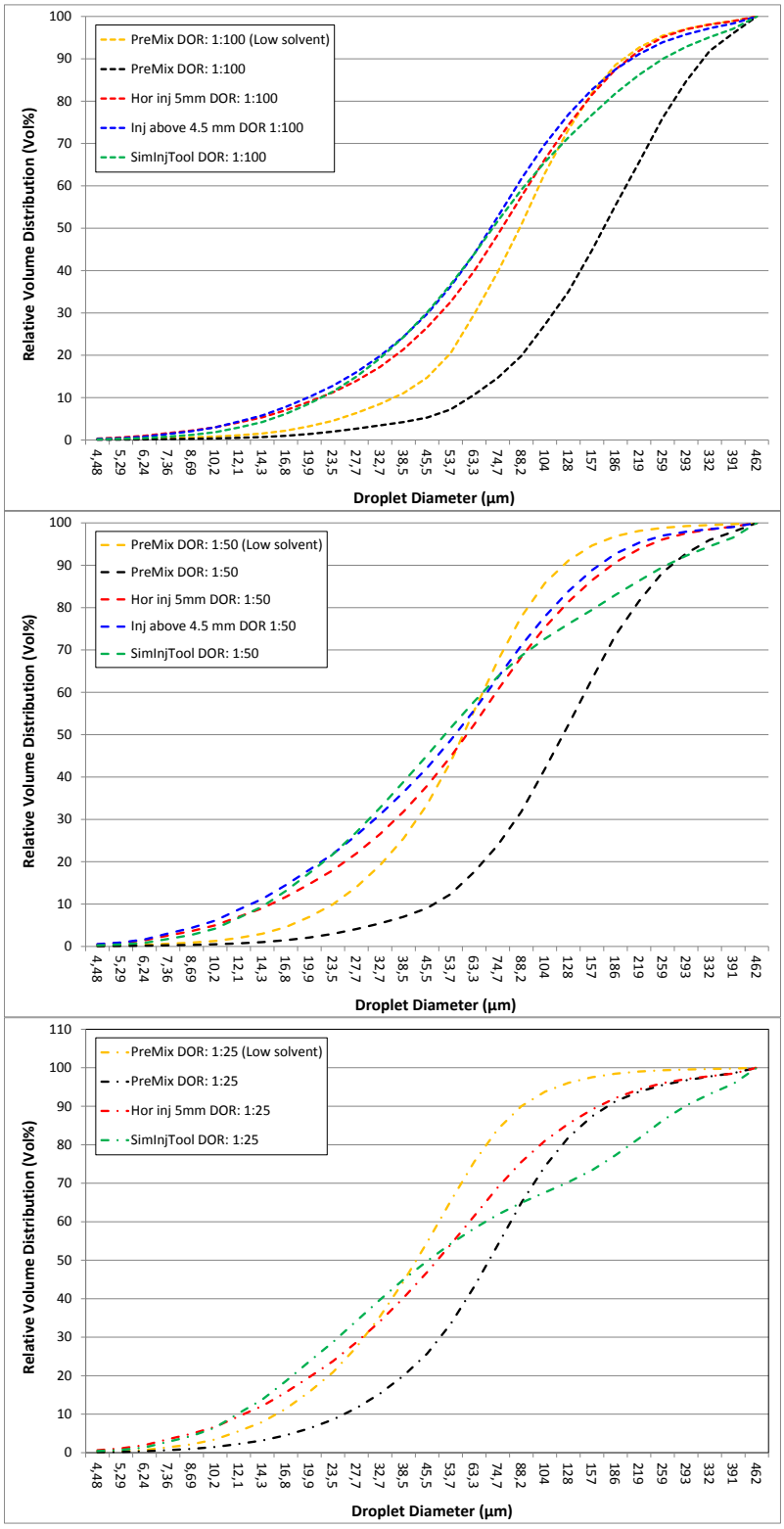

Figure 6.22: Cumulative droplet size distribution (volume %) for all the injection methods at Dispersant to Oil Ratio (DOR) 1:100/50/25 with the Oseberg oil measured with the LISST in the SINTEF Tower Basin. Release conditions 1,5 mm and 1,2 L/min.

6.9 Comparison of dispersant injection at different nozzle sizes

The down-scaling of the Tower basin experiments compared to field conditions and the strategy behind the design of the injection experiments are both based on using the release diameter as a scaling factor. To compare one of the injection methods (Injection above nozzle) with different nozzle sizes, experiments were performed with 0.5, 1.5 and 3 mm nozzle. The dispersant was injected 3 release diameters above the nozzle in each experiment, see figures on next page.

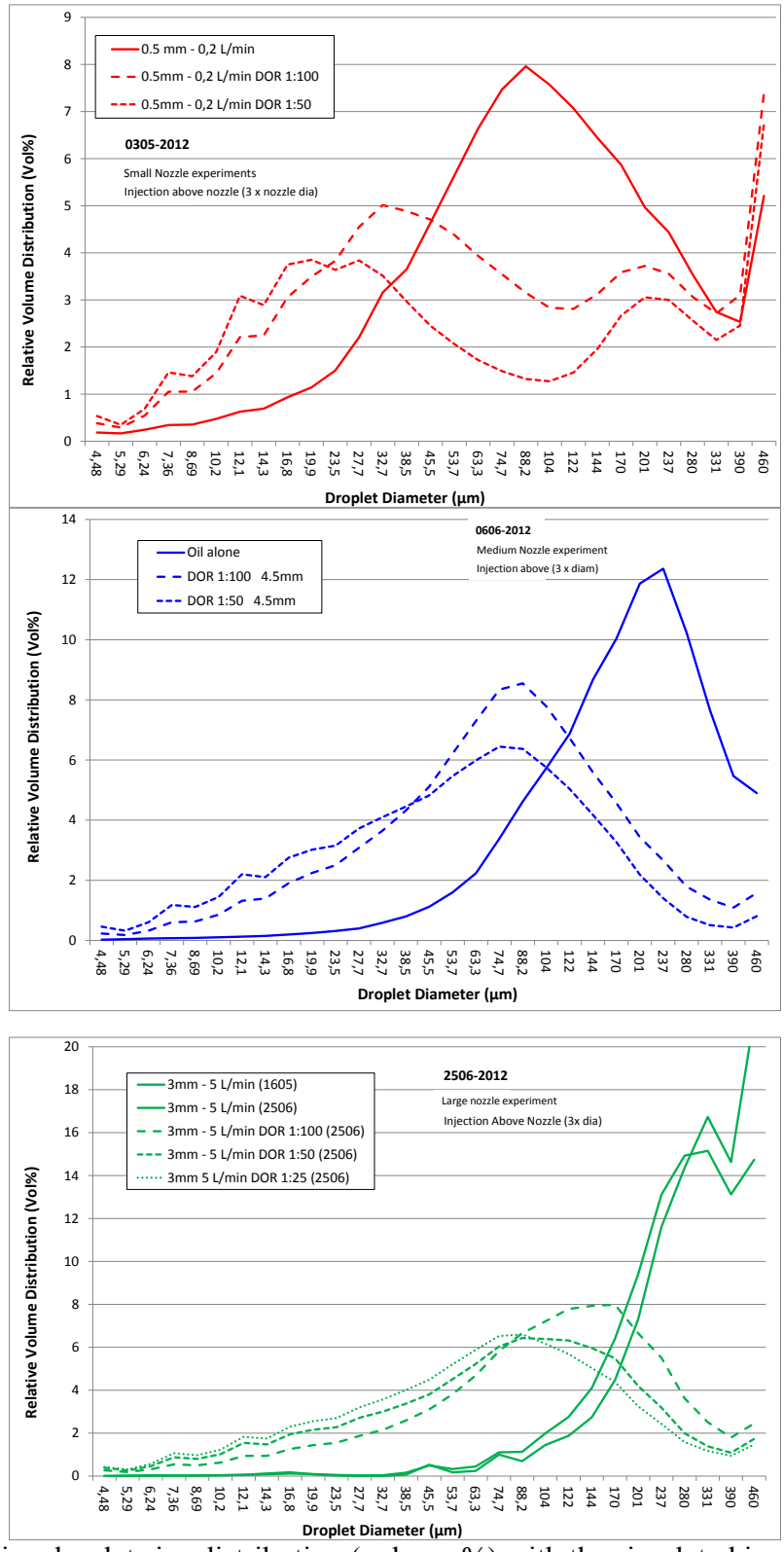

Figure 6.23: Relative droplet size distribution (volume %) with the simulated insertion tool with different Dispersant to Oil Ratio (DOR: 100, 50 and 25) on the Oseberg oil measured with LISST instrumentation in the SINTEF Tower Basin. Release conditions nozzle size: 0.5, 1.5 and 3.0 mm and release rate: 0.2, 1.5 and 5 L/min.

Table 6.14: VMD as a function of nozzle size (0.5, 1.5 and 3 mm) and dispersant injected 3 nozzle diameters above release (DOR: 1:100, 50 and 25) for the Oseberg oil measured with LISST instrumentation in the SINTEF Tower Basin.

Dispersant	**0.5 mm – 0.5 L/min**		**1.5 mm – 1.2 L/min**		**3 mm – 5 L/min**	
DOR	VMD (µm)	Relative shift in VMD	VMD (µm)	Relative shift in VMD	VMD (µm)	Relative shift in VMD (µm)
Oil alone	88,2	1	259	1	332	1
1:100	32,7	0,34	88,2	0,34	128	0,38
1:50	23,5	0,28	74,7	0,29	104	0,31
1:25					74,7	0,23

6.10 Experiments with combined releases of oil & gas (air)

This section presents the initial experiments that were performed with oil, gas (air) and dispersants.

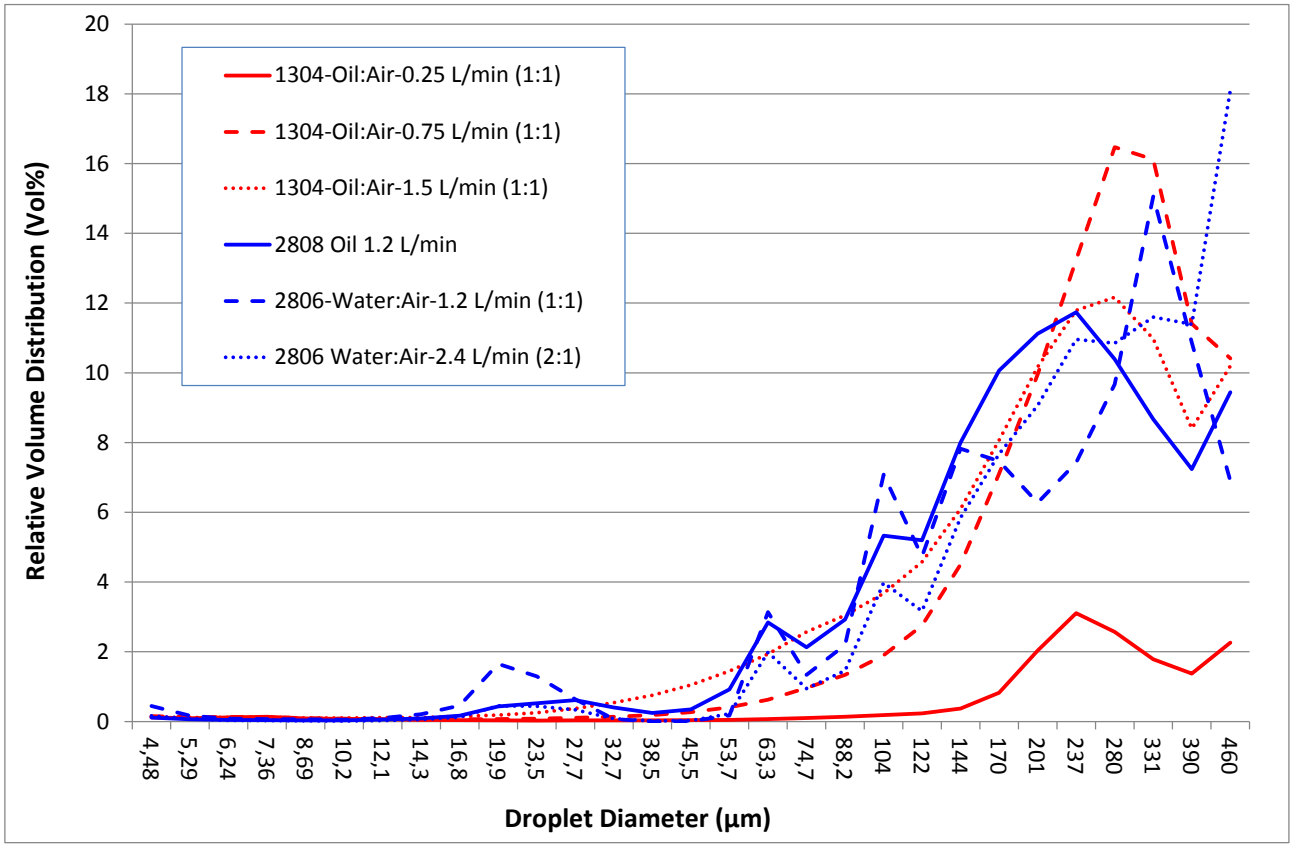

Figure 6.24: Relative droplet size distribution (volume %) with and without gas (air). Nozzle size (1.5 mm) and total flow rate (both oil and gas) of 0.25 to 2.4 L/min) for water and Oseberg blend measured with LISST instrumentation in the SINTEF Tower Basin.

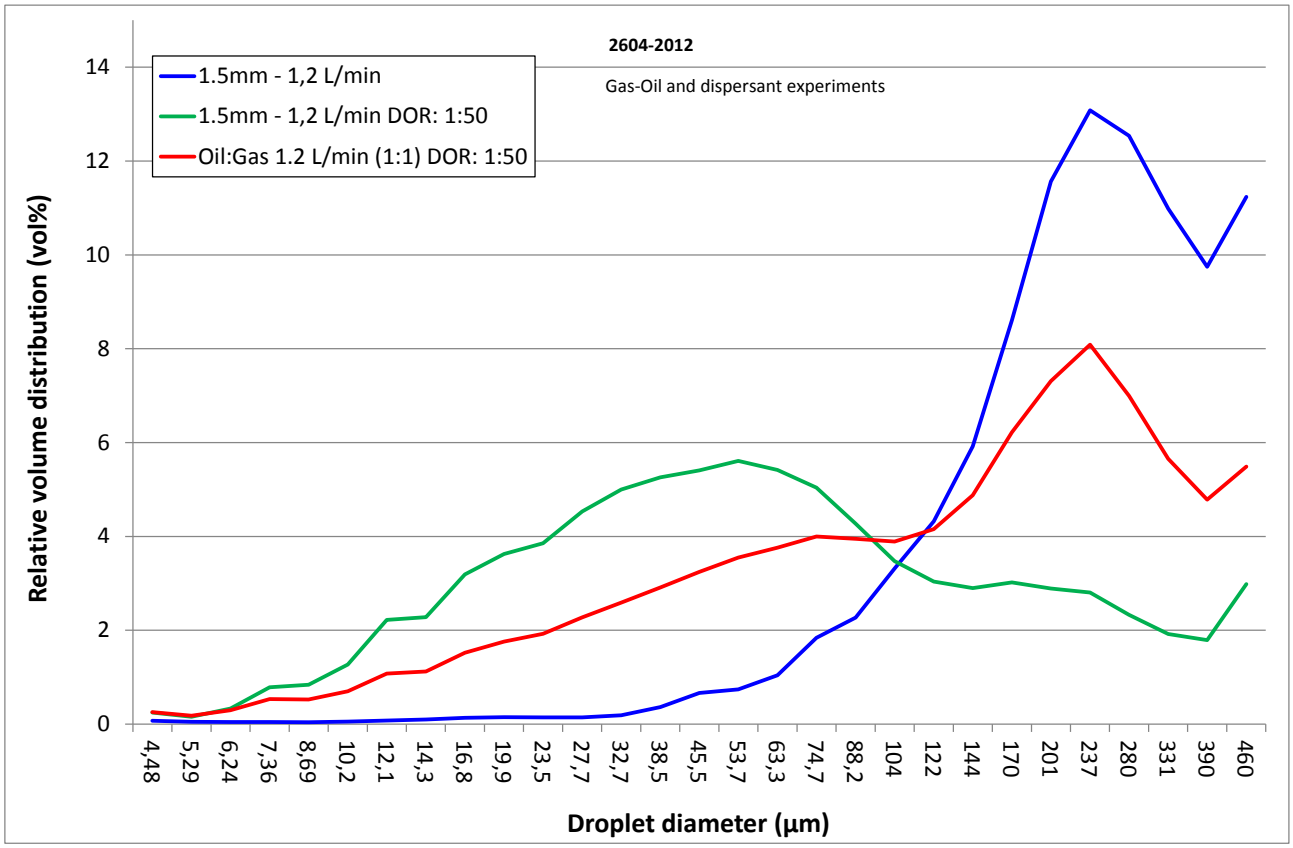

Figure 6.25: Relative droplet size distribution (volume %) with and without gas (air) and dispersant (DOR: 1:50). Nozzle size (1.5 mm) and total flow rate (both oil and gas) of 1.2 L/min for water and Oseberg blend measured with LISST instrumentation in the SINTEF Tower Basin.

7 Discussions

This chapter contains the discussion of the results presented in Chapter 6.

7.1 Initial experiment

7.1.1 Measurement of oil concentrations

In the initial experiment, both the UniLux UVF sensor and the LISST instrument were used to monitor oil concentrations. The latter gave results that best correlated with the concentrations measured in the water samples. The LISST also had a larger linear range and was able to report droplet size distributions. However, the oil concentration in the rising plume is not critical and can be calculated from the release rate and dilution factor.

7.1.2 Verification of droplet distributions measured with the LISST instrument

Droplet size distributions measured with the LISST instrument and sizes of mono disperse particle standards are presented in Figure 6.3. This calibration experiment showed a very good fit between the standard particles and the distribution reported from the LISST.

7.1.3 Verification of mass flow regulators

The set values and the obtained flow rate values for the three different mass flow regulators are presented in Table 6.1. There are some minor deviations for some of the settings (low values for Digimesa or high values for the Burkert 5-100). However, as long as the deviations are small and the real flow rates are used in the calculations, these deviations are not regarded as a problem. Each Tower basin experiment also had a separate flow rate log, where the actual flow rate from each part of the experiment can be calculated.

7.1.4 Reproducibility within and between experiments

The ability of the control and monitoring system in the Tower basin to reproduce droplet size distributions at the most frequent used conditions (1.5 mm nozzle and oil rate 1.2 L/min) is presented in Figure 6.4 and Figure 6.5. The first figure presents variations between 7 different Tower basin experiments performed over a two month period. We can see from the figure that three of these experiments have a slightly larger VMD than the others (VMD of 237 compared to 201 microns). This is probably caused by a slightly lower release rate (approximately 1.1 compared to 1.2 L/min). However, this can be compensated for in the calculations in chapter 8 using the correct flow from the flow rate logs that were recorded for each experiment.

The second figure shows the droplet distributions for the different experimental periods (90 seconds) within one Tower basin experiment. This showed very little variation of droplet size distributions (and flow rate) within one experiment.

7.2 Flow rate experiments - droplet sizes versus release conditions

The droplet size data for the different release experiments utilizing three nozzle sizes (0.5, 1.5 and 3) and three different flow rates for each nozzle (0,1 – 8 L/min) are presented in Figure 6.6. An overview of all the Volume Median Diameters (VMD) for these experiments is also given in Table 6.3.

Most of the data are from the LISST instrumentation, which is used as the main sensor for droplet size measurements. The data obtained from the two image based techniques (In-situ macro camera and the external PVM) contained very limited information regarding sizes of the large droplets in most experiments. This is probably due to the small focusing area of these macro methods (mm range) combined with the short time for data acquisition (usually 30 seconds). During this period a very limited number of large droplets were captured and quantified on the images.

Due to this limitation, the images were only analysed and used for the large nozzle experiments (3 mm) and low flow rates (5 and 8 L/min). In these experiments the maximum peak of the distributions was not visually identified in the 2-500 micron range obtained by the LISST. For these experiments, droplet data is provided by image analysis of the PVM images, see legends in Table 6.3.

Assuming a log normal distribution, both the peak value from the relative volume distributions and the 50% from the cumulative distribution should give similar estimates of VMD. However, use of the cumulative distribution assumes that we actually have data for the complete range of droplets. This is not the case for distributions with a significant amount of droplets above the LISST range of 500 microns. However, since the Relative droplet distributions have a limited resolution (30 bins) and the cumulative distributions can be used to interpolate between the bins exactly, the same numerical values cannot be expected. When comparing these two measures of VMD in Table 6.3, we observe that the values based on the cumulative distributions are generally slightly smaller compared to their counterparts.

The experiments give a consistent data set with droplet sizes as expected based on the earlier used algorithm for Weber number scaling of droplet sizes. These data will be used to verify earlier published work (Johansen et al., 2013) to improve existing algorithms for predicting droplet size distributions for different release conditions (modified Weber scaling). See section 8 for further details.

7.3 Droplet sizes versus Dispersant to oil ratio (DOR)

To study the influence on dispersant to oil ratio (DOR) on the interfacial tension and the droplet size distributions, experiments were performed with a wide range of DORs. The relative distributions for two different experiments are presented in Figure 6.8, Table 6.5 and Table 6.6. The only difference between these two experiments is the flow rate of the oil. The second experiment is performed with a lower flow rate (1.2 L/min opposed to 1.5 L/min in the first experiment).

The dispersant (C9500A) was injected into the oil stream 3 meters or 2000 nozzle diameters upstream of the nozzle. It is assumed that the dispersant blends into the oil along this distance upfront of the nozzle. For this reason, this method of upstream dispersant injected is regarded as premixing of dispersant. The residence time of the dispersant/oil from the injection point to the nozzle is less than 2 seconds (1.2 L/min).

The lower figure (1.2 L/min) show that the lowest concentrations (1:1000-500-250) have a very limited effect on the droplet size distributions. It is very difficult to visually see any difference on these three droplet size distributions. However, the three highest concentrations (1:100, 50 and 25)

give a shift towards smaller droplets. The upper figure with a higher flow rate (1.5 L/min) shows some effect of the dispersant at low dosage rates (1:500 and 1:250).

The lack of shift in droplet size distribution with the lowest dosages of dispersant is surprising since the Interfacial tension (oil-water) is lowered (see Table 6.5 and Table 6.6.). The relatively large bin sizes could mask small shifts in droplet size distribution. However, a more probable explanation could be insufficient mixing of the dispersant into the oil despite the 2000 release diameters between injection of the dispersant and the release nozzle. At the lowest dispersant dosages, the injection of the dispersant into the 4 mm oil tubing is probably too small compared to the turbulence level to give sufficient mixing of dispersant and oil before release into the Tower basin. The combinations of flow and oil properties used in these experiments give a Reynolds number (Re) of 1000-1300. A Re lower than 2000 is usually taken as an indication of tubular flow which gives low turbulence and reduced mixing during this short residence time (< 2 seconds). The fact that increased oil flow rate (1.5 versus 1.2 L/min) gives better mixing (higher effectiveness at 1:500/250) supports this hypothesis.

In future DOR experiments, a "mixing-chamber" should be installed to locally raise Re and ensure sufficient turbulence and mixing of oil and dispersants, especially at low dispersant treatment rates (DOR 1:1000 – 1:250).

7.4 Effectiveness of different dispersant injection techniques

Three different dispersant injection techniques were tested in this project;

1. Simulated insertion tool, injection of dispersant 6 nozzle diameters before the outlet
2. Injection in the centre of the rising plume at different heights above the nozzle
3. Horizontal Injection into the plume from outside at different distances

The effectiveness of these injection techniques, evaluated by the relative shift in droplet size distribution, was compared with the premixed results from the previous chapter.

7.4.1 Simulated insertion tool

During the Macondo deep water dispersant injection in the Gulf of Mexico in 2010, dispersant was injected with an "insertion tool". This was a nozzle on the tip of an approximately 2-3 meter long tube which was inserted into the broken riser. In our case this was not possible to simulate directly because inserting some device into these small nozzles (0.5 – 3 mm) would reduce the diameter and restrict the flow. For this reason the dispersant was injected into a separate tube attached orthogonal to the outlet 6 diameters before the nozzle opening.

The results from the simulated insertion tool are presented in Figure 6.12 and the VMD are summarized in Table 6.8. The observed shifts in droplet size distributions are consistent with the dispersant concentrations. This means that an increased dispersant concentration reduces the droplets (VMD). The experiments give systematic shifts in droplet sizes from 259 microns (oil alone), to 75 microns (1:100), 54 microns (1:50) and finally 24 for the 1:25. This is the same trend as for the premixed experiments, but the measured droplet sizes are significant smaller for the simulated inserted tool. No oil samples have been collected for IFT analysis during this type of experiment.

For the highest dispersant treatment, a bimodal distribution can be seen in Figure 6.12, indicating that the dispersant is not completely mixed into the oil stream and that some of the oil is not treated.

7.4.2 Injection at different heights above the nozzle

To simulate the injection of dispersant with the "wand" during the Macondo deep water dispersant injection, dispersant was injected into the rising oil plume at different heights above the nozzle. The results from this dispersant injection are presented in Figure 6.14 and Figure 6.15 (relative droplet distribution - DOR 1:50 and 1:100) and in Table 6.9 and Table 6.10.

These figures show that to be effective in our Tower basin, the dispersant has to be injected rather close to the nozzle. There was a significant difference in droplet size distribution between the experiments where the dispersant was injected close to the nozzle (1.5 to 8 mm or 1 to 6 nozzle diameters) compared to injecting higher above the nozzle. Both the experiments at DOR 1:50 and 1:100 show this trend.

A liquid jet from a nozzle will form a solid cone up to 4-6 nozzle diameters (Or et al., 2011). This is called the zone of flow establishment (ZFE). Above this zone the solid cone will break up and form a spray of droplets (zone established flow – ZEF). Injecting the dispersant in ZFE seems to be most efficient. Then the dispersant is injected directly into the oil cone and mixed into the oil, lowering the IFT before the oil enters the more turbulent ZEF, where the droplets are formed. See illustration in Figure 7.1.

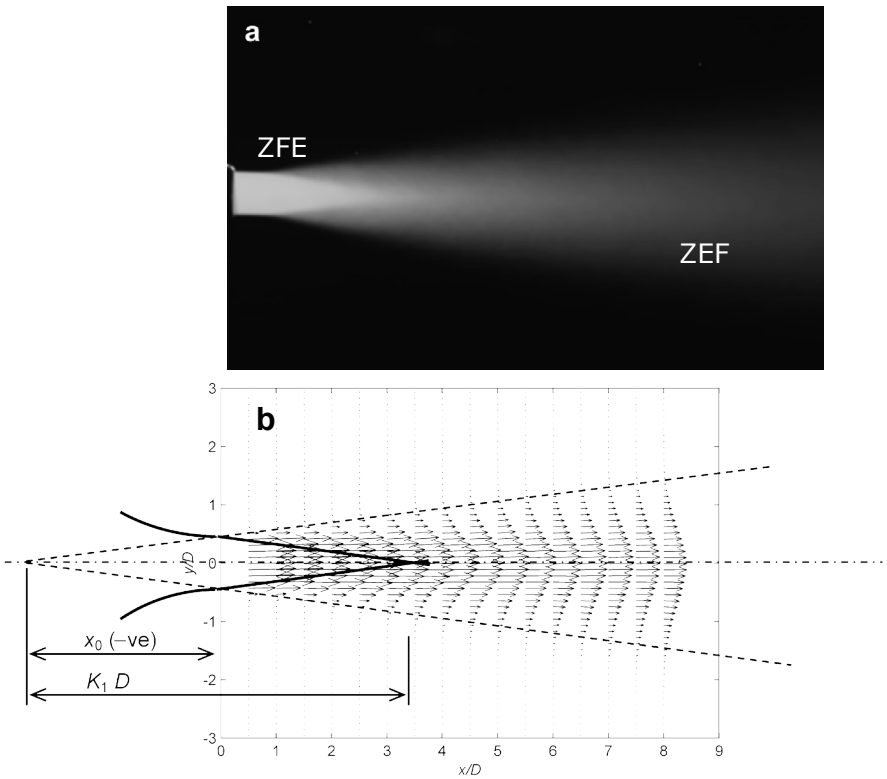

Figure 7.1: Mean concentration field of a jet shown as a grey-level image (a) and mean velocity fields for a simple jet (B). x_0 is the virtue origin and K_1 is a decay constant (Or et al., 2011).

The shear forces in ZEF are much higher compared to further above the nozzle. Injecting the dispersant in and above ZEF is less effective due to reduced mixing (loss of dispersant due to injection into the water instead of into oil cone) and less turbulent conditions. The reduced effectiveness can be seen in the red lines for 15mm (10D) and 45mm (30D) in Figure 6.14. This reduced effectiveness of the dispersant injection high above the nozzle can be explained by;

1. the droplets are already formed
2. reduced turbulence/shear forces in this zone compared to closer to the nozzle
3. further splitting into smaller droplets demands higher turbulence
4. less effective use of dispersant, since some is injected into the water phase instead of the oil

This can also be seen from the measured IFT from oil samples collected in the Tower basin during experiments Table 6.9 and Table 6.10 where the oil samples collected close to the nozzle have significantly lower IFT and corresponding smaller VMDs.

When the dispersant is injected directly into an oil cone in the zone of established flow (e.g. 4.5 mm or 3D) it looks like there is a limited effect of increasing the dispersant dosage (DOR) from 1:100 to 1:50. The shift in VMD from 1:100 to 1:50 is only from 88 to 75 microns.

7.4.3 Injection horizontally into the plume

These experiments were originally designed to study dispersant released on the side of the rising plume and then drawn into the plume. However, the tube or nozzle used for dispersant injection was so small that instead of releasing the dispersant into the water it had sufficient release velocity to be injected into the zone of flow establishment (4.5 mm or three release diameters) of the rising oil (see Figure 6.11 and Figure 6.16).

Injection experiments were performed with two dispersant treatment ratios (DOR: 1:100 and 1:50) and a series of different injection distance (0 – 20 mm). Single experiments were also performed at DOR: 1:25 and 1:12.5 with a distance of 5 mm (see Figure 6.17, Table 6.11 and Table 6.12).

The horizontal distance has limited effect on the shift in droplet size distribution in our Tower basin, as long as the dispersant beam enters directly into the oil cone close to the release nozzle (4.5 mm or 3 nozzle diameters). The differences in VMD versus dispersant treatment ratios are (at a horizontal distance of 5 mm) for DOR: 1:100/50/25 and 12.5; 88, 75, 63 and 54 microns.

This means that doubling the dispersant volume from DOR 1:100 to 1:50 in our Tower basin, will only lower the VMD from 88 to 75 or 0.40 to 0.34 relative to oil alone (219 microns), see Table 6.11and Table 6.12.

7.5 Release of warm oil

This experiment was not a part of the original experimental design, but was included later in the process, since we omitted some dispersant injection experiments (dispersant ring).

The dispersant was injected with the simulated insertion tool to ensure good contact and mixing of the dispersant into the warm oil before release.

Not all the experimental data presented in Figure 6.17 and Figure 6.18 was as initially expected. The "cold" and "warm" oil distributions show slightly smaller droplets for the warm oil due to lower viscosity. For the oil treated with dispersants the opposite trend can be seen. For all three treatment ratios (1:100, 1:50 and 1:25) the warm oil gives distributions with slightly larger droplets compared to the cold oil.

This was not as initially expected, and possible factors that might explain this behaviour are listed below:

1. Cooling effect from the injected dispersant could reduce the effect of the warm oil
2. Increased viscosity difference between warm (low viscous) oil and more viscose dispersant give less efficient mixing
3. The critical micelle concentrations (CMC) for the surfactants and the resulting IFT (water/oil) could change at elevated oil temperatures.

Since the treatment ratio is in the range of 1-4%, the cooling effect from the cold dispersant should be minimal (1). Regarding viscosity (2), reduced mixing due to increased difference in viscosity is difficult to justify. It should actually be the other way around with increased mixing since the continuous phase (the oil) is warm and less viscous. The heat from the warm oil should also quickly warm the injected dispersant and lower its viscosity.

Concerning the third point, some studies (Rewick et al., 1984 and Mohajeri & Noudeh, 2012) indicate that CMC of surfactants could decrease with increased temperature. A possible temperature sensitivity of the CMC could also be different for the main groups of surfactants in most dispersants (sorbitan esters, etoxylated sorbitanesters, sulfosuccinate sodiumsalts and branched octanols). This difference could change the internal ratio of the surfactants available for the oil-water interphase, which could increase the IFT and reduce effectiveness of the dispersant.

Measurement at SINTEF on samples from the Tower basin and premixed oil samples (DOR 1:50) show that the IFT increase in the range of 2-10 times going from 10 and 50°C. The significance of this increase in IFT (from ultralow to low) should be verified in both small-scale (spinning drop) and in the Tower basin. This is suggested as an important topic for a possible phase-II study.

7.6 Modified dispersant with reduced amount of solvent

A modified version of Corexit 9500A with reduced amount of solvent was tested with "upstream injection" at varying DOR (1:1000 – 1:25), see Figure 6.19 and Table 6.13. When comparing the shift in droplet sizes as a function of varying DORs for the new product compared to the ordinary version of C9500A (Figure 6.8, Table 6.5 and Table 6.6.) the modified version is significantly more effective.

At a DOR of 1:100 the VMD of the ordinary C9500A is 186 microns and with the modified product 104 microns. At DOR 1:50 and 1:25, the corresponding values are 157 versus 63 and 88 versus 54 microns. This means that the relative shift in VMD at DOR 1:100 is 0.72 for ordinary C9500A and 0.40 for the modified product.

It is difficult to evaluate the significance of this effect (0.72 versus 0.40) without evaluating the exact increased surfactant content in the modified product, since the DOR are similar for the two tests.

7.7 Comparison of the different injection techniques

To easier compare the effectiveness of the different injection techniques, the resulting droplet size distributions are presented in Figure 6.21 and Figure 6.22. The comparison is made for the same nozzle and flow rate (1.5 mm and 1.2 L/min).

The main conclusions from these summary figures are as long as the dispersant is injected close to the nozzle, in the zone of flow establishment before the droplets are formed, all three injection methods (simulated insertion tool, horizontal injection and injection above the nozzle) produce similar droplet size distributions at DOR 1:100.

At DOR 1:50 and 1:25 the insertion tool produces slightly smaller droplets compared to the other injection methods.

7.8 Comparison of dispersant injection at different nozzle sizes

Dispersant was injected above the nozzle at three different nozzle diameters (0.5, 1.5 and 3 mm). The dispersant was in all cases injected 3 nozzle diameters above the nozzles. The droplet distributions for three different DORs (1:100, 1:50 and 1:25) are given in Figure 6.23 and Table 6.14.

The nozzle diameter is a main scaling parameter for the design of the experiments in the SINTEF Tower basin. In the three series of experiments that range over a relatively large range of nozzle diameters (the largest nozzle was six times larger than the smallest) the dispersant was injected in the same position relatively to the nozzle size.

It is not easy to see the strong similarities between the graphs in Figure 6.23, but it is easier comparing the relative shift in droplet sizes (VMD) in Table 6.14. For all three nozzles, a dispersant treatment of DOR 1:100 gives a relative reduction in VMD of 0.34-0.38. This means that for all three nozzle sizes, the droplets (VMD) are reduced to a third at DOR 1:100.

The results from these experiments are very supportive for the basic idea behind SINTEFs down-scaled Tower basin approach. The fact that scaled dispersant experiments gave consistent results is very encouraging for utilizing these results in operational oil spill models.

7.9 Experiments with combined releases of oil & gas (air)

The experiments with oil, gas (air) and dispersants are discussed in section 8.4.

8 Data analyses - Modelling

8.1 Droplet breakup model

The present understanding is that the characteristic droplet size generated by a turbulent oil jet injected into water will follow a Weber number scaling. With the characteristic droplet size represented by the median droplet diameter d_{50}, this implies:

$$d_{50}/D = A\ We^{-3/5} \quad (8.1)$$

where D is the diameter of the exit, A is an empirical coefficient, and We is the exit Weber number, $We = \rho U^2 D/\sigma$, where ρ is the density of the oil, σ is the interfacial tension between oil and water (IFT), and U is the exit velocity. This relationship is valid for interfacial tension limited breakup, but under certain conditions, viscous forces may be of importance (Wang and Calabrese 1986). If these forces are dominant, the characteristic droplet size will instead be related to the exit Reynolds number

$$d_{50}/D = C\ Re^{-3/4} \quad (8.2)$$

where C is an empirical coefficient and the Reynolds number is $Re = \rho U D/\mu$, where μ is the dynamic viscosity of the oil. Wang and Calabrese (1986) derived a semi-empirical equation for the intermediate case, where both interfacial tension and viscous forces are influencing droplet breakup:

$$d_{50}/D = A\ We^{-3/5} (1 + B\ Vi\ (d_{50}/D)^{1/3})^{3/5} \quad (8.3)$$

where B is an empirical coefficient and Vi is the Viscosity number, $Vi \equiv We/Re = \mu U/\sigma$.
For large values of the viscosity number, $Vi >> 1$, Eq. 8.3 can be approximated by the equation

$$(d_{50}/D)^{4/5} = A\ We^{-3/5} (B\ Vi)^{3/5} \quad (8.4)$$

By taking into account that the viscosity number is the ratio between the Weber number and the Reynolds number, Eq. 8.4 can also be expressed in terms of the Reynolds number:

$$(d_{50}/D)^{4/5} = A\ B^{3/5}\ Re^{-3/5}, \text{ or } d_{50}/D = A^{5/4}\ B^{3/4}\ Re^{-3/4} \quad (8.5)$$

This implies that the coefficient C in Eq. 8.2 is $C = A^{5/4}\ B^{3/4}$. Wang and Calabrese's equation (Eq. 8.3) thus changes smoothly from a Weber number scaling to a Reynolds number scaling when the viscosity number increases and eventually becomes very large ($Vi >> 1$). This condition can be met for high exit velocities, high oil viscosities, or for low interfacial tensions. The latter may result from injection of a chemical dispersant into the oil, which may reduce IFT by a factor of 100 or more.

8.2 Empirical model for predicting droplet sizes

We have used Wang and Calabrese's model (Eq. 8.3) as the basis for developing a new algorithm for prediction of droplet sizes in oil jets. The values that were used are obtained from experiments with untreated oil, and experiments with dispersants injected upstream in the oil line in different

dispersant to oil ratios (DOR), and in addition, results from experiments where the dispersants were injected a short distance before the outlet (simulated injection tool) and a short distance after the outlet (vertical injection 1.5 mm above the outlet). The main results are summarized in **Table 8.1**, which also include the test conditions (nozzle size and volume flow rate, and various derived variables, such as exit velocity, Weber number and viscosity number). For the cases with dispersants, the interfacial tension values were measured on oil samples taken from the plume. In some cases with low DOR (i.e in the range 1:1000 to 1:250, marked with grey shading in **Table 8.1**), we have noted that the peak droplet size is practically insensitive to the observed variations in the reported IFT values. This discrepancy might indicate that the dispersant has been inefficiently mixed into the oil line before the exit nozzle, and thus having limited effect on oil droplet breakup. However, during handling and storage of the samples, oil and dispersants would have been blended in the sampling flasks, causing a significant reduction in the measured IFT values. Due to this uncertainty, we have excluded these tests from the data analyses.

Table 8.1: Data from tower tank tests. Grey shading indicates tests that have been excluded from the analyses due to uncertainties in the recorded IFT values (see text). Here, D is the nozzle size; Q the oil flow rate; DOR the dispersant to oil ratio; We the Weber number; U the exit velocity; Vi the viscosity number and d_p the peak droplet diameter obtained from the LISST droplet size measurements. IFT data in bold are estimated as mean values from other experiments with same DOR.

Date	D, mm	Q, L/min	DOR	IFT, mN/m	U, m/s	We	Vi	d_p, um
17.04 2012	1.5	1.5	-	16.5	14.1	1.53E+04	9	144.0
	1.5	1.5	1:1000	14.7	14.1	1.72E+04	10	144.0
	1.5	1.5	1:500	13.2	14.1	1.91E+04	11	104.0
	1.5	1.5	1:250	4.5	14.1	5.60E+04	31	88.2
	1.5	1.5	1:100	1.5	14.1	1.68E+05	94	88.2
	1.5	1.5	1:50	0.002	14.1	1.26E+08	70 736	74.7
	1.5	1.5	1:25	0.07	14.1	3.60E+06	2 021	53.7
26.04 2012	1.5	0.5	-	15	4.7	1.87E+03	3	391.0
	1.5	1.2	-	15	11.3	1.08E+04	8	237.0
	1.5	2.8	-	15	26.4	5.86E+04	18	104.0
Simulated	1.5	1.2	1:100	**0.66**	11.3	2.45E+05	172	74.7
inj. tool	1.5	1.2	1:50	**0.056**	11.3	2.88E+06	2021	53.7
	1.5	1.2	1:25	**0.055**	11.3	2.93E+06	2058	27.7
03.05 2012	0.5	0.1	-	15	8.5	2.02E+03	6	170.0
	0.5	0.2	-	15	17.0	8.07E+03	11	88.2
	0.5	0.5	-	15	42.4	5.04E+04	28	27.6
Injection	0.5	0.2	-	0.658	17.0	1.84E+05	258	32.7
above	0.5	0.2	-	0.056	17.0	2.16E+06	3032	19.9
06.06 2012	1.5	1.2	-	18.2	11.3	8.87E+03	6	237.0
Injection	1.5	1.2	1:100	0.5	11.3	3.23E+05	226	74.5
1.5 mm ab.	1.5	1.2	1:50	0.001	11.3	1.61E+08	113177	63.3

Date	D, mm	Q, L/min	DOR	IFT, mN/m	U, m/s	We	Vi	d_p, um
28.06 2012	1.5	1.2	-	18.1	11.3	8.92E+03	6	237.0
	1.5	1.2	1:1000	7.5	11.3	2.15E+04	15	237.0
	1.5	1.2	1:500	2.4	11.3	6.72E+04	47	237.0
	1.5	1.2	1:250	0.7	11.3	2.31E+05	162	170.0
	1.5	1.2	1:100	0.09	11.3	1.79E+06	1 258	104.0
	1.5	1.2	1:50	0.07	11.3	2.31E+06	1 617	63.3
	1.5	1.2	1:25	0.05	11.3	3.23E+06	2 264	53.7

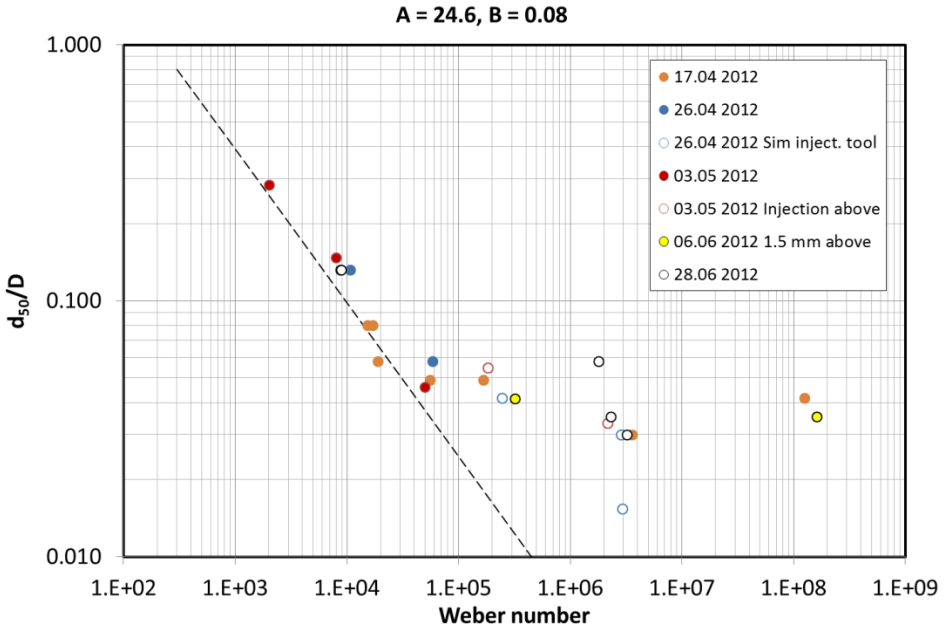

Figure 8.1 shows a plot of the relative median droplet size (d_{50}/D) vs. the exit Weber number for untreated oil and oil with premixed dispersants. The median droplet size is derived from the peak droplet diameter by assuming $d_{50} = d_p/1.2$, where the factor 1.2 is based on a presumed Rosin Rammler type droplet size distribution (Johansen et al. in press). The graph shows clearly that the Weber number scaling does not hold for a large number of the cases. As expected, the largest deviations were found for cases with premixed dispersants. Figure 8.2 shows the same results versus the outlet Reynolds number.

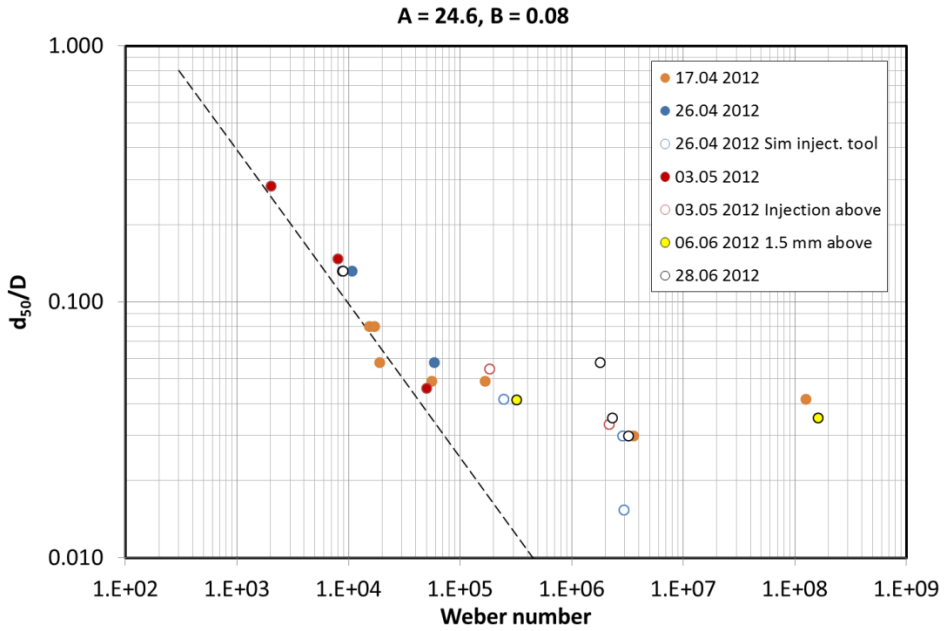

Figure 8.1: Weber number plot of median droplet size data for Oseberg Blend – results with no treatment and with dispersants. The broken line shows the Weber number scaling model (Eq. 8.1).

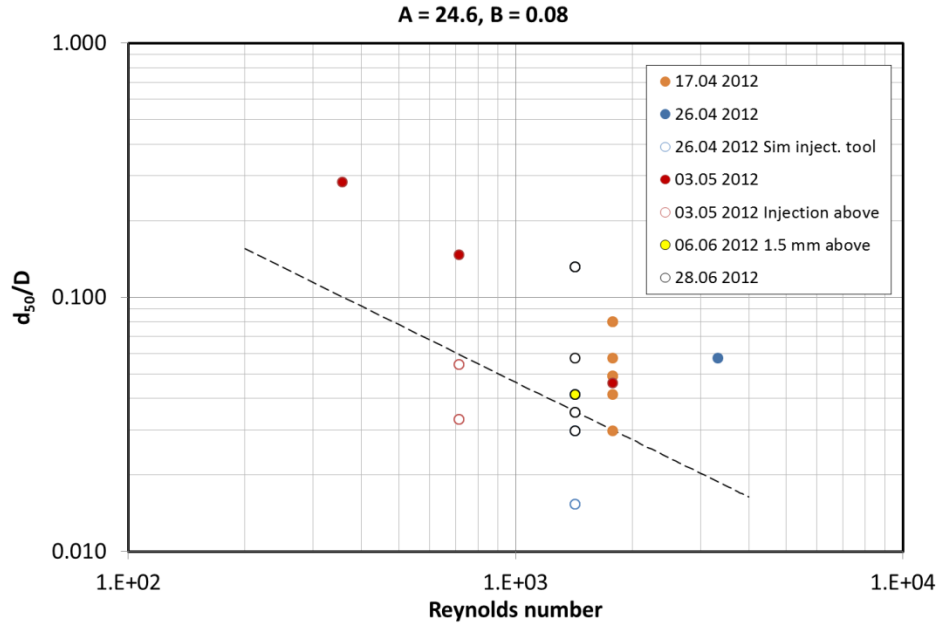

Figure 8.2: Reynolds number plot of median droplet size data for experiments with no treatment and with dispersants. The broken line shows the Reynolds number scaling model (Eq. 8.2).

Figure 8.3 shows a plot of the same results based on Wang and Calabrese's model, with coefficients A and B determined by best fit for all data. Figure 8.4 shows the best fit correlation (computed vs. measured values of d_{50}/D).

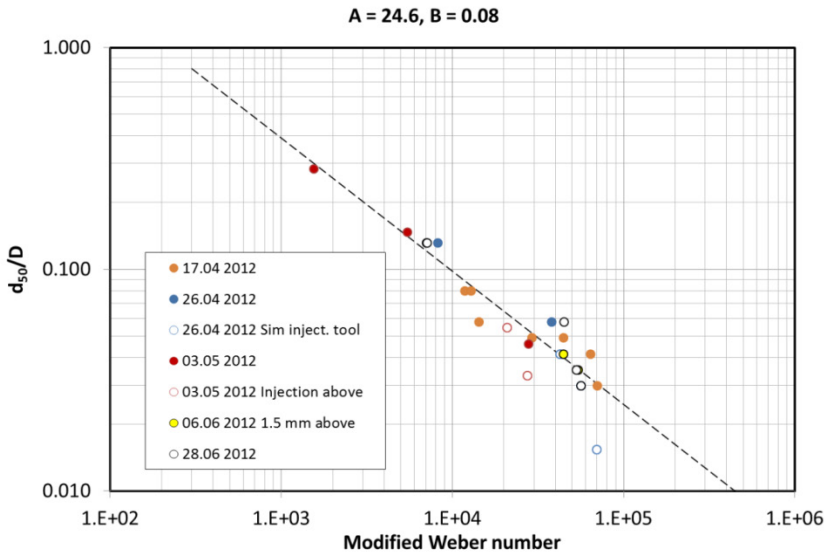

Figure 8.3: Modified Weber number plot of median droplet size data for experiments with no treatment and with dispersants. The modified Weber number includes the correction for the viscosity effect, and is defined as $We^* = We/[1 + B\ Vi\ (d_{50}/D)^{1/3}]$. The broken line represents the Wang and Calabrese model with coefficients A = 24.6 and B = 0.08.

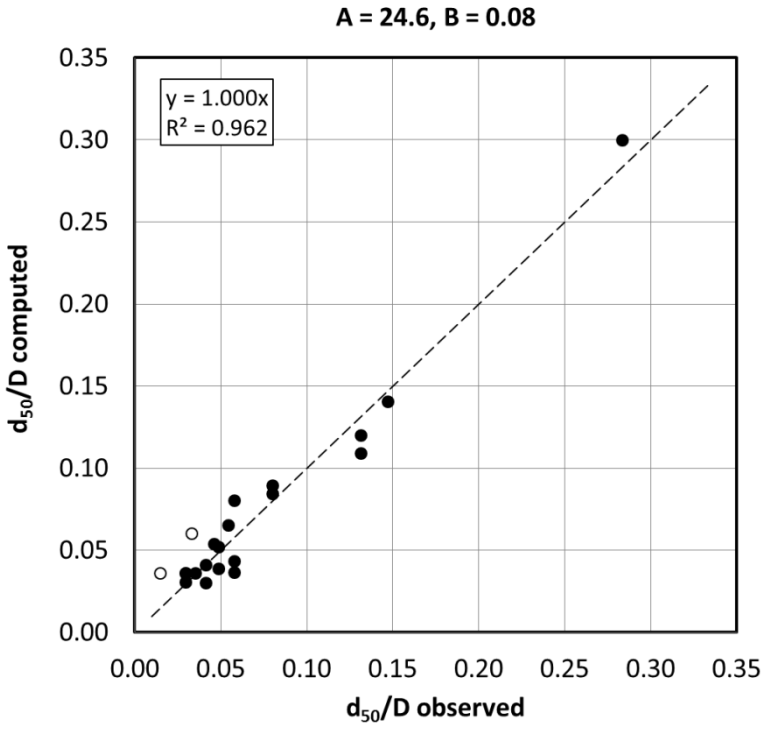

Figure 8.4: Measured and computed relative median droplet sizes d_{50}/D from all experiments. The computed values are determined with the Wang and Calabrese model with best fit coefficients A = 24.8 and B = 0.08. The data points with open markers are excluded from the correlation (see text).

In order to demonstrate the implications of the modified Weber number model, we have used results from the April 17 experiments (Figure 8.5). The figure shows measured median droplet diameters as a function of the corresponding viscosity number Vi = μ U/σ, where μ is the dynamic viscosity of the oil, U is the exit velocity and σ is the interfacial tension. Since the oil viscosity and the exit velocity are constant in these experiments, increasing values of Vi is caused by reduced interfacial tension due to injection of dispersants with increasing DOR. The computed line shows an asymptotic behavior with increasing values of Vi, with the median droplet diameter approaching a lower limiting value (broken line), determined by the exit Reynolds number (Eq. 8.5). The measured median droplet diameters follow a comparable trend, with deviations most probably related to uncertainties in the determination of the interfacial tension. Further details can be found in Johansen et al., 2013.

This demonstration has two important implications:

- Below a certain DOR, further increase in DOR will have minor effect on the median droplet size
- The achievable minimum droplet size will be limited by the exit Reynolds number

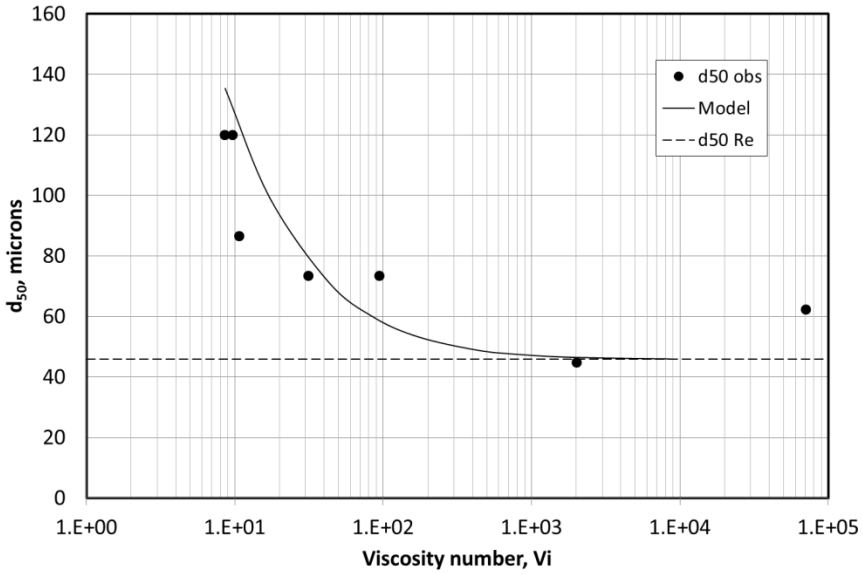

Figure 8.5: Measured and computed median droplet sizes d_{50} from the April 17 experiment with 1.5 mm nozzle diameter and 1.5 l/min oil flow rate. The viscosity number increases due to reduced IFT caused by injection of dispersants with increasing DOR. The computed values (marked "Model") are determined with the Wang and Calabrese model with the coefficient A and B as found above. The broken line marked "d50 Re" represent the lowest achievable median droplet size for the given Reynolds number (Eq. 6.5).

8.3 Droplet size distributions

The analysis above provides a method for estimating the median droplet size depending on outlet conditions and IFT, but in order to predict the actual droplet size distribution, an appropriate size distribution function and its parameters must be known. Here, we will consider to distribution functions commonly used for representing droplet and particle size distribution; the lognormal distribution and the Rosin Rammler distribution.

The lognormal distribution is in principle a normal distribution based on the logarithm of the observed droplet sizes, and may be expressed as Normdist(x, mean, stdev) where x = ln(d), mean = arithmetic mean of x and stdev is the standard deviation of the x-values. The Rosin Rammler distribution is expressed by the equation $V = 1 - \exp[k\,(d/d_{50})^{\alpha}]$, where V is the cumulative volume fraction, the coefficient k = 0.693, d_{50} is the volume median droplet size, and α is the spreading parameter. The validity of a chosen distribution function can be tested by linearization. If the observations fall on a straight line after certain transformations of the variables, the chosen distribution function applies, and the parameters for the distribution can be determined.
For the lognormal distribution, linearization is obtained by plotting normalized deviations from the mean as a function of the logarithm of the droplet size. The normalized deviations S are expressed in units of standard deviations, and may be determined from the cumulative probabilities P by the function S = NormInv(P, mean = 0, stdev = 1). The Rosin Rammler distribution can be linearized by plotting the logarithm of Y = -ln(1-V) as a function of the logarithm of the droplet size. When several data sets are involved, it is convenient to rather use a relative measure of the droplet size, i.e. $\delta = d/d_{50}$, where d_{50} is the volume median droplet diameter.

We have applied this approach to two series of experiments – the series from April 14 2012 with upstream injection of dispersants in a wide range of DOR, and the vertical dispersant injection experiments conducted on July 6 2012. The cumulative distributions that were obtained from the LISST data are shown in Figure 8.6. Note that the distributions are limited upwards by the 500 microns upper detection limit of the LISST instrument. The cumulative volume fraction at the detection limit is estimated from the observed peak diameter – presumed to corresponding to 50% by volume – and a best fit logarithmic standard deviation for the whole set. The graphs show a clear left-hand shift in the droplet distributions with increasing DOR values and decreasing injection heights, while the shape of the distributions seems to be more or less unchanged. Figure 8.7 and Figure 8.8 show the same distributions in linearized form.

Figure 8.7 indicates distinct differences between the two tests series. To the extent that a lognormal distribution applies to the data, the vertical injection tests from June 6 implies a significantly larger standard deviation than the upstream injection test series from April 17 (stdev = 1.1 vs. 0.7). Moreover, the April 17 series gives a good fit to a lognormal distribution for S-values down to -2, corresponding to a cumulative volume fraction of 2%. The data from the June 6 test series also shows a reasonably good fit to a lognormal distribution, even while the data deviates more from a straight line. However, these deviations may to some extent be due to variations in the standard deviations between the different tests.

The Rosin Rammler plot in Figure 8.8 indicates that the data from the April test series gives the best fit to the Rosin Rammler distribution in the low to medium range of the distribution. Distinct deviations from a straight line are seen for Y-values below 0.01 and above 2.3, corresponding to cumulative volume fractions of respectively 1% and 90%. For the June 6 test series, the results indicate significant variations in the spreading parameter of the Rosin Rammler distribution. A good fit is found with α = 1.8 for the whole range of the oil only data, but to the extent that the Rosin Rammler function applies, data from the injection tests implies smaller values of the spreading parameter.

In total, these findings point in favour of the lognormal distribution, but with the implication of possible variations in the standard deviations depending of the injection method. For the upstream injection tests, the best fit overall to the lognormal was obtained with stdev = 0.7, while a larger standard deviation (stdev = 1.1) was found for the vertical injection tests.

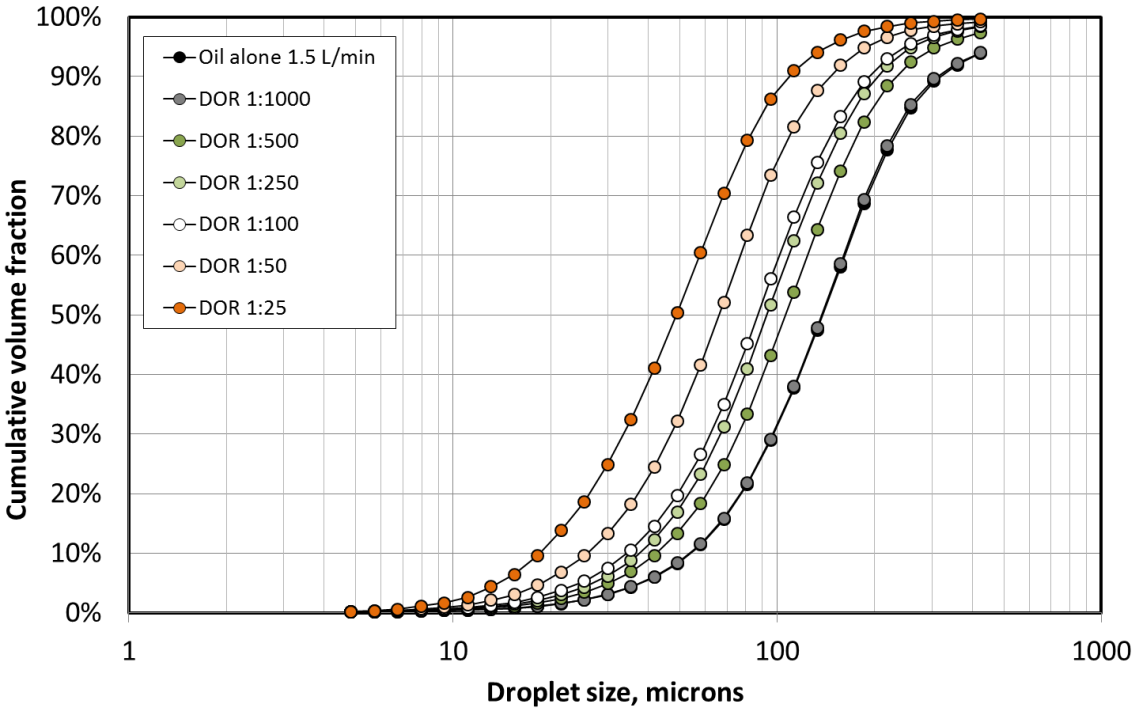

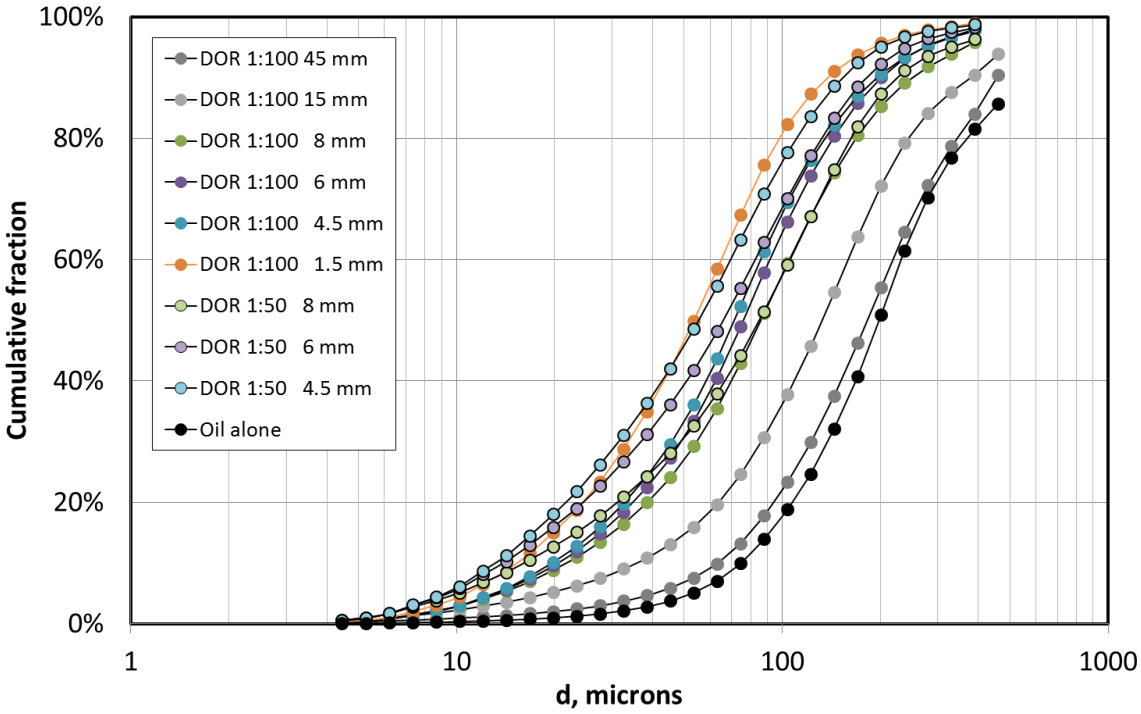

Figure 8.6: Measured droplet size distributions from the April 17 experiments with upstream injection of dispersants (top) and the June 6 experiments with injection of dispersants at various heights above the nozzle (bottom). Corresponding DOR values and heights are given in the legend. Note that the distributions are limited upwards by the 500 microns upper detection limit of the LISST instrument. See text for more details.

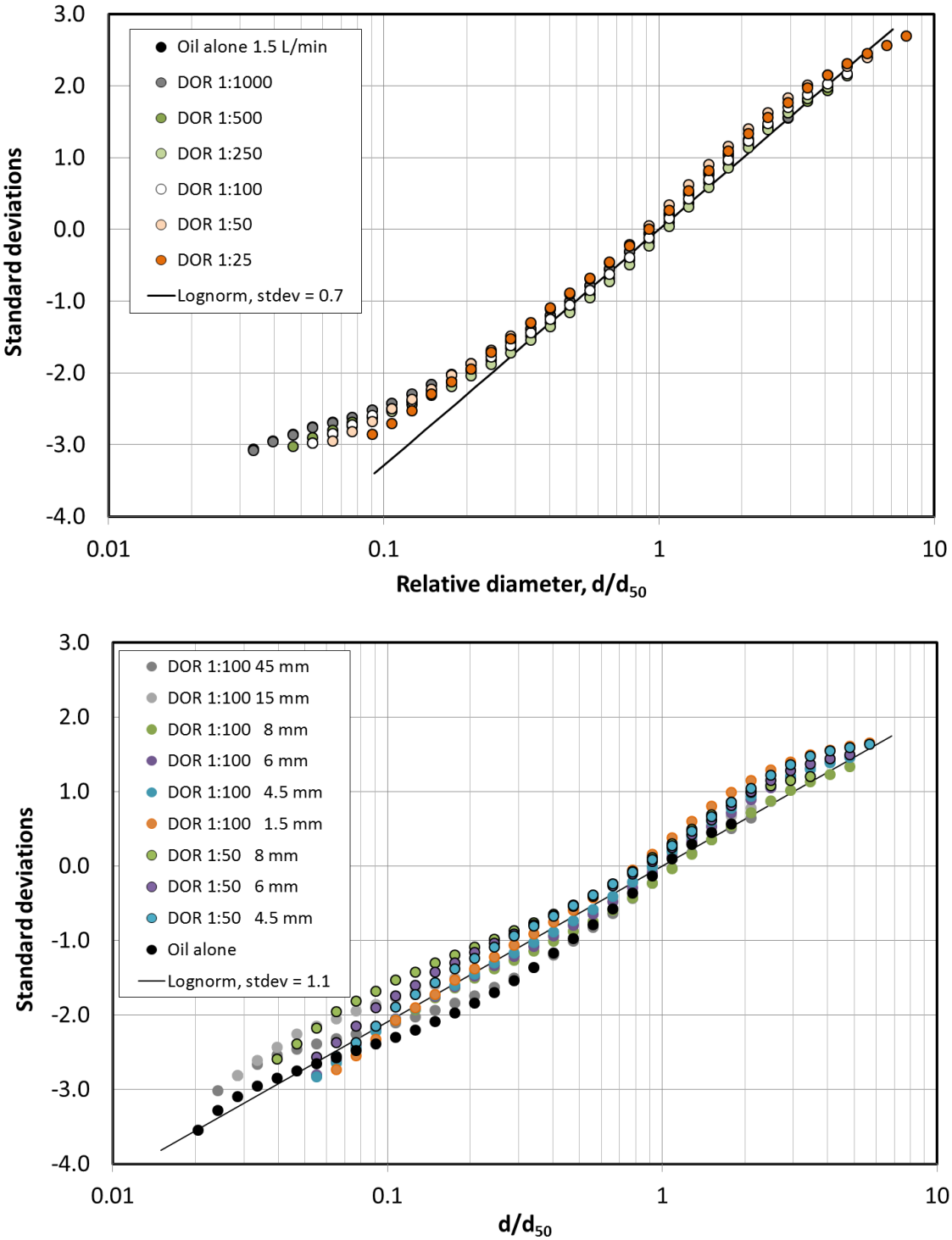

Figure 8.7: Lognormal linearized droplet size distributions from the April 17 experiments and the June 6 experiments. Corresponding DOR values and heights are given in the legend. Note that the distributions are limited upwards by the 500 microns upper detection limit of the LISST instrument. See text for more details.

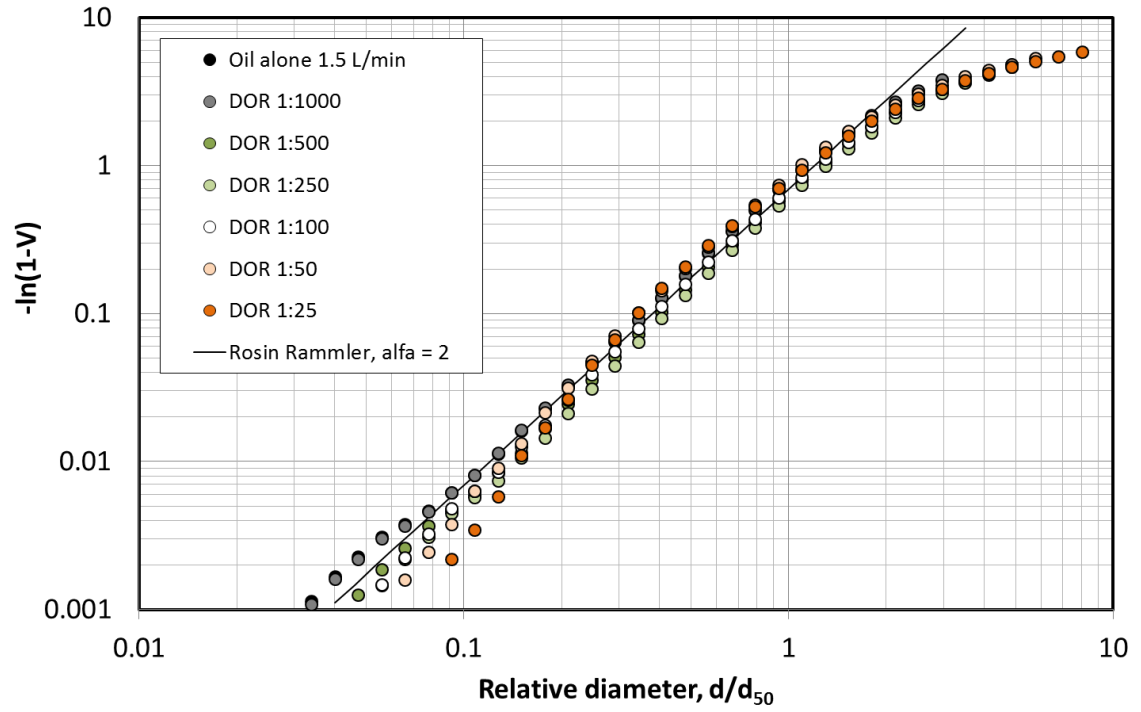

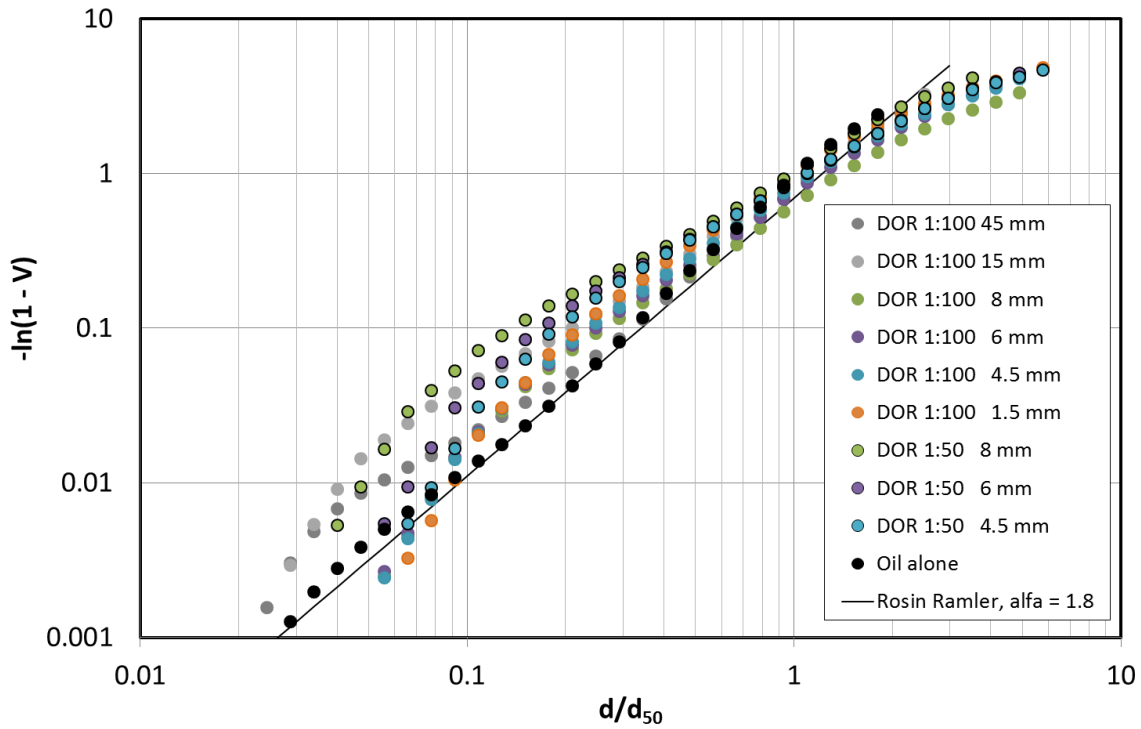

Figure 8.8: Rosin Rammler linearized droplet size distributions from the April 17 experiments and the June 6 experiments. Corresponding DOR values and heights are given in the legend. Note that the distributions are limited upwards by the 500 microns upper detection limit of the LISST instrument. See text for more details.

8.4 Effects of air injection

In the chapter on the theory of droplet breakup in turbulent jets (Chapter 3), we found that the effect of gas released together with oil could be accounted for in terms of an efficient exit velocity expressed by the equation $U_e = U_{oil} (1 - n)^{-1/2}$, where U_{oil} is the oil only exit velocity (i.e. the oil volume flow rate divided by the nozzle cross section), and n is the gas void fraction in the exit flow. Due to the fact that the LISST instrument does not discriminate between gas bubbles and oil droplets, the present experimental setup makes it difficult to test this assumption directly. However, in this section, we will make an attempt to separate gas bubbles from oil droplets on a theoretical basis. For this purpose, we have selected two experiments with injection of dispersants at a DOR of 1:50 with the simulated injection tool. The first experiment was conducted with oil only, while in the second experiment, air was injected together with oil at a 1:1 ratio. Figure 8.9 shows the droplet size distributions obtained with the LISST instrument in both cases. The nozzle diameter was 1.5 mm, and the total flow rate was 1.2 L/min in both cases, but made up of equal volume parts of air and oil in the second case, corresponding to a gas void fraction of 50%.

The oil only experiment has a peak droplet diameter of 53.5 microns, while the peak diameter is shifted to 237 microns in the second experiment. However, the second distribution seems to be bimodal, with a secondary peak at about 75 microns. This secondary peak coincides reasonably well with the expected shift in the median droplet size due to the mixed oil and gas flow: with equal total flow rate, but a void fraction of 50%, the effective exit velocity will be reduced by a factor of 1.4 (square root of two). With a Reynolds number correlation for the median droplet size with an exponent of -3/4, this implies an increase in the median droplet size with a factor of 1.3, i.e. from 53.5 to 69.3 microns.

Assuming that the bimodal distribution reflects a sum of the distributions of oil droplets and gas bubbles, the main peak will be related to the peak diameter of the gas bubble distribution. Figure 8.10 shows an attempt to explain the total distribution in terms of two distinct distributions, one representing oil droplets, and one representing gas bubbles. Both distributions are presumed to be log-normal distributions, defined be the median droplet/bubble diameter and the logarithmic standard deviation.

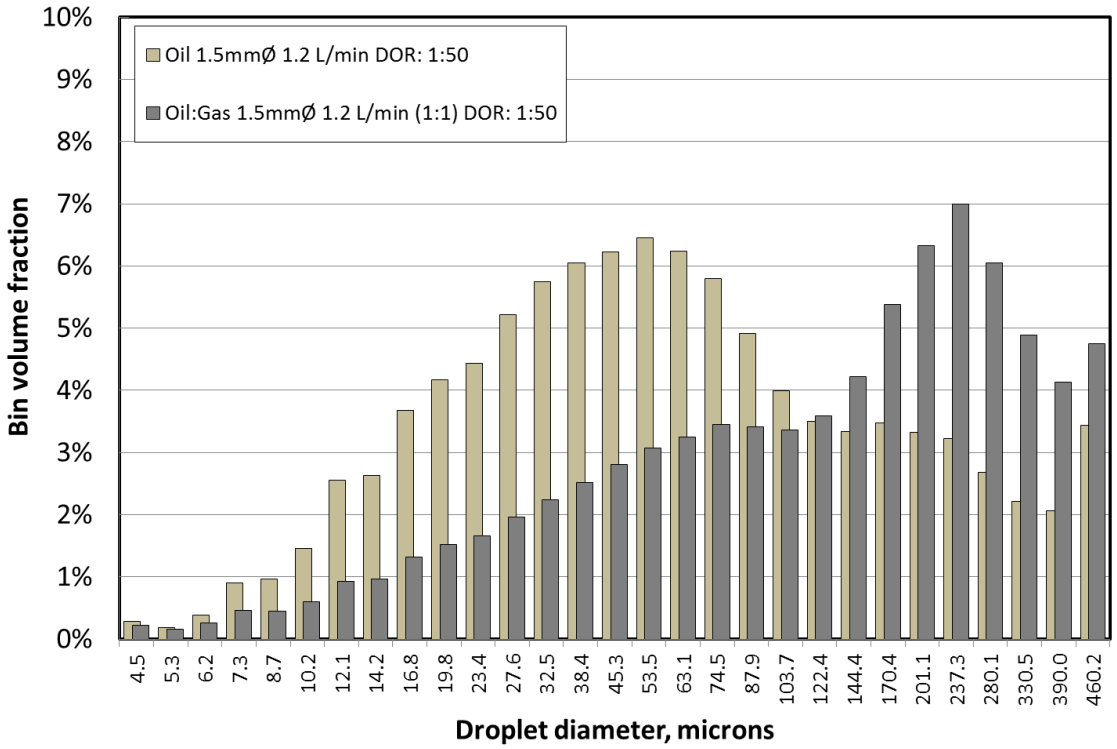

Figure 8.9: Droplet size distributions obtained with the LISST instrument for two experiments with injection of dispersants, one with oil only and one with gas together with oil (see legend).

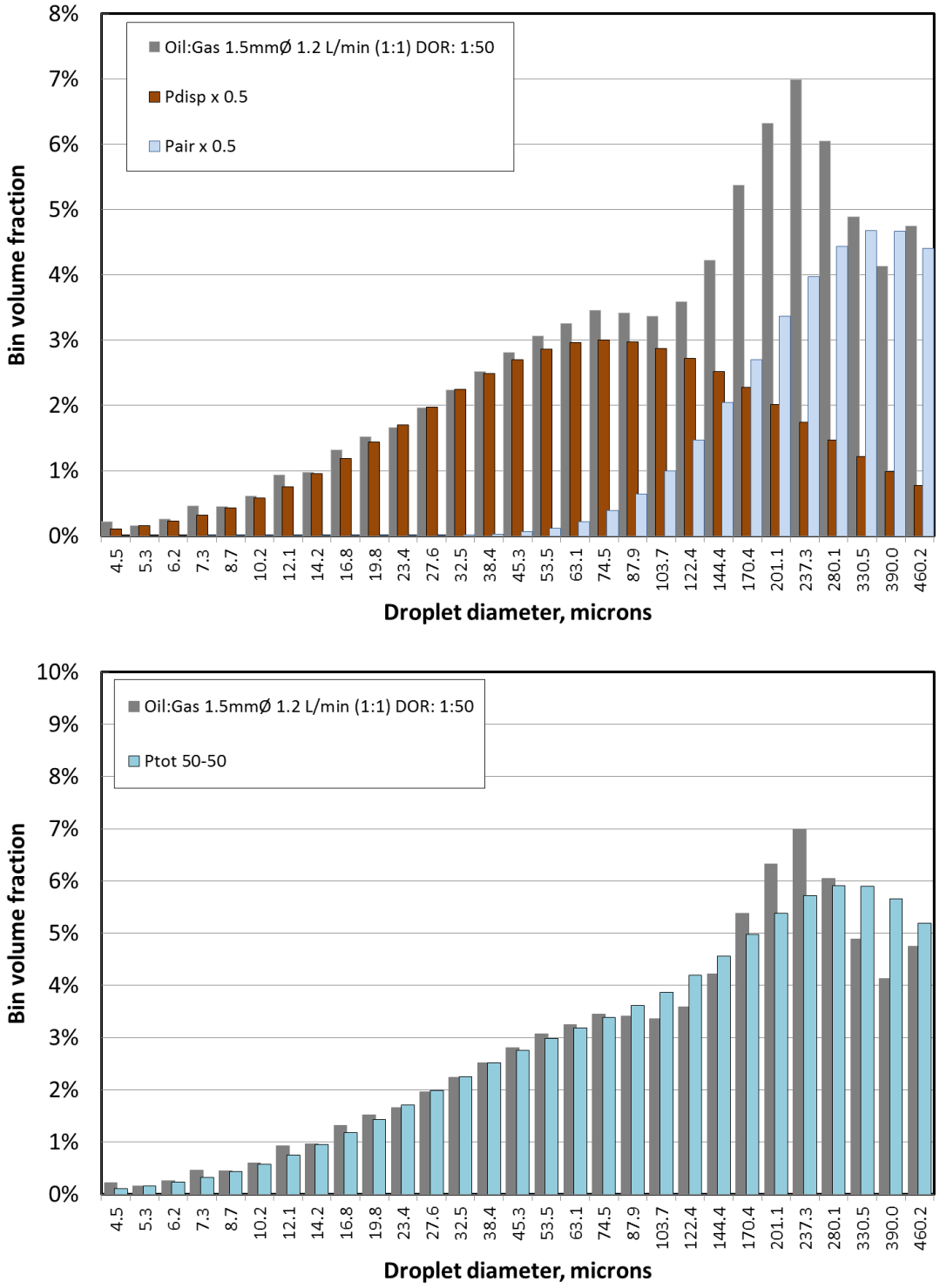

Figure 8.10: Bimodal droplet size distributions composed of equal amounts of oil and gas. The top graph shows the presumed distributions for oil droplets and gas bubbles (each reduced by a factor of 0.5) on the background of the observed bimodal distribution (grey columns). The bottom graph shows the combined distribution on the background of the observed distribution (grey).

The median diameter for the oil droplet distribution is taken as 70 microns, according to the assumption above on the effect of a 50% void fraction, while the standard deviation is chosen as 1.1 in natural log units based on the observed distribution (see top graph in Figure 8.10). For the air bubble distribution, the standard deviation was set to 0.7 in natural log units, and the median air bubble diameter was chosen as 330 microns. The latter is larger than the observed main peak at 237 microns, but is meant to account for the left-hand shift in the visible peak due to the superposition of the droplet size distribution. However, the median bubble size of 330 microns also corresponds to the peak diameter observed in a parallel experiment with 1:1 flow rates of water and air, where the nozzle size and the total flow rate was the same as in the oil-air experiments, but with water replacing oil. Figure 8.10 shows that the bimodal character of the distribution is less pronounced in the computed composite distribution, but when presented in cumulative form, the correspondence between the observed and computed distributions is striking, as shown in Figure 8.11.

Thus, in total, the present analysis of the results from the experiment with dispersant injection in a mixed oil and air flow is found to provide a plausible explanation of the observed increase in the peak droplet size as an effect of the presence of gas bubbles. Secondly, it also gives support to the assumption of the momentum related effect of gas on the median droplet size.

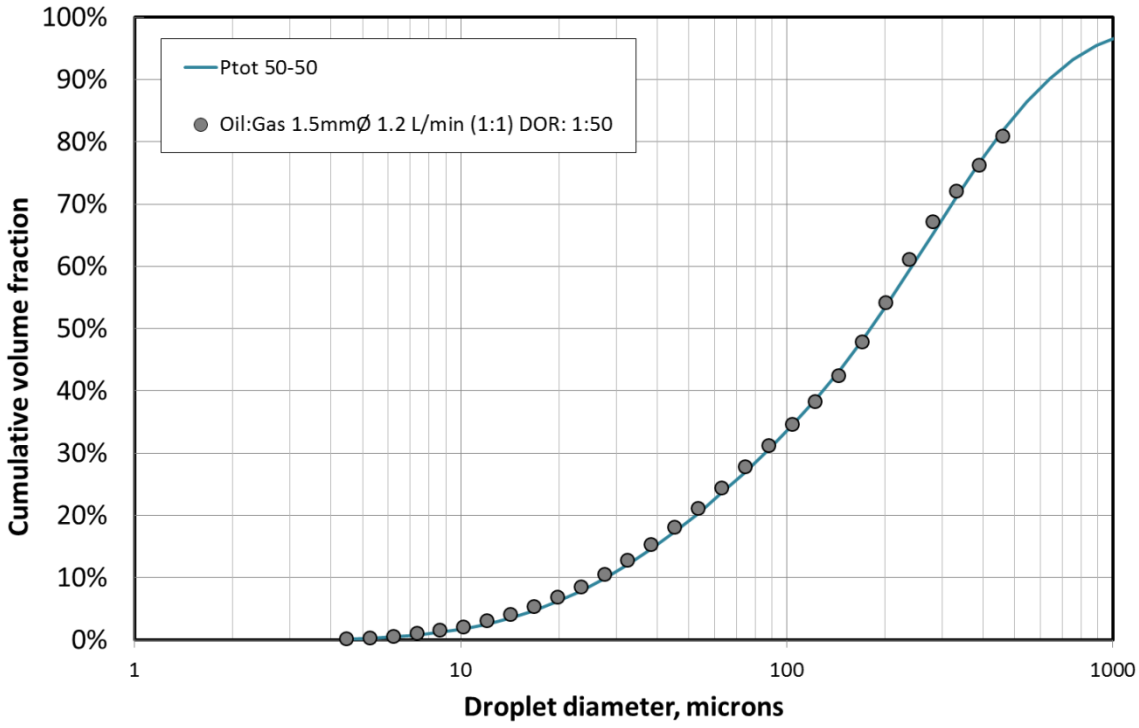

Figure 8.11: Cumulative droplet size distributions composed of equal amounts of oil and gas. The markers show the observed cumulative distribution from the experiment discussed above with dispersant injection with DOR 1:50 in a mixed (1:1) oil and air flow. The solid line shows the computed distribution composed of separate oil droplet and gas bubble distributions.

8.5 Up-scaling from lab to field

Up-scaling of the results from the tower tank experiments to full scale conditions may in principle be based on a Weber number scaling. By assuming a certain full scale outlet diameter D, we can determine the oil flow rate Q that corresponds to a Weber number in one of the laboratory experiments. From the expression for the outlet volume flow $Q = \pi/4\ D^2\ U$ we can eliminate the outlet velocity U and get an expression for the Weber number in terms of volume flow:

$$We = (\rho/\sigma)\ (4/\pi)^2\ Q^2/D^3 \qquad (8.6)$$

Solving for Q gives us an expression for the equivalent oil volume flow Q_{eq} for a given outlet diameter and Weber number:

$$Q_{eq} = \pi/4\ We^{1/2}\ (\sigma/\rho)^{1/2}\ D^{3/2} \qquad (8.7)$$

The corresponding oil only outlet velocity will be:

$$U = Q/\ (\pi/4\ D^2) \qquad (8.8)$$

For releases with both gas and oil, we must also apply the void fraction adjustment as described in Chapter 3. For large volume flows which might be buoyancy dominated, an exit Froude number adjustment must also be applied, also described in Chapter 3:

Adjustment for void fraction:

$$U_n = U/(1 - n)^{1/2}, \qquad (8.9)$$

where U is the oil only outlet velocity and n is the gas void fraction at the exit.

Adjustment for buoyancy (large volume flows):

$$U' = U_n\ (1 + Fr^{-1}), \qquad (8.10)$$

where $Fr = U_n\ /(g'\ D)^{1/2}$ with $g' = g\ [\rho_w - \rho_{oil}\ (1 - n)]/\rho_w$.

The adjusted velocity U´ is used in the Weber and Reynolds numbers to get respectively $We' = \rho\ U'^2\ D/\sigma$ and $Re' = \rho\ U'\ D/\mu$, and these corrected non-dimensional numbers are then used in the modified Weber number correlations to predict the volume median droplet size.

Table 8.2 shows two examples where these principles have been applied to up-scaling. The different variables in the table are explained in the following.

Table 8.2: Up-scaling from tower tank tests to field test and full scale conditions. Variables are explained in the text.

	D, mm	Q_{oil}	Void	U_{oil}, m/s	U', m/s	We'	Re'	d_{50} oil	d_{50} disp
Lab. exp.	1.5	1.5 L/mn	0 %	14.1	14.1	15 283	1 783	133 µm	45 µm
Field exp.	120	64 m^3/h	50 %	1.6	2.5	38 273	25 230	5.4 mm	0.5 mm
Full scale	400	392 m3/h	50%	0.9	2.7	153 670	92 300	7.7 mm	0.76 mm

The equivalent oil flow rate Q_{oil}, is determined from the Weber number and the chosen up-scaled outlet diameter D by use of Eq. 8.7. The corresponding oil only outlet velocity U_{oil} is computed from Eq. 8.8. This velocity is adjusted for gas void fraction (Eq. 8.9) and Froude number (Eq. 8.10) to get the adjusted velocity U'. The volume median droplet sizes d_{50} are computed from the modified Weber number model (Eq. 8.3) for untreated oil (d_{50} oil) and treated oil (d_{50} disp), with

dispersant injection presumed to cause a reduction in IFT by a factor of 200. Two up-scaled diameters are shown – one representing the DeepSpill field experiment with an outlet diameter of 120 mm, and one full scale corresponding to a diameter consistent with a blow-out scenario with an outlet diameter of 400 mm.

The resulting droplet size distributions are shown in Figure 8.12. The distributions are based on the volume median diameters shown in Table 8.2. Lognormal distributions with a standard deviation of 0.7 are used for treated oil and untreated oil for lab conditions. For the field experiment conditions and the full scale condition lognormal distributions with the same standard deviation are used for treated oil, while Rosin Rammler distributions with a spreading parameter of 1.8 are used for untreated oil.

Compared to the laboratory conditions, the results for the field experiment and the full scale conditions show considerably larger median droplet sizes, but at the same time, a larger shift is found in the median droplet size from untreated to treated oil. The first effect is due to increased outlet diameters as expected by the Weber number scaling: $d_{50} = D\ A\ We^{-3/5}$, implying $d_{50} \sim D$ for constant We. However, it should be noted that the computed increase in the median droplet will be much less than proportional to the increase in diameter when the effects of void fraction and buoyancy is taken into account. Keeping in mind that the median droplet size for treated oil may be expected to follow a Reynolds number correlation, the increased relative effect on treatment for the field experiment and full scale conditions may be related to the large increase in the Reynolds number caused by the increased outlet diameters: assuming constant Weber number and increasing outlet diameter, the Reynolds number will increase in proportion to the square root of the diameter. In addition, since the adjustment for void fraction and buoyancy will cause an increase in the effective outlet velocity, a further increase in the Reynolds number will follow, as shown in Table 8.2.

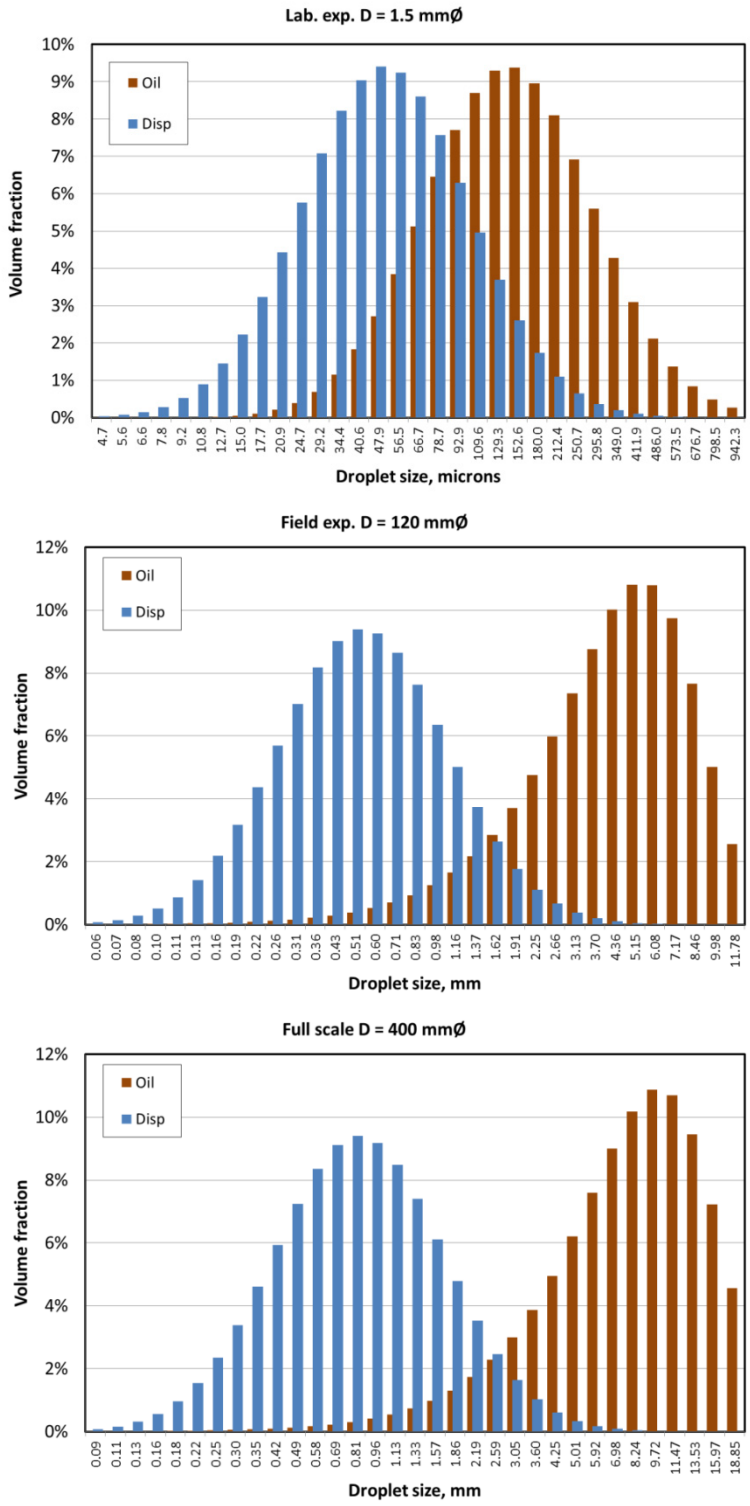

Figure 8.12: Droplet size distributions for laboratory scale (top), field scale (middle) and full scale discharges (bottom), with oil only flow rates computed from the Weber number corresponding to the experimental conditions. Blue columns represent treated oil (labeled "Disp"), while brown columns represent untreated oil (labeled "Oil").

9 Conclusions

The major findings from the discussions are summarized in this chapter.

9.1 Dispersant dosages

The dosage experiments were performed with varying dispersant to oil ratios (DOR) from 1:1000 (0.1%) to 1:25 (4%). Two experiments were performed with Corexit 9500 and one with a reduced solvent version of C9500 (giving approximate 100% more active material).

- A clear correlation between DOR and the shift in droplet size distribution towards smaller droplets was observed. Very limited effect was observed for the lowest concentrations, steadily increasing up to shift corresponding to a third of the initial VMD at the highest concentration.
- The effect of the more concentrated version of Corexit gave shifts in MVD that corresponded to the increased content of active material (double concentration) and corresponding reduction in IFT.

9.2 Dispersant injection techniques

Three different injection techniques were tested; Simulated insertion tool, injection above nozzle into the rising oil and sidewise injection into the rising oil.

- The tested injection methods gave similar results (reduction or shift in VMD), independent of whether the dispersant was injected immediately before the outlet (simulated injection tool) or immediately after the outlet.
- An oil jet sprayed from a nozzle, like in a subsurface blow-out or in our down-scaled experiments, will form a solid oil cone up to approximately 6 nozzle diameters. Injecting the dispersant into this solid oil cone seems to be most efficient. With this approach the dispersant will mix into the oil and reduce the IFT before the oil enters the highly turbulent zone where the droplets are formed.

9.3 Experiments with warm oil

An initial experiment with warm oil (58 °C) was performed. The results indicated a reduced effect of dispersant injection, since larger droplets (VMDs) were measured compared to experiments with lower oil temperature (11 °C). However, the validity of this single initial experiment is uncertain and the effect of oil temperature will be studied more in detail in Phase-II of this project.

9.4 Experiments with different nozzle sizes to verify scaling approach

The nozzle diameter is a main scaling parameter for the design of the experiments in the SINTEF Tower basin. The following experiments were performed to verify the validity of this approach:

- A series of experiments with varying nozzle size (0.5, 1.5 and 3mm)
- Dispersant was injected in the same position relatively to the nozzle size (3 D above).

Dispersant treatment with all three nozzles sizes gave a similar relative reduction in VMD, e.g. 0.34-0.38 for DOR 1:100. This means that for all three nozzle sizes, the diameter of the droplets (VMD) are reduced to a third when using a DOR 1:100.

The results from these experiments are very supportive for the basic idea behind SINTEFs down-scaled Tower basin approach. The fact that scaled dispersant experiments gave consistent results is very encouraging for utilizing these results in operational oil spill models. These models can then be

used both for contingency planning, environmental risk assessments and guidance for operative subsurface releases including dispersant injection (see next chapter).

9.5 Data analysis – Modelling

The major findings from the analysis of the experimental data may be summarized as follow:

Droplet size model:

- The analysis of the results from the tower tank experiment with and without dispersant injection gives support to a modified Weber number model with coefficients A ≈ 25 and B ≈ 0.08. For cases with injection of dispersants at high DOR, this correlation tends to change into a Reynolds number scaling. Further details can be found in Johansen et al., 2013.
- The droplet size distributions for treated oils tend to follow lognormal distributions, while the Rosin Rammler distribution may provide a better fit for untreated oils.

Mixed oil and gas flows:

- The effect of mixed oil and gas flows is difficult to assess directly because the LISST instrument does not discriminate between oil droplets and gas bubbles. However, we have made an indirect assessment by considering droplet size distribution data obtained from two tower tank experiments with upstream injection of dispersants, one with and one without air mixed into the oil line.
- The apparent increase in the peak droplet size with mixed oil and air flows has been explained as an effect of a gas bubble distribution superimposed on an oil droplet size distribution.
- This case study also gives support to the assumption of the momentum related effect of gas on the median droplet size.

Up-scaling from lab to full scale:

- Up-scaling from lab to full scale can occur by choosing a representative full scale outlet diameter and keeping the Weber number constant. On this basis an equivalent oil flow rate can be computed for the full scale conditions.
- Calculations of oil droplet size distributions for up-scaled conditions with untreated oil show an increase in the volume median droplet size with increasing outlet diameters, but when adjustments are made for void fraction and buoyancy flux, this increase is considerably less than expected from a simple Weber number scaling.
- For up-scaled conditions with dispersant injection, a larger relative shift in droplet size is found than in the lab tests. This is explained by the observation that the median droplet size will be expected to follow a Reynolds number correlation for treated oils. Assuming constant Weber number and increasing outlet diameter, the Reynolds number will increase in proportion to the square root of the diameter. In addition, since the adjustment for void fraction and buoyancy will cause an increase in the effective outlet velocity, a further increase in the Reynolds number will follow.

10 Recommendations

The following questions or topics have been identified during the discussion of this report and should be evaluated for further studies:

1. How does the temperature of the released oil influence the droplet size distribution of the oil, both with and without injection of dispersants? The preliminary results from this study should be verified with additional experiments.

2. Does the presence of gas (air), released together with oil, influence the droplet size distribution of the oil, both with and without injection of dispersants? The results obtained so far have been difficult to interpret since the main instrumentation (LISST) cannot distinguish between oil droplets and gas bubbles. Other methods to quantify size of gas bubbles should be evaluated.

3. How does dispersant effectiveness, measured by shift in droplet size distribution, vary as a function of oil properties (different oil types), dispersant type (commercial available products) and dispersant dosage? Several, carefully selected, oil types and dispersants should be tested.

4. How does the deep water pressure (100-300 bars) influence droplet formation and effect of dispersant injection? How can this be studied in pressurized tanks under controlled conditions similar to the SINTEF Tower basin?

5. How does "live oil" influence the formation of droplets and the effect of dispersant injection? How will the release of gas (degassing), precipitation of waxes and asphaltenes, hydrate formation etc. during the release influence oil droplet formation? Can such experiments be performed in pressured tanks as indicated above? Can also additional natural gas be added in these experiments?

6. How do different release or turbulence conditions for the oil release influence droplet formation? Experiments should also be studied with significantly less turbulence, not only in the "Atomizing range", but also in the "Transition" and "Pendant drop" zone.

7. The upper limit for nozzle size and flow rates should be explored. It should be possible to do short term experiments (30-120 seconds?) in the SINTEF Tower Basin with significant higher flow rates (10-15 mm nozzle and 100-200 L/min).

8. How does dispersant treatment influence possible coalescence and droplet splitting in the plume after the initial droplet sizes are formed? Experiments with multiple instruments (LISST at different heights?) could be performed.

9. As an alternative to the resource demanding experiments in the SINTEF Tower basin (42 m^3), bench-scale testing in the new MiniTower (80 L) should be evaluated and compared.

11 References

Brandvik, P.J., Johansen, Ø., Leirvik,F., Farooq, U., and Daling, P.S. 2013. Droplet breakup in sub-surface oil releases – Part 1: Experimental study of droplet breakup and effectiveness of dispersant injection. Mar. Pollut. Bull. 2013 Volume 73, Issue 1, 15 2013, pp. 319-326.

Khelifa and So. (2011). Effects of chemical dispersants on oil-brine interfacial tension and droplet formation. *34th AMOP Technical seminar on environmental contamination and response.* Alberta.

Liu, S. (2007). Alkaline surfactant polymer enhanced oil recovery process. Rice University, USA: PhD Thesis.

Miller et al., R. F. (2001). Characterization of water/oil interfaces. I J. Sjoblom, *Encyclopedic handbook of emulsion technology* (ss. 1-41). New York: Marcel Dekker, Inc.

Standness and Austad. (2000). Wettability alteration in chalk: 2. Mechanism for wettability alteration from oil-wet to water-wet using surfactants. *JPSE, 28*, 123-148.

Zhang et al. (2002). Studies of synergism/antagonism for lowering dynamic interfacial tensions in surfactant/alkali/acidic oil systems 1. synergism/antagonism in surfactant/model oil systems. *J. Colloid Interface Sci., 249*, 187–193.

Zhang et al., H. B. (2001). Determination of low interfacial tension with a laser light scattering technique and a comparative analysis with drop shape methods. *J. Colloid Interface Sci., 237*, 11-20.

Zhu et al., Y. X. (2008). Production of ultra-low interfacial tension between crude oil and mixed brine solution of Triton X-100 and its oligomer Tyloxapol with cetyltrimethylammonium bromide induced by hydrolyzed polyacrylamide. *Colloids Surf. A., 332*, 90-97.

Or, C.M., Lam, K.M. and Liu, P. 2011: Potential core lengths of round jets in stagnant and moving envirionments. Journal of Hydro-environment Research, Vol. 5, pp. 81-91.

Mohajeri, E and Noudeh, G.D. 2012: Effect of temperature on the critical micelle concentration and micellization Thermodynamic of non-ionic surfactants: Polyoxyethylene sorbitan fatty acid esters. www.ejchem.net E-Journal of Chemistry. 2012, 9(4) 2268-2274. ISSN: 0973-4945.

Hinze, J.O., 1955: Fundamentals of the hydrodynamic mechanism of splitting in dispersion processes. A.I.Ch.E. Journal, Vol. 1, pp. 289-295.

Masutani, S.M. and E.E. Adams, 2000: Experimental study of multiphase plumes and application to deep ocean oil spills. Final report to the U.S. Department of Interior, Minerals Management Service, contract No. 1435-01-98-CT-30946.

Neto, I.E.L., D.Z. Zhu and N. Rajaratnam, 2008: Bubbly jets in stagnant water. International Journal of Multiphase Flow, 34, pp. 1130-1141.

L. Tang and S.M. Masutani, 2003: Laminar and Turbulent Flow Liquid-liquid Jet Instability and Breakup. Proceedings of the Thirteenth International Offshore and Polar Engineering Conference, Honolulu, Hawaii, USA, pp. 317-324.

Hinze, J.O., 1955: Fundamentals of the hydrodynamic mechanism of splitting in dispersion processes. A.I.Ch.E. Journal, Vol. 1, pp. 289-295.

Johansen, Ø., Brandvik, P.J., and Farooq, U. 2013. Droplet breakup in sub-surface oil releases – Part 2: Predictions of droplet size distributions with and without injection of chemical dispersants. Mar. Pollut. Bull. 2013 Volume 73, Issue 1, 15 2013, pp. 327-335.

Lefebvre, AH, 1989: Atomization and Sprays, Taylor & Francis, 421 pp.

Masutani, S.M. and E.E. Adams, 2000: Experimental study of multiphase plumes and application to deep ocean oil spills. Final report to the U.S. Department of Interior, Minerals Management Service, contract No. 1435-01-98-CT-30946.

Neto, I.E.L., D.Z. Zhu and N. Rajaratnam, 2008: Bubbly jets in stagnant water. International Journal of Multiphase Flow, 34, pp. 1130-1141.

Papanicolaou, P.N. and E.J. List, 1988: Investigation of round vertical turbulent buoyant jets. J. Fluid Mech. Vol. 195, pp. 341-391.

Tang L., and S.M. Masutani, 2003: Laminar and Turbulent Flow Liquid-liquid Jet Instability and Breakup. Proceedings of the Thirteenth International Offshore and Polar Engineering Conference, Honolulu, Hawaii, USA, pp. 317-324.

Wang, C.Y. and R.V. Calabrese, 1986: Drop Brekup in Turbulent Stirred-Tank Contractors. Part II: Relative Influence of Viscosity and Interfacial Tension. AIChE Journal, Vol. 32, pp. 667-676.

Appendix A:
Summary overview of all Tower Basin experiments.

API D3 - Tower basin experiments – Summary log for all experiments (March – June 2012)

Exper no	Date	Nozzle size (mm)	Type of experiment					
			Rate (L/min)	Oil	Gas	Disp GOR Injection	Comments	WS
1	210312	1.5	0.5/1.5/3	OB	N	1:50	Initial experiment and testing of acoustic sensors (Paul Panetta) Problems with flow regulations (low flows). Acoustic data was good and LISST data on 1.5 and 3 L/min. Water sampling	6
2	130412	1.5	0.5/1.5/3	W OB	Yes	No	Experiments with: water/gas, oil/gas and oil only. Constant total flow. No water sampling Oil alone and Water: Air data were bad Oil alone: Air data is good	
3	170412	1.5	1.5	OB	N	DOR	DOR experiments (Upstream injection) Water sampling (IFT) Good LISST data, very good IFT measurements and Cam/Still data	7
4	190412	1.5	0.5/1.5/3	OB	N		New test with oil alone + Sim Insertion tool injection. Not meaningful droplet distributions? Probably polluted/dirty LISST lenses.	10
5	260412	1.5	0.5/1.2/3	OB		SimInjTool	New round with Oil alone 0.5/1.2/3 Regulators OK/Calibrated.	0
6	030512	0.5	0.1/0.2/0.5	OB	N	Rate exp + Inj above nozzle	Problems with autoregulation of flow. Operated manually ➔ OK	0
7	160512	3.0	2 + 5	OB	N	Rate exp + Inj above nozzle	Problems with autoregulation of flow. Operated manually ➔ OK Samples for IFT analysis. Injection too high above nozzle (30 mm)	4

8	290512	1.5	1.2	OB	N	Vert. Inject. DOR 1:50/100	Flow operated manually ➔ OK. Samples for IFT analysis (PJ). Problems with particle in dispersant tube, causing overpressure and rapture of tube. No dispersant injected. Very nice replicate experiments with no dispersant injection.	7
9	010612	1.5	1.2	OB	N	Vert. Inject. DOR 1:50/100	Flow operated manually ➔ OK. Samples for IFT analysis. Problems with LISST instrument ➔ No data saved..!	7
10	060612	1.5	1.2	OB	N	Vert. Inject. DOR 1:50/100	Flow operated manually ➔ OK. Samples for IFT analysis. Injection centered with support rods (se video). Moved UW light and installed extra "Diver lights". Very nice video and LISST data	9
11	080612	1.5	1.2	OB	N	DOR 1:1000-1:25	Flow operated manually ➔ OK. New DOR experiment at reduced flow rate (1.2 L/min) to produce slightly larger and comparable droplet distributions. Very good video/Still (only nozzleCam/still) and LISST data	7
12	140612	1.5	1.2	OB	N	Horzontal inj DOR 1:50/100	Very successful experiment. Nice pictures with new macro still/video camera.	8
13	200612	1.5		OB	N	Sim inj. tool DOR: 1:100/50/25	Warm vs. cold oil, first experiment, problems with heater only 58C	
14	250612	3.0	2 + 5 + 8	OB	N	Rate exp + Inj above nozzle	New flow rate experiment with 3 mm nozzle. Dispersant injected 9 mm (3 x dia) above nozzle. "Problems" with dispersant pump overpressure at highest disp rate.	
15	280612	1.5	0.5/1.2/3	W	Yes		Water:air Experiment (repeated from experiment 21.03)	8
16	280612	1.5	1.2	OB	N	DOR 1:1000-25	Alternative dispersant (C9500 with less solvent). Viscous disp, but no problems at these low rates. Tried also Sim.inj. Tool but run out of oil..?	

Red: Not successful experiment
Yellow: Partly successful experiment
Green: Completely successful experiment

WS: Water samples (oil analysis, surfactant analysis or IFT measurements)

Appendix B:
Experimental data: Numerical distributions of oil and experimental conditions.

SINTEF

1704-2012

Date 1704-2012

Date: DDMM-YYYY of experiment – Used to identify each experiments in the report

Conditions C9500-Premixed DOR 1:1000-1:25
Comments DOR experiment
Nozzle size 1,5mm, 1,5L/min

This field is used to define the experimental conditions and the purpose or type of experiment

Name Oil alone 1,5 L/min
Average start 550 15:51:58
Average stop 600 15:52:48
Number of records 50

One experiments contains many runs with different flow rates, injection techniques and/or dispersant to oil ratios (DORs). This section identifies each run or data segment.
Name: Used as identifier (legends) in many of the figures in the report.
Start/Stop and **Number of records** identifies the data records averaged and used to represent this run or data segment.

Bins	2,73	3,22	3,8	4,48	5,29	6,24	7,36	8,69	10,2	12,1	14,3	16,8	19,9	23,5	27,7	32,7	38,5	45,5	53,7
	63,3	74,7	88,2	104	122	144	170	201	237	280	331	390	460						
Average conc	5,28	2,17	0,72	0,22	0,11	0,12	0,16	0,13	0,17	0,30	0,37	0,63	0,93	1,27	1,84	2,53	3,42	4,63	
	6,46	8,75	12,05	15,10	17,90	20,00	21,71	21,60	18,56	14,36	9,23	5,60	4,00	4,67					
Stdev conc	0,74	0,31	0,11	0,04	0,02	0,03	0,05	0,04	0,07	0,12	0,16	0,26	0,38	0,49	0,69	0,94	1,25	1,68	
	2,27	2,97	3,90	4,75	5,59	6,30	7,08	7,36	6,63	5,18	3,32	2,02	1,60	2,38					

Bins: Midpoint in microns for each of the 32 log distributed bins. These are not given for each of the data sets.

Average conc: Averaged concentration in ppm (10 measurements per second/record, usually 300-500 measurements) for all droplets within each bin.
Stdev conc: Standard deviation in concentration for all droplets within each bin. Reflects both experimental variation and the size variation within each bin.

Date 0305-2012
Conditions Small Nozzle experiments
Comments Injection above nozzle (3 x nozzle dia)
Nozzle size 0.5mm - 0.1 / 0.2 / 0.5 L/min
Name 0.5 mm - 0.1 L/min

Average start	348	15:12:8																
Average stop	402	15:13:2																
Number of records	54																	
Average conc	0,35	0,23	0,15	0,10	0,10	0,13	0,16	0,15	0,20	0,23	0,22	0,26	0,27	0,36	0,57	0,88	1,00	1,34
1,82	2,41	3,03	3,88	4,44	5,38	5,91	6,29	5,39	4,28	2,61	1,69	1,30	1,87					
stdev	0,03	0,02	0,01	0,01	0,01	0,01	0,01	0,01	0,02	0,03	0,04	0,05	0,06	0,08	0,13	0,21	0,26	0,34	0,46
0,59	0,77	0,97	1,15	1,45	1,97	2,62	2,70	2,39	1,58	1,11	1,10	2,26						

Name 0.5 mm - 0,2 L/min

Average start	1259	15:51:42																
Average stop	1289	15:52:12																
Number of records	30																	
Average conc	0,62	0,38	0,23	0,14	0,13	0,19	0,27	0,28	0,37	0,49	0,54	0,73	0,89	1,17	1,72	2,46	2,85	3,62
4,40	5,17	5,82	6,20	5,90	5,51	5,02	4,58	3,87	3,46	2,76	2,14	1,97	4,06					
stdev	0,10	0,06	0,03	0,02	0,02	0,03	0,04	0,05	0,06	0,10	0,12	0,17	0,23	0,29	0,40	0,55	0,67	0,84	1,04
1,25	1,50	1,70	1,74	1,67	1,48	1,13	0,77	0,69	0,79	1,00	1,45	4,51						

Name 0.5mm - 0,5 L/min

Average start	1427	15:54:30																
Average stop	1457	15:55:0																
Number of records	30																	
Average conc	11,54	4,69	1,62	0,65	0,54	1,20	2,63	2,81	4,03	6,39	6,56	9,01	10,20	10,68	11,62	11,35	9,24	7,08
5,05	3,46	2,43	1,75	1,37	1,27	1,44	1,82	2,27	2,71	2,73	2,36	2,51	6,30					
stdev	5,36	1,84	0,50	0,15	0,11	0,28	0,75	0,82	1,20	2,01	1,91	2,49	2,60	2,47	2,56	2,35	1,90	1,43	1,03
0,69	0,46	0,31	0,23	0,19	0,21	0,25	0,38	0,58	0,63	0,50	0,68	2,73						

Name	0.5mm - 0,2 L/min DOR 1:100																	
Average start	1697	15:59:0																
Average stop	1727	15:59:30																
Number of records	30																	
Average conc	7,22	2,98	1,05	0,42	0,32	0,59	1,15	1,15	1,58	2,41	2,45	3,34	3,81	4,18	4,96	5,47	5,33	5,13
	4,78	4,29	3,87	3,44	3,09	3,06	3,41	3,91	4,06	3,88	3,35	2,96	3,39	8,06				
stdev	5,34	1,88	0,53	0,16	0,11	0,21	0,49	0,48	0,67	1,11	1,06	1,43	1,54	1,53	1,66	1,56	1,34	1,06	0,91
	0,87	0,93	0,96	0,88	0,78	0,68	0,64	0,68	0,66	0,56	0,66	1,17	3,99					

Name	0.5mm - 0,2 L/min DOR 1:50																	
Average start	1787	16:0:30																
Average stop	1817	16:1:0																
Number of records	30																	
Average conc	27,14	8,92	2,35	0,69	0,45	0,89	1,89	1,78	2,44	3,98	3,73	4,84	4,97	4,70	4,95	4,53	3,83	3,16
	2,66	2,22	1,92	1,71	1,64	1,88	2,53	3,44	3,94	3,87	3,31	2,78	3,17	8,69				
stdev	16,67	4,01	0,61	0,10	0,07	0,10	0,24	0,25	0,46	1,09	1,06	1,53	1,56	1,36	1,39	1,15	0,90	0,67	0,53
	0,40	0,30	0,21	0,17	0,18	0,21	0,32	0,46	0,48	0,44	0,47	0,73	2,85					

Date 2604-2012
Type of experiment Medium Nozzle experiments
Injection medods Simulated injection tool - C9500
Flow and Nozzle size 1.5 mm 0.5-3.0 L/min

Name 1.5mm - 0,5 L/min
Average start 359 13:46:50
Average stop 389 13:47:20
Number of records 30

Average conc	0,71	0,39	0,18	0,08	0,04	0,03	0,03	0,03	0,04	0,07	0,09	0,11	0,09	0,05	0,04	0,04	0,09	0,20
0,17	0,23	0,41	0,40	0,64	0,85	1,15	2,41	5,27	8,90	12,20	13,37	13,42	12,57					
stdev	0,02	0,01	0,01	0,01	0,00	0,00	0,00	0,00	0,00	0,01	0,01	0,01	0,01	0,00	0,00	0,00	0,01	0,02	0,02
0,03	0,07	0,08	0,13	0,18	0,26	0,56	1,14	1,71	2,36	2,78	4,00	6,42						

Name 1.5mm - 1,2 L/min
Average start 474 13:48:45
Average stop 504 13:49:15
Number of records 30

Average conc	0,71	0,50	0,33	0,21	0,15	0,13	0,14	0,13	0,16	0,23	0,30	0,41	0,45	0,42	0,42	0,56	1,09	1,97
2,20	3,10	5,47	6,76	9,86	12,85	17,61	25,60	34,40	38,90	37,30	32,67	28,99	33,43					
stdev	0,05	0,04	0,05	0,05	0,05	0,05	0,05	0,04	0,05	0,07	0,08	0,12	0,14	0,16	0,18	0,25	0,44	0,75	0,91
1,28	2,13	2,64	3,69	4,82	6,48	8,37	10,25	12,46	12,84	12,08	11,86	16,39						

Name 1.5mm - 2,8 L/min
Average start 609 13:51:00
Average stop 639 13:51:30
Number of records 30

Average conc	4,72	2,43	1,15	0,57	0,41	0,58	0,90	0,93	1,28	1,98	2,38	3,61	4,87	6,38	8,77	12,24	16,40	21,72
26,98	32,79	40,34	44,09	46,13	44,80	42,50	37,48	29,27	20,58	12,77	7,96	5,95	6,94					
stdev	2,95	1,20	0,40	0,13	0,09	0,18	0,37	0,41	0,60	1,02	1,17	1,80	2,38	3,07	4,22	5,67	6,94	8,43	10,33
11,85	13,44	14,12	13,87	12,93	11,65	9,37	6,50	4,02	2,25	1,42	1,34	2,14						

Name	1.5mm - 1,2 L/min DOR: 1:100																	
Average start	1239	14:1:30																
Average stop	1269	14:2:0																
Number of records	30																	
Average conc	10,18	4,00	1,34	0,48	0,31	0,54	1,09	1,21	1,87	3,32	3,87	5,80	7,25	8,50	10,62	12,93	15,02	17,39
	19,79	21,62	23,19	22,07	19,73	17,43	16,00	15,13	13,13	11,28	8,66	6,68	5,95	8,77				
stdev	5,78	1,85	0,44	0,11	0,06	0,16	0,45	0,52	0,86	1,63	1,81	2,70	3,28	3,72	4,65	5,54	6,12	6,75	7,69
	8,21	8,52	7,99	6,77	5,46	4,22	2,95	1,69	0,97	0,77	0,82	1,03	2,29					

Name	1.5mm - 1,2 L/min DOR: 1:50																	
Average start	1329	14:3:00																
Average stop	1359	14:3:30																
Number of records	30																	
Average conc	25,73	8,61	2,30	0,67	0,43	0,91	2,14	2,28	3,45	6,03	6,19	8,66	9,84	10,46	12,30	13,56	14,27	14,68
	15,23	14,70	13,67	11,59	9,43	8,25	7,86	8,20	7,85	7,61	6,33	5,21	4,86	8,10				
stdev	16,79	5,25	1,30	0,36	0,22	0,49	1,21	1,29	1,98	3,55	3,58	5,00	5,61	5,87	6,85	7,47	7,79	7,93	8,20
	7,87	7,27	6,11	4,90	4,23	3,98	4,12	3,95	3,85	3,23	2,70	2,62	4,64					

Name	1.5mm - 1,2 L/min DOR: 1:25																	
Average start	1416	14:4:27																
Average stop	1417	14:4:28																
Number of records	1	(single measurements due to saturation of LISST due high concentration of small droplets)																
Average conc	41,23	13,31	3,37	0,93	0,60	1,31	3,13	3,14	4,57	7,81	7,48	10,03	10,69	10,53	11,62	11,56	10,94	10,06
	9,43	8,39	7,49	6,46	5,62	5,65	6,43	8,17	9,19	9,75	8,17	6,27	5,55	8,76				
stdev	5,18	1,24	0,18	0,02	0,01	0,06	0,23	0,23	0,37	0,75	0,65	0,85	0,78	0,64	0,65	0,65	0,63	0,56	0,50
	0,31	0,13	0,02	0,08	0,13	0,12	0,16	0,05	0,21	0,31	0,24	0,31	0,42					

Name	Oil:Gas 1.2 L/min (1:1) DOR: 1:50																	
Average start	1598	14:7:29																
Average stop	1628	14:7:59																
Number of records		30																
Average conc	8,42	3,67	1,36	0,54	0,38	0,63	1,12	1,11	1,48	2,28	2,37	3,21	3,72	4,07	4,81	5,47	6,16	6,86
	7,50	7,95	8,45	8,35	8,23	8,78	10,31	13,15	15,45	17,09	14,79	11,95	10,11	11,60				
stdev	2,57	0,97	0,29	0,10	0,07	0,14	0,29	0,29	0,39	0,61	0,59	0,78	0,87	0,92	1,09	1,19	1,21	1,19	1,23
	1,19	1,09	0,96	0,82	0,78	0,79	0,93	1,06	1,29	1,49	1,88	2,35	3,53					

Date 2506-2012
Conditions Flow rate exp.
Comments Injection above Nozzle (3x dia)
Nozzle size 3mm, 2+5+8L/min

Name 3mm - 8 L/min (2506)
Average start 264 12:56:30
Average stop 294 12:57:0
Number of records 30

Average conc	0,01	0,01	0,02	0,04	0,08	0,12	0,14	0,16	0,20	0,28	0,39	0,51	0,48	0,33	0,23	0,31	0,89	2,02
	1,81	2,49	5,09	5,79	9,46	13,17	18,98	27,54	38,15	49,80	53,96	50,22	41,55	40,73				
stdev	0,01	0,01	0,02	0,04	0,06	0,08	0,07	0,06	0,07	0,09	0,13	0,15	0,17	0,16	0,14	0,20	0,44	0,79	0,86
	1,17	2,08	2,56	4,07	5,61	7,88	10,73	14,29	18,40	20,73	21,56	21,85	27,31					

Name 3mm - 5 L/min (2506)
Average start 704 13:3:50
Average stop 734 13:4:20
Number of records 30

Average conc	0,00	0,00	0,01	0,02	0,05	0,07	0,06	0,06	0,08	0,11	0,23	0,32	0,15	0,04	0,02	0,02	0,13	0,95
	0,32	0,44	1,79	1,25	2,60	3,37	4,90	8,02	13,09	20,80	25,75	29,98	26,22	38,37				
stdev	0,00	0,00	0,01	0,03	0,05	0,05	0,04	0,04	0,04	0,05	0,08	0,11	0,05	0,04	0,02	0,02	0,09	0,43	0,19
	0,26	0,71	0,58	1,01	1,45	2,18	3,45	5,04	7,48	9,77	11,76	12,79	25,95					

Name 3mm - 5 L/min DOR 1:100 (2506)
Average start 780 13:5:5
Average stop 810 13:5:35
Number of records 30

Average conc	13,02	5,45	1,96	0,77	0,55	0,90	1,56	1,43	1,79	2,68	2,68	3,58	4,09	4,41	5,33	6,12	7,36	8,82
	10,82	13,30	16,53	18,89	20,46	22,09	22,50	22,66	18,89	15,64	10,29	7,14	5,10	6,97				
stdev	12,58	4,43	1,25	0,38	0,23	0,43	0,87	0,79	1,04	1,68	1,62	2,22	2,54	2,74	3,36	3,79	4,28	4,85	6,06
	7,27	8,60	9,51	9,82	10,44	10,73	11,05	9,34	7,97	5,57	4,20	3,41	5,97					

Name	3mm - 5 L/min DOR 1:50 (2506)																	
Average start	839	13:6:4																
Average stop	869	13:6:34																
Number of records	30																	
Average conc	23,87	9,19	2,94	1,02	0,69	1,22	2,29	2,08	2,65	4,03	3,84	5,06	5,62	5,92	7,07	7,82	8,78	9,89
	11,73	13,58	15,68	16,70	16,61	16,43	15,50	14,26	10,93	8,29	5,19	3,61	2,84	4,51				
stdev	18,86	6,76	1,99	0,65	0,43	0,77	1,51	1,38	1,79	2,80	2,64	3,50	3,86	4,04	4,81	5,29	5,86	6,52	7,72
	8,89	10,22	10,87	10,80	10,63	10,04	9,27	7,23	5,68	3,78	2,93	2,85	6,18					

Name	3mm 5 L/min DOR 1:25 (2506)																	
Average start	894	13:6:59																
Average stop	924	13:7:29																
Number of records	30																	
Average conc	14,75	5,94	2,04	0,77	0,57	1,04	1,92	1,75	2,21	3,30	3,15	4,14	4,61	4,86	5,77	6,43	7,23	8,09
	9,38	10,59	11,75	11,88	11,11	10,24	9,07	7,90	5,86	4,38	2,85	2,11	1,70	2,65				
stdev	14,84	5,47	1,70	0,60	0,43	0,79	1,54	1,42	1,82	2,81	2,65	3,49	3,85	4,02	4,77	5,26	5,82	6,42	7,44
	8,37	9,24	9,32	8,72	8,14	7,39	6,62	5,15	4,14	3,07	2,78	2,77	5,32					

Date 1605-2012
Conditions Flow rate experiment
Comments Injection above nozzle (3 x nozzle dia)
Nozzle size 3mm, 2 + 5 ml/min

Name 3mm - 2 L/min (1605)
Average start 472 15:41:56
Average stop 502 15:42:26
Number of records 30

Average conc	0,04	0,03	0,02	0,01	0,02	0,02	0,01	0,01	0,02	0,04	0,08	0,12	0,03	0,00	0,00	0,00	0,01	0,12
	0,02	0,03	0,19	0,09	0,32	0,44	0,61	1,38	2,42	3,37	4,12	5,40	5,39	17,21				
stdev	0,03	0,02	0,01	0,01	0,01	0,01	0,01	0,01	0,03	0,03	0,02	0,05	0,01	0,00	0,00	0,00	0,01	0,08	0,01
	0,02	0,14	0,06	0,20	0,27	0,32	0,76	1,65	2,23	2,70	4,31	4,10	15,22					

Name 3mm - 5 L/min (1605)
Average start 601 15:44:5
Average stop 631 15:44:35
Number of records 30

Average conc	0,00	0,00	0,01	0,01	0,03	0,06	0,07	0,09	0,13	0,18	0,28	0,38	0,31	0,17	0,11	0,14	0,52	1,60
	1,08	1,45	3,56	3,64	6,41	8,88	13,19	20,62	30,28	42,24	48,09	48,81	42,27	47,46				
stdev	0,01	0,01	0,01	0,02	0,03	0,06	0,05	0,05	0,06	0,07	0,09	0,14	0,12	0,11	0,08	0,11	0,27	0,69	0,53
	0,76	1,32	1,60	2,39	3,19	4,86	7,70	11,84	16,51	19,58	18,84	18,83	30,57					

Name 3mm - 5 L/min DOR: 1:100 (1605)
Average start 1242 15:54:46
Average stop 1272 15:55:16
Number of records 30

Average conc	7,17	2,87	1,00	0,40	0,29	0,48	0,82	0,75	0,95	1,43	1,44	1,94	2,22	2,39	2,89	3,36	4,08	4,96
	5,98	7,32	9,15	10,70	12,20	13,92	15,92	17,98	17,82	17,17	14,44	11,84	10,34	13,48				
stdev	13,48	4,81	1,41	0,45	0,29	0,52	0,99	0,91	1,19	1,90	1,86	2,56	2,95	3,19	3,93	4,49	5,20	6,11	7,49
	9,08	11,05	12,81	14,16	15,89	17,98	20,30	20,28	19,20	15,30	12,08	10,79	14,36					

Name	3mm - 5 L/min DOR: 1:50 (1605)																	
Average start	1131	15:52:55																
Average stop	1161	15:53:25																
Number of records	30																	
Average conc	15,73	5,72	1,71	0,56	0,36	0,64	1,19	1,06	1,36	2,12	2,03	2,72	3,03	3,20	3,83	4,25	4,76	5,41
	6,50	7,64	8,87	9,53	9,56	9,58	9,15	8,47	6,56	5,06	3,37	2,45	2,08	3,19				
stdev	21,54	7,47	2,11	0,66	0,42	0,74	1,43	1,28	1,66	2,64	2,51	3,40	3,78	3,97	4,76	5,24	5,82	6,56	7,87
	9,22	10,66	11,41	11,38	11,37	10,85	10,06	7,79	6,00	3,97	2,90	2,63	4,64					

Name	3mm - 5 L/min DOR: 1:25 (1605)																	
Average start	1267	15:55:11																
Average stop	1297	15:55:41																
Number of records	30																	
Average conc	0,31	0,19	0,11	0,07	0,06	0,08	0,10	0,09	0,10	0,14	0,15	0,19	0,16	0,10	0,07	0,08	0,16	0,30
	0,25	0,33	0,59	0,63	0,94	1,23	1,67	2,27	2,55	2,94	3,34	3,52	3,55	5,25				
stdev	0,15	0,10	0,07	0,06	0,05	0,07	0,09	0,07	0,08	0,09	0,08	0,08	0,08	0,08	0,08	0,09	0,11	0,13	0,15
	0,19	0,25	0,32	0,41	0,47	0,54	0,66	0,90	1,50	2,33	2,95	3,53	6,82					

Date 1704-2012
Conditions C9500-Premixed DOR 1:1000-1:25
Comments High flowrate experiment
Nozzle size 1,5mm, 1,5L/min

Name DOR 1:1000
Average start 597 15:52:45
Average stop 627 15:53:15
Number of records 30

Average conc	5,58	2,31	0,77	0,24	0,12	0,13	0,18	0,15	0,20	0,35	0,43	0,74	1,09	1,48	2,14	2,94	3,98	5,39
	7,49	10,09	13,84	17,39	20,70	23,17	25,30	25,13	21,33	16,16	10,11	6,02	4,29	5,10				
stdev	0,71	0,30	0,11	0,04	0,02	0,03	0,04	0,04	0,06	0,11	0,15	0,25	0,36	0,48	0,67	0,91	1,21	1,61	2,18
	2,85	3,75	4,59	5,42	6,16	6,79	6,73	5,87	4,56	2,90	1,77	1,39	2,02					

Name DOR 1:500
Average start 672 15:54:0
Average stop 702 15:54:30
Number of records 30

Average conc	6,24	2,50	0,80	0,25	0,12	0,14	0,21	0,19	0,26	0,47	0,59	1,03	1,50	2,02	2,90	4,00	5,41	7,28
	9,95	12,94	16,81	19,60	21,07	20,74	19,47	16,42	11,89	7,96	4,72	2,87	2,20	2,79				
stdev	0,98	0,37	0,12	0,04	0,02	0,03	0,06	0,06	0,09	0,17	0,23	0,38	0,54	0,69	0,96	1,29	1,69	2,23	2,97
	3,75	4,70	5,33	5,61	5,35	4,89	4,10	3,06	2,12	1,36	0,94	0,81	1,10					

Name DOR 1:250
Average start 747 15:55:15
Average stop 777 15:55:45
Number of records 30

Average conc	6,65	2,65	0,85	0,26	0,13	0,16	0,25	0,22	0,31	0,56	0,69	1,18	1,73	2,34	3,40	4,74	6,40	8,54
	11,48	14,43	17,89	19,61	19,50	17,65	15,33	12,13	8,44	5,53	3,22	1,88	1,38	1,74				
stdev	2,08	0,77	0,23	0,07	0,04	0,07	0,13	0,13	0,20	0,38	0,47	0,80	1,12	1,47	2,05	2,77	3,57	4,56	5,82
	6,99	8,24	8,75	8,65	7,93	6,95	5,57	4,09	2,84	1,74	1,04	0,75	0,94					

Name	DOR 1:100																	
Average start	812	15:56:20																
Average stop	842	15:56:50																
Number of records	30																	
Average conc	7,41	2,95	0,95	0,30	0,15	0,20	0,32	0,30	0,44	0,80	1,01	1,70	2,42	3,18	4,50	6,15	8,14	10,62
	13,97	17,19	20,75	22,13	21,36	18,72	15,64	11,88	8,00	5,12	2,97	1,76	1,32	1,73				
stdev	1,44	0,52	0,16	0,05	0,03	0,05	0,10	0,10	0,16	0,30	0,38	0,63	0,87	1,10	1,51	2,01	2,57	3,25	4,11
	4,87	5,64	5,80	5,46	4,73	3,97	3,06	2,18	1,55	1,06	0,74	0,65	0,93					

Name	DOR 1:50																	
Average start	882	15:57:30																
Average stop	912	15:58:0																
Number of records	30																	
Average conc	12,34	4,41	1,26	0,36	0,19	0,30	0,58	0,60	0,94	1,82	2,22	3,65	4,97	6,25	8,55	11,26	14,29	17,64
	21,65	24,09	25,69	23,16	18,72	13,79	9,75	6,78	4,13	2,64	1,50	0,96	0,74	1,16				
stdev	5,27	1,64	0,40	0,10	0,06	0,11	0,27	0,31	0,51	1,03	1,24	1,99	2,59	3,11	4,08	5,12	6,09	7,06	8,21
	8,70	8,86	7,67	5,81	4,14	2,80	1,91	1,21	0,82	0,51	0,36	0,31	0,58					

Name	DOR 1:25																	
Average start	1006	15:59:34																
Average stop	1030	15:59:58																
Number of records	24																	
Average conc	25,45	8,45	2,22	0,60	0,34	0,64	1,45	1,59	2,56	4,93	5,70	8,97	11,52	13,59	17,35	20,89	23,81	25,88
	28,33	27,48	24,75	19,26	13,11	8,79	5,76	3,90	2,38	1,53	0,88	0,56	0,46	0,78				
stdev	8,48	2,36	0,49	0,11	0,06	0,16	0,44	0,51	0,88	1,77	1,93	2,94	3,51	3,82	4,63	5,23	5,63	5,79	6,01
	5,68	4,92	3,76	2,54	1,70	1,16	0,81	0,56	0,40	0,26	0,17	0,14	0,24					

Name	Oil alone 1,5 L/min																	
Average start	550	15:51:58																
Average stop	600	15:52:48																
Number of records		50																
Average conc	5,28	2,17	0,72	0,22	0,11	0,12	0,16	0,13	0,17	0,30	0,37	0,63	0,93	1,27	1,84	2,53	3,42	4,63
	6,46	8,75	12,05	15,10	17,90	20,00	21,71	21,60	18,56	14,36	9,23	5,60	4,00	4,67				
stdev	0,74	0,31	0,11	0,04	0,02	0,03	0,05	0,04	0,07	0,12	0,16	0,26	0,38	0,49	0,69	0,94	1,25	1,68	2,27
	2,97	3,90	4,75	5,59	6,30	7,08	7,36	6,63	5,18	3,32	2,02	1,60	2,38					

Date 0806-2012
Conditions Premixed DOR 1:1000-1:25
Comments Reduced flow rate exp.
Nozzle size 1,5mm, 1,2L/min

Name DOR: 1:1000
Average start 308 15:42:35
Average stop 338 15:43:5
Number of records 30

Average conc	0,25	0,15	0,09	0,05	0,04	0,04	0,04	0,04	0,04	0,07	0,10	0,19	0,34	0,51	0,59	0,49	0,35	0,46
	1,23	2,97	2,60	3,43	6,26	6,18	9,53	11,98	15,03	18,20	18,86	17,23	14,84	17,95				
stdev	0,05	0,03	0,03	0,02	0,02	0,02	0,02	0,02	0,02	0,03	0,04	0,06	0,09	0,12	0,18	0,22	0,21	0,27	0,55
	0,95	1,10	1,49	2,30	2,59	3,52	4,28	5,21	6,70	7,37	8,08	9,01	15,49					

Name DOR: 1:500
Average start 375 15:43:42
Average stop 405 15:44:12
Number of records 30

Average conc	0,28	0,16	0,09	0,05	0,03	0,04	0,05	0,04	0,05	0,07	0,10	0,20	0,36	0,53	0,65	0,58	0,44	0,58
	1,43	3,28	3,07	4,12	7,31	7,41	11,19	13,79	15,98	16,92	14,74	11,16	8,16	8,85				
stdev	0,04	0,02	0,02	0,02	0,02	0,02	0,02	0,02	0,03	0,03	0,04	0,06	0,09	0,14	0,19	0,24	0,24	0,32	0,61
	1,01	1,23	1,64	2,41	2,77	4,03	5,23	5,99	6,46	5,85	4,65	4,05	6,63					

Name DOR: 1:250
Average start 453 15:45:0
Average stop 483 15:45:30
Number of records 30

Average conc	0,32	0,17	0,09	0,04	0,03	0,03	0,04	0,04	0,05	0,08	0,12	0,23	0,40	0,58	0,69	0,63	0,51	0,67
	1,61	3,57	3,37	4,42	7,50	7,46	10,78	12,67	14,33	15,62	14,68	12,49	9,71	10,03				
stdev	0,05	0,02	0,02	0,02	0,02	0,02	0,02	0,02	0,02	0,04	0,05	0,08	0,11	0,15	0,21	0,27	0,29	0,39	0,73
	1,20	1,43	1,80	2,47	2,90	4,13	5,30	6,28	6,58	6,55	6,77	6,97	10,34					

Name	DOR: 1:100																	
Average start	543	15:46:30																
Average stop	573	15:47:0																
Number of records	30																	
Average conc	0,71	0,39	0,19	0,10	0,07	0,09	0,13	0,13	0,17	0,27	0,35	0,56	0,81	1,06	1,33	1,44	1,49	1,98
	3,68	6,54	7,51	9,78	13,87	14,83	18,45	19,95	19,24	19,76	16,37	13,55	7,85	7,52				
stdev	0,21	0,11	0,06	0,03	0,02	0,03	0,04	0,04	0,06	0,10	0,12	0,19	0,26	0,35	0,48	0,64	0,79	1,07	1,72
	2,64	3,54	4,47	5,62	6,23	7,47	8,26	7,94	8,30	7,03	6,47	4,86	6,71					

Name	DOR: 1:50																	
Average start	633	15:48:0																
Average stop	663	15:48:30																
Number of records	30																	
Average conc	1,14	0,58	0,27	0,12	0,09	0,12	0,18	0,18	0,24	0,40	0,50	0,82	1,19	1,56	2,07	2,42	2,79	3,71
	6,04	9,50	11,42	14,33	18,32	18,96	19,59	18,77	14,62	12,32	8,08	5,83	3,47	3,81				
stdev	0,49	0,22	0,09	0,04	0,03	0,04	0,07	0,08	0,11	0,17	0,21	0,33	0,45	0,60	0,83	1,11	1,41	1,87	2,65
	3,55	4,87	6,20	7,35	8,30	8,35	8,10	6,20	4,82	2,99	2,21	1,78	2,65					

Name	DOR: 1:25																	
Average start	723	15:49:30																
Average stop	753	15:50:0																
Number of records	30																	
Average conc	4,49	1,85	0,67	0,26	0,18	0,33	0,67	0,73	1,06	1,74	1,95	2,94	3,90	4,90	6,53	8,19	10,04	12,45
	16,78	21,10	23,36	23,79	20,57	16,35	11,85	8,50	5,37	3,82	2,62	2,14	1,90	3,05				
stdev	3,32	1,15	0,32	0,10	0,07	0,15	0,37	0,43	0,65	1,12	1,20	1,78	2,21	2,56	3,28	4,08	5,12	6,21	7,79
	9,28	10,34	10,23	8,43	6,82	4,80	3,19	1,88	1,28	0,95	0,91	1,12	2,99					

Name	Oil alone																	
Average start	184	15:40:31																
Average stop	191	15:40:38																
Number of records	7	(reduced number of measurements due to noisy signals in initiation of experiments)																
Average conc	0,29	0,12	0,04	0,02	0,01	0,01	0,01	0,01	0,01	0,02	0,04	0,10	0,21	0,31	0,29	0,13	0,05	0,06
	0,28	1,12	0,64	0,85	2,16	1,94	3,82	5,10	7,15	9,13	9,07	7,94	6,52	8,27				
stdev	0,07	0,01	0,02	0,01	0,01	0,01	0,01	0,01	0,01	0,01	0,01	0,02	0,03	0,05	0,09	0,07	0,04	0,05	0,15
	0,38	0,30	0,40	0,78	0,83	1,40	2,02	3,74	5,80	6,32	5,36	4,80	7,96					

Date 0606-2012
Conditions Vertical Injection
Comments DOR 1:100 and DOR 1:50
Nozzle size 1,5mm, 1,2 L/min

Name DOR 1:100 45mm
Average start 589 15:7:15
Average stop 619 15:7:45
Number of records 30

Average conc	0,44	0,33	0,24	0,19	0,18	0,22	0,24	0,21	0,22	0,27	0,29	0,38	0,46	0,56	0,73	0,96	1,23	1,63
2,23	3,09	4,44	6,01	7,37	8,67	10,23	11,45	12,16	12,10	10,28	8,56	7,05	8,44					
stdev	0,33	0,23	0,15	0,10	0,09	0,11	0,12	0,10	0,11	0,13	0,13	0,16	0,20	0,24	0,32	0,41	0,53	0,69	0,96
1,31	1,75	2,24	2,81	3,27	3,74	4,61	5,31	5,39	4,79	4,65	5,28	9,11						

Name DOR 1:100 15mm
Average start 669 15:8:35
Average stop 699 15:9:5
Number of records 30

Average conc	2,79	1,52	0,75	0,40	0,33	0,50	0,72	0,63	0,71	0,93	0,91	1,16	1,32	1,47	1,84	2,21	2,66	3,27
4,20	5,47	7,20	8,96	10,30	11,66	12,98	13,42	12,28	10,29	7,23	5,12	4,15	4,95					
stdev	1,57	0,76	0,33	0,15	0,11	0,17	0,27	0,23	0,26	0,35	0,33	0,42	0,47	0,52	0,66	0,78	0,94	1,15	1,47
1,87	2,37	2,86	3,30	3,79	4,24	4,39	4,20	4,29	3,63	2,73	2,38	3,41						

Name DOR 1:100 8mm
Average start 759 15:10:5
Average stop 789 15:10:35
Number of records 30

Average conc	3,69	1,73	0,72	0,33	0,26	0,46	0,82	0,83	1,08	1,60	1,63	2,17	2,50	2,75	3,35	3,95	4,64	5,51
6,78	8,23	9,89	10,88	10,84	10,37	9,45	8,18	6,36	5,05	3,54	2,79	2,59	4,71					
stdev	1,80	0,76	0,28	0,11	0,08	0,16	0,31	0,31	0,41	0,62	0,60	0,79	0,90	0,98	1,21	1,42	1,64	1,92	2,31
2,77	3,34	3,70	3,83	4,00	4,10	4,14	3,66	3,31	2,47	2,16	3,21	10,41						

Name	DOR 1:100 6mm																	
Average start	826	15:11:12																
Average stop	856	15:11:42																
Number of records	30																	
Average conc	3,63	1,71	0,72	0,33	0,25	0,43	0,77	0,80	1,06	1,59	1,66	2,24	2,64	2,94	3,62	4,28	5,06	6,02
	7,40	8,88	10,41	10,99	10,38	9,36	8,04	6,74	5,13	4,01	2,63	1,83	1,34	1,82				
stdev	2,53	1,06	0,38	0,15	0,11	0,20	0,39	0,39	0,52	0,81	0,81	1,09	1,27	1,41	1,75	2,06	2,41	2,83	3,49
	4,14	4,71	4,72	4,29	3,86	3,41	3,12	2,57	2,31	1,71	1,39	1,26	1,96					

Name	DOR 1:100 4.5mm																	
Average start	929	15:12:55																
Average stop	959	15:13:25																
Number of records	30																	
Average conc	3,35	1,53	0,62	0,28	0,22	0,39	0,72	0,75	1,02	1,57	1,66	2,26	2,67	2,97	3,66	4,33	5,13	6,08
	7,38	8,67	9,90	10,16	9,25	7,99	6,64	5,43	4,08	3,16	2,12	1,61	1,30	1,88				
stdev	2,67	1,07	0,36	0,13	0,09	0,18	0,38	0,39	0,54	0,85	0,87	1,19	1,39	1,54	1,91	2,27	2,66	3,08	3,74
	4,30	4,80	4,84	4,48	4,01	3,40	2,89	2,31	1,93	1,30	1,08	1,02	1,78					

Name	DOR 1:100 1.5mm																	
Average start	1038	15:14:44																
Average stop	1068	15:15:14																
Number of records	30																	
Average conc	8,42	3,32	1,13	0,43	0,33	0,63	1,29	1,33	1,82	2,86	2,90	3,94	4,56	5,03	6,18	7,27	8,29	9,33
	10,65	11,48	11,95	10,99	8,96	6,80	4,99	3,63	2,53	1,81	1,16	0,80	0,65	1,05				
stdev	8,99	2,83	0,70	0,19	0,12	0,27	0,70	0,70	1,02	1,77	1,69	2,32	2,57	2,66	3,19	3,55	3,89	4,18	4,70
	4,89	4,89	4,29	3,36	2,57	1,89	1,39	0,98	0,78	0,56	0,39	0,33	0,66					

Name	DOR 1:50 8mm																	
Average start	1814	15:27:40																
Average stop	1844	15:28:10																
Number of records	30																	
Average conc	8,11	3,63	1,42	0,62	0,48	0,83	1,39	1,24	1,49	2,07	1,95	2,46	2,67	2,80	3,30	3,66	4,07	4,58
	5,42	6,37	7,58	8,61	9,22	9,56	9,35	8,44	6,46	4,60	2,83	1,89	1,42	1,84				
stdev	7,48	2,88	0,91	0,31	0,21	0,38	0,71	0,61	0,74	1,09	0,99	1,27	1,38	1,43	1,71	1,85	2,02	2,21	2,60
	3,00	3,43	3,69	3,80	4,05	4,18	4,11	3,26	2,50	1,67	1,35	1,28	1,93					

Name	DOR 1:50 6mm																	
Average start	1882	15:28:48																
Average stop	1912	15:29:18																
Number of records	30																	
Average conc	17,34	6,99	2,38	0,90	0,65	1,20	2,25	2,06	2,58	3,78	3,54	4,54	4,95	5,16	6,11	6,74	7,40	8,16
	9,43	10,64	11,94	12,50	12,17	11,59	10,38	8,65	6,19	4,33	2,63	1,71	1,31	1,93				
stdev	9,64	3,23	0,84	0,23	0,13	0,25	0,56	0,50	0,67	1,12	1,02	1,36	1,45	1,45	1,72	1,80	1,92	2,04	2,35
	2,64	2,91	2,86	2,49	2,24	2,11	2,12	1,92	1,56	1,06	0,79	0,66	1,09					

Name	DOR 1:50 4.5mm																	
Average start	1969	15:30:15																
Average stop	1999	15:30:45																
Number of records	30																	
Average conc	20,42	7,78	2,49	0,88	0,63	1,17	2,28	2,15	2,79	4,24	4,06	5,31	5,83	6,08	7,19	7,91	8,58	9,31
	10,55	11,55	12,43	12,29	11,11	9,72	8,06	6,31	4,22	2,71	1,52	0,98	0,82	1,55				
stdev	15,77	5,02	1,22	0,32	0,18	0,36	0,82	0,77	1,08	1,84	1,72	2,32	2,50	2,51	2,92	3,09	3,20	3,36	3,74
	3,95	4,09	3,80	3,21	2,66	2,18	1,89	1,45	1,03	0,66	0,66	0,92	2,88					

Name	DOR 1:50 1.5mm																	
Average start	2104	15:32:30																
Average stop	2134	15:33:0																
Number of records		30																
Average conc	27,97	9,93	2,88	0,92	0,63	1,29	2,76	2,65	3,58	5,68	5,40	7,18	7,89	8,23	9,77	10,70	11,42	12,01
	13,00	13,27	13,05	11,57	9,38	7,44	5,72	4,30	2,88	1,95	1,17	0,79	0,65	1,11				
stdev	13,94	4,25	0,99	0,25	0,14	0,27	0,67	0,64	0,93	1,66	1,53	2,10	2,24	2,23	2,57	2,67	2,73	2,80	3,06
	3,07	2,92	2,44	1,82	1,35	1,06	0,93	0,82	0,79	0,61	0,50	0,49	0,91					

Name	Oil alone																	
Average start	450	15:4:56																
Average stop	500	15:5:46																
Number of records		50																
Average conc	0,01	0,01	0,01	0,02	0,04	0,05	0,06	0,07	0,09	0,11	0,13	0,17	0,21	0,27	0,34	0,50	0,68	0,96
	1,37	1,91	2,90	3,96	4,91	5,89	7,44	8,60	10,17	10,60	8,77	6,56	4,69	4,20				
stdev	0,01	0,01	0,01	0,01	0,02	0,02	0,02	0,02	0,03	0,04	0,05	0,06	0,08	0,10	0,13	0,20	0,30	0,44	0,61
	0,87	1,33	1,85	2,51	3,21	4,18	5,11	6,14	6,85	6,20	4,73	3,75	3,99					

Date 1406-2012
Conditions Horizontal Injection
Comments DOR 1:25/50/100
Nozzle size 1,5mm, 1,2L/min

Name DOR 1:100 20mm
Average start 248 15:50:10
Average stop 278 15:50:40
Number of records 30

Average conc	0,36	0,25	0,17	0,12	0,09	0,10	0,10	0,08	0,09	0,13	0,17	0,25	0,30	0,29	0,32	0,39	0,72	1,19
	1,23	1,74	2,69	3,29	4,36	5,52	7,04	9,16	10,19	10,17	8,13	5,58	4,00	4,47				
stdev	0,09	0,06	0,04	0,03	0,03	0,03	0,03	0,03	0,03	0,05	0,06	0,09	0,12	0,14	0,17	0,21	0,32	0,46	0,55
	0,77	1,15	1,55	1,98	2,40	2,98	3,55	3,65	3,55	3,09	2,79	3,18	4,31					

Name DOR 1:100 10mm
Average start 308 15:51:10
Average stop 338 15:51:40
Number of records 30

Average conc	1,68	0,88	0,42	0,22	0,17	0,24	0,35	0,33	0,41	0,60	0,66	0,92	1,08	1,18	1,43	1,71	2,25	2,89
	3,31	4,10	5,05	5,62	5,99	5,92	5,57	4,96	3,78	2,57	1,45	0,80	0,58	0,84				
stdev	1,64	0,71	0,27	0,11	0,08	0,14	0,25	0,24	0,32	0,48	0,49	0,67	0,79	0,91	1,15	1,37	1,61	1,88	2,31
	2,79	3,32	3,72	3,74	3,40	2,77	2,10	1,59	1,29	0,91	0,59	0,51	0,89					

Name DOR 1:100 5mm
Average start 388 15:52:30
Average stop 418 15:53:0
Number of records 30

Average conc	2,77	1,39	0,63	0,30	0,23	0,37	0,58	0,55	0,70	1,03	1,11	1,54	1,82	2,02	2,50	2,99	3,78	4,72
	5,53	6,65	7,80	8,21	8,04	7,41	6,52	5,44	4,04	2,89	1,74	1,02	0,73	1,02				
stdev	1,13	0,54	0,23	0,10	0,08	0,13	0,21	0,20	0,25	0,36	0,36	0,49	0,58	0,66	0,84	1,01	1,20	1,41	1,74
	2,09	2,38	2,48	2,42	2,32	2,01	1,54	1,25	1,23	0,92	0,63	0,56	0,88					

Name	DOR 1:100 0mm																	
Average start	468	15:53:50																
Average stop	498	15:54:20																
Number of records	30																	
Average conc	4,66	2,16	0,88	0,39	0,29	0,48	0,84	0,83	1,09	1,67	1,79	2,47	2,91	3,22	3,96	4,69	5,80	7,08
	8,48	10,13	11,74	12,19	11,66	10,71	9,42	8,27	6,25	4,66	2,83	1,83	1,28	1,79				
stdev	2,14	0,82	0,26	0,09	0,06	0,12	0,26	0,26	0,36	0,59	0,59	0,81	0,94	1,04	1,31	1,55	1,80	2,09	2,55
	3,01	3,39	3,56	3,46	3,23	2,88	2,57	2,18	2,06	1,68	1,35	1,09	1,81					

Name	DOR 1:50 5mm																	
Average start	530	15:54:52																
Average stop	560	15:55:22																
Number of records	30																	
Average conc	8,09	3,45	1,28	0,53	0,40	0,69	1,23	1,16	1,49	2,23	2,23	2,97	3,36	3,62	4,39	5,04	5,86	6,73
	7,60	8,40	8,97	8,66	7,74	6,65	5,62	4,68	3,46	2,53	1,61	1,01	0,71	0,97				
stdev	7,06	2,49	0,70	0,21	0,14	0,29	0,64	0,59	0,78	1,24	1,15	1,52	1,66	1,73	2,08	2,31	2,45	2,58	2,89
	3,00	3,04	2,82	2,36	1,90	1,67	1,65	1,42	1,17	0,75	0,47	0,40	0,68					

Name	DOR 1:50 10mm																	
Average start	588	15:55:50																
Average stop	618	15:56:20																
Number of records	30																	
Average conc	11,48	4,66	1,63	0,64	0,47	0,83	1,51	1,40	1,78	2,67	2,60	3,43	3,83	4,07	4,90	5,54	6,30	7,12
	8,03	8,75	9,15	8,61	7,48	6,29	5,17	4,15	2,98	2,08	1,27	0,81	0,69	1,24				
stdev	9,92	3,45	0,94	0,26	0,16	0,35	0,80	0,73	0,99	1,60	1,47	1,96	2,13	2,19	2,64	2,90	3,11	3,35	3,85
	4,14	4,29	4,03	3,41	2,81	2,22	1,74	1,31	1,10	0,80	0,63	0,69	1,55					

Name DOR 1:50 20mm
Average start 628 15:56:30
Average stop 658 15:57:0
Number of records 30

Average conc	8,52	3,71	1,40	0,58	0,44	0,76	1,34	1,23	1,54	2,26	2,22	2,94	3,30	3,54	4,26	4,85	5,57	6,34
	7,17	7,92	8,36	7,92	6,89	5,81	4,83	3,92	2,83	1,99	1,22	0,77	0,65	1,20				
stdev	6,03	2,28	0,72	0,25	0,18	0,33	0,65	0,59	0,75	1,13	1,06	1,40	1,54	1,64	1,98	2,22	2,47	2,69	3,16
	3,44	3,54	3,30	2,75	2,20	1,66	1,22	0,86	0,71	0,51	0,48	0,69	1,55					

Name DOR 1:50 5mm
Average start 688 15:57:30
Average stop 718 15:58:0
Number of records 30

Average conc	6,29	2,82	1,10	0,47	0,36	0,60	1,02	0,94	1,17	1,70	1,69	2,23	2,51	2,70	3,25	3,72	4,36	5,08
	5,73	6,44	7,01	6,92	6,35	5,59	4,78	4,01	3,01	2,12	1,27	0,75	0,59	1,00				
stdev	5,62	2,29	0,79	0,29	0,20	0,36	0,67	0,61	0,76	1,12	1,06	1,38	1,54	1,66	2,03	2,31	2,55	2,80	3,27
	3,63	3,96	3,97	3,56	2,99	2,35	1,81	1,32	0,92	0,60	0,42	0,40	0,88					

Name DOR 1:25 5mm
Average start 743 15:58:25
Average stop 773 15:58:55
Number of records 30

Average conc	9,18	3,68	1,28	0,50	0,36	0,65	1,18	1,08	1,39	2,10	2,05	2,72	3,02	3,18	3,77	4,19	4,67	5,12
	5,50	5,70	5,68	5,07	4,21	3,42	2,81	2,32	1,71	1,25	0,82	0,57	0,52	1,15				
stdev	8,70	2,80	0,77	0,25	0,17	0,32	0,66	0,61	0,81	1,32	1,24	1,66	1,81	1,87	2,23	2,40	2,47	2,49	2,63
	2,50	2,29	1,93	1,45	1,07	0,79	0,61	0,47	0,44	0,38	0,37	0,55	1,78					

Name	DOR 1:12,5 5mm																	
Average start	791	15:59:13																
Average stop	821	15:59:43																
Number of records	30																	
Average conc	17,41	6,30	1,90	0,65	0,45	0,83	1,61	1,46	1,91	2,97	2,82	3,73	4,07	4,18	4,87	5,22	5,50	5,72
	5,89	5,74	5,36	4,51	3,61	2,90	2,41	2,05	1,58	1,17	0,73	0,46	0,37	0,68				
stdev	16,35	4,78	1,05	0,26	0,15	0,30	0,68	0,63	0,87	1,52	1,42	1,93	2,06	2,03	2,33	2,33	2,22	2,06	2,04
	1,85	1,62	1,27	0,91	0,66	0,53	0,48	0,43	0,36	0,26	0,19	0,18	0,39					

Name	Oil alone 1,2 L/min																	
Average start	133	15:48:15																
Average stop	163	15:48:45																
Number of records	30																	
Average conc	0,24	0,18	0,14	0,10	0,08	0,07	0,07	0,05	0,06	0,08	0,11	0,17	0,19	0,17	0,18	0,21	0,48	0,93
	0,91	1,38	2,31	2,81	3,92	5,02	6,65	9,16	10,33	10,00	7,98	6,16	5,33	7,21				
stdev	0,03	0,02	0,02	0,02	0,02	0,02	0,02	0,01	0,02	0,02	0,03	0,05	0,06	0,06	0,07	0,09	0,17	0,31	0,35
	0,53	0,89	1,13	1,53	1,95	2,75	4,05	5,15	5,77	5,04	4,40	5,65	9,95					

Date 2006-2012
Conditions Sim.Inj.Tool, DOR 1:100/50/25
Comments Warm Vs. Cold oil, 1st experiment
Nozzle size 1,5mm, 1,2L/min

Name DOR 1:100 Cold
Average start 300 15:43:31
Average stop 330 15:44:1
Number of records 30

Average conc	5,02	2,10	0,76	0,30	0,22	0,40	0,81	0,90	1,31	2,17	2,42	3,53	4,39	5,12	6,38	7,69	9,07	10,58
	12,42	13,94	15,18	14,86	13,25	11,07	8,64	6,56	4,35	2,97	1,81	1,24	0,98	1,45				
stdev	3,43	1,26	0,38	0,12	0,08	0,17	0,40	0,43	0,65	1,12	1,18	1,70	2,05	2,31	2,86	3,33	3,76	4,22	4,90
	5,30	5,55	5,32	4,60	3,88	3,18	2,67	2,01	1,50	1,01	0,81	0,76	1,36					

Name DOR 1:50 Cold
Average start 461 15:46:12
Average stop 470 15:46:21
Number of records 9

Average conc	16,06	6,15	1,96	0,68	0,49	0,98	2,02	1,97	2,66	4,17	4,07	5,46	6,11	6,47	7,64	8,42	9,03	9,51
	10,17	10,13	9,53	7,87	5,82	4,25	3,13	2,40	1,70	1,27	0,87	0,67	0,60	1,12				
stdev	3,81	1,48	0,50	0,18	0,12	0,20	0,34	0,31	0,40	0,62	0,61	0,83	0,91	0,98	1,14	1,17	1,16	1,11	1,11
	1,10	1,13	1,05	0,86	0,72	0,57	0,48	0,46	0,48	0,45	0,40	0,38	0,84					

Name DOR 1:25 Cold
Average start 548 15:47:39
Average stop 549 15:47:40
Number of records 1 (saturation of LISST due to high concentration of small droplets)

Average conc	27,49	9,60	2,70	0,84	0,55	1,08	2,24	2,07	2,73	4,28	3,97	5,11	5,37	5,26	5,83	5,74	5,54	5,19
	4,87	4,22	3,47	2,60	1,80	1,33	1,02	0,87	0,70	0,60	0,41	0,26	0,20	0,32				
stdev	21,08	6,27	1,32	0,25	0,11	0,29	0,85	0,80	1,17	2,09	1,90	2,53	2,58	2,43	2,68	2,61	2,54	2,33	2,08
	1,52	1,06	0,71	0,44	0,27	0,19	0,12	0,05	0,05	0,08	0,09	0,09	0,11					

Name	DOR 1:100 Warm																	
Average start	1005	15:55:16																
Average stop	1035	15:55:45																
Number of records	30																	
Average conc	1,29	0,64	0,30	0,15	0,12	0,18	0,30	0,32	0,45	0,72	0,87	1,30	1,69	2,07	2,62	3,35	4,38	5,70
	7,21	9,12	11,41	12,88	14,21	14,73	15,12	14,95	12,86	10,68	7,42	5,25	3,66	3,93				
stdev	1,52	0,65	0,24	0,09	0,06	0,11	0,22	0,25	0,37	0,63	0,73	1,08	1,39	1,67	2,14	2,66	3,25	3,89	4,74
	5,47	6,14	6,24	5,73	5,40	5,61	6,39	6,26	5,63	4,35	3,57	2,87	3,23					

Name	DOR 1:50 Warm																	
Average start	1060	15:56:10																
Average stop	1090	15:56:40																
Number of records	30																	
Average conc	6,70	2,83	1,03	0,41	0,30	0,56	1,10	1,15	1,59	2,51	2,64	3,67	4,36	4,90	5,98	6,99	8,00	9,02
	10,24	11,00	11,20	10,04	8,20	6,47	4,96	3,80	2,56	1,76	1,03	0,67	0,54	0,89				
stdev	4,27	1,64	0,53	0,19	0,13	0,25	0,54	0,56	0,79	1,27	1,29	1,77	2,05	2,24	2,70	3,05	3,32	3,52	3,82
	3,82	3,61	2,99	2,18	1,72	1,50	1,36	1,04	0,75	0,43	0,37	0,42	0,89					

Name	DOR 1:25 Warm																	
Average start	1136	15:57:26																
Average stop	1160	15:57:50																
Number of records	24																	
Average conc	16,00	5,84	1,75	0,58	0,41	0,83	1,76	1,70	2,29	3,59	3,39	4,39	4,68	4,70	5,27	5,41	5,31	5,06
	4,83	4,29	3,61	2,73	1,91	1,37	1,06	0,87	0,63	0,44	0,28	0,18	0,17	0,34				
stdev	16,58	5,59	1,54	0,48	0,33	0,68	1,47	1,41	1,92	3,06	2,86	3,71	3,92	3,89	4,34	4,42	4,31	4,07	3,88
	3,44	2,90	2,20	1,55	1,12	0,87	0,72	0,53	0,40	0,27	0,19	0,19	0,48					

Name	Oil Cold																	
Average start	194	15:41:45																
Average stop	224	15:42:15																
Number of records		30																
Average conc	0,00	0,00	0,01	0,01	0,03	0,04	0,05	0,06	0,07	0,09	0,11	0,15	0,18	0,21	0,22	0,30	0,47	0,75
	1,01	1,50	2,26	2,92	4,29	5,60	7,93	10,85	13,96	17,27	17,95	15,94	11,41	11,15				
stdev	0,00	0,01	0,01	0,01	0,02	0,03	0,04	0,04	0,04	0,04	0,05	0,06	0,08	0,09	0,10	0,13	0,20	0,33	0,46
	0,72	1,08	1,41	1,91	2,37	3,41	4,73	6,44	8,53	10,04	10,83	9,11	10,94					

Name	Oil warm																	
Average start	937	15:54:8																
Average stop	967	15:54:38																
Number of records		30																
Average conc	0,07	0,06	0,05	0,06	0,06	0,08	0,09	0,09	0,11	0,15	0,19	0,29	0,39	0,47	0,55	0,73	1,11	1,72
	2,39	3,63	5,45	7,20	9,97	12,02	14,91	17,49	18,16	16,75	12,55	8,40	5,98	6,46				
stdev	0,02	0,01	0,02	0,02	0,03	0,03	0,03	0,03	0,04	0,04	0,05	0,07	0,11	0,15	0,18	0,27	0,43	0,70	1,02
	1,55	2,37	3,24	4,57	5,63	6,98	7,93	8,24	8,10	6,75	5,29	4,85	6,06					

Date 2806-2012
Conditions DOR 1:1000-1:25
Comments New low solvent Dispersant & Water-air experiment
Nozzle size 1,5mm - 1.2 L/min

Name 2806-Water:Air-1.2 L/min (1:1)
Average start 594 14:5:1
Average stop 624 14:5:31
Number of records 30

Average conc	0,30	0,23	0,14	0,07	0,03	0,01	0,01	0,01	0,01	0,02	0,03	0,07	0,25	0,19	0,10	0,01	0,00	0,00
	0,03	0,47	0,20	0,33	1,06	0,71	1,17	1,12	0,94	1,11	1,45	2,25	1,62	1,03				
stdev	0,02	0,01	0,00	0,00	0,00	0,00	0,00	0,00	0,00	0,00	0,00	0,00	0,00	0,01	0,01	0,00	0,00	0,00	0,01
	0,09	0,04	0,05	0,17	0,20	0,48	0,66	0,66	0,80	1,06	1,50	1,93	1,49					

Name 2806 Water:Air-2.4 L/min (2:1)
Average start 1000 14:11:47
Average stop 1030 14:12:17
Number of records 30

Average conc	0,19	0,18	0,15	0,09	0,05	0,02	0,01	0,01	0,01	0,02	0,03	0,07	0,27	0,26	0,20	0,05	0,01	0,02
	0,13	1,18	0,56	0,86	2,35	1,87	3,46	4,54	5,36	6,48	6,42	6,86	6,74	10,71				
stdev	0,06	0,03	0,01	0,01	0,01	0,01	0,00	0,00	0,00	0,00	0,00	0,01	0,02	0,03	0,04	0,02	0,01	0,01	0,06
	0,31	0,21	0,36	0,87	0,81	1,53	2,14	2,78	3,33	3,28	4,14	4,78	9,71					

Name DOR 1:1000
Average start 1802 14:29:19
Average stop 1832 14:29:49
Number of records 30

Average conc	0,36	0,28	0,21	0,13	0,08	0,06	0,06	0,05	0,05	0,08	0,12	0,22	0,50	0,62	0,79	0,65	0,51	0,72
	1,56	3,82	3,45	4,72	7,78	7,94	10,92	12,65	13,63	13,90	10,98	7,49	5,17	5,56				
stdev	0,07	0,05	0,05	0,05	0,05	0,04	0,04	0,04	0,04	0,05	0,07	0,12	0,19	0,26	0,40	0,50	0,53	0,75	1,25
	2,08	2,54	3,34	4,40	4,86	6,37	8,02	9,86	11,14	9,19	6,19	4,27	4,43					

Name	DOR 1:500																	
Average start	1883	14:30:40																
Average stop	1913	14:31:10																
Number of records		30																
Average conc	0,40	0,30	0,22	0,14	0,09	0,07	0,07	0,07	0,08	0,12	0,18	0,31	0,64	0,78	0,98	0,86	0,69	1,00
2,08	4,74	4,48	6,04	9,36	9,56	13,03	14,87	15,64	16,59	14,90	11,92	8,19	7,93					
stdev	0,07	0,04	0,03	0,02	0,02	0,02	0,03	0,02	0,03	0,05	0,06	0,10	0,14	0,18	0,23	0,28	0,29	0,41	0,67
1,01	1,29	1,79	2,50	3,00	4,16	5,00	5,58	6,33	6,20	5,70	5,06	7,74						

Name	DOR 1:250																	
Average start	1962	14:31:59																
Average stop	1992	14:32:29																
Number of records		30																
Average conc	1,33	0,81	0,45	0,24	0,15	0,16	0,22	0,23	0,29	0,48	0,64	0,98	1,54	1,72	2,06	2,00	2,04	2,70
4,47	7,65	8,79	11,75	15,86	17,86	21,03	22,70	21,05	20,80	16,73	13,84	6,78	5,57					
stdev	0,50	0,25	0,12	0,06	0,04	0,05	0,06	0,06	0,08	0,13	0,15	0,24	0,35	0,47	0,66	0,80	0,97	1,30	1,99
2,94	3,71	5,01	6,45	7,60	8,30	8,77	8,38	8,88	7,29	7,23	4,48	4,73						

Name	DOR 1:100																	
Average start	2052	14:33:29																
Average stop	2082	14:33:59																
Number of records		30																
Average conc	1,16	0,67	0,35	0,17	0,11	0,11	0,15	0,16	0,21	0,35	0,47	0,73	1,21	1,48	2,05	2,44	2,91	4,16
6,54	10,46	11,27	12,63	13,80	11,76	9,76	7,54	4,63	3,21	1,82	1,25	0,90	1,19					
stdev	0,54	0,26	0,11	0,05	0,03	0,04	0,07	0,08	0,11	0,18	0,23	0,35	0,50	0,68	1,02	1,42	1,88	2,59	3,60
4,68	5,86	6,40	6,16	5,68	4,63	3,94	2,58	1,75	1,06	0,78	0,75	1,57						

Name	DOR 1:50																	
Average start	2143	14:35:0																
Average stop	2173	14:35:30																
Number of records		30																
Average conc	3,33	1,53	0,61	0,24	0,15	0,22	0,38	0,42	0,62	1,14	1,52	2,49	3,75	4,68	6,38	8,06	9,87	12,58
	15,81	19,03	18,36	16,31	12,45	8,39	5,54	3,46	1,97	1,14	0,62	0,39	0,32	0,49				
stdev	1,74	0,70	0,24	0,09	0,05	0,08	0,17	0,20	0,32	0,60	0,76	1,19	1,58	1,95	2,59	3,38	4,27	5,23	6,13
	6,66	6,76	5,82	4,26	2,93	1,92	1,26	0,76	0,45	0,28	0,22	0,22	0,38					

Name	DOR 1:25																	
Average start	2228	14:36:25																
Average stop	2258	14:36:55																
Number of records		30																
Average conc	11,36	4,22	1,32	0,45	0,31	0,61	1,42	1,64	2,48	4,33	4,78	6,95	8,85	10,22	13,16	16,12	18,21	20,44
	21,61	20,52	16,99	12,01	7,64	4,62	2,94	1,87	1,13	0,68	0,39	0,25	0,22	0,42				
stdev	7,82	2,48	0,62	0,17	0,11	0,25	0,67	0,77	1,26	2,35	2,51	3,66	4,33	4,78	5,91	6,98	7,62	8,07	8,14
	7,32	6,14	4,34	2,79	1,82	1,30	0,95	0,64	0,42	0,26	0,19	0,18	0,42					

Name	Oil 1,2 L/min																	
Average start	1596	14:25:54																
Average stop	1626	14:26:24																
Number of records		30																
Average conc	0,32	0,25	0,17	0,10	0,06	0,04	0,04	0,03	0,03	0,05	0,08	0,16	0,40	0,49	0,57	0,37	0,23	0,32
	0,86	2,65	1,98	2,73	4,97	4,85	7,46	9,38	10,37	10,94	9,69	8,08	6,75	8,80				
stdev	0,04	0,02	0,02	0,03	0,03	0,02	0,02	0,02	0,02	0,03	0,04	0,07	0,11	0,16	0,24	0,26	0,21	0,30	0,61
	1,26	1,38	1,93	2,95	3,09	4,32	5,62	6,95	8,58	9,64	9,80	9,08	12,92					

Technology for a better society
www.sintef.no